

Feynman-Dyson Perturbation Theory Applied to Model Linear Polyenes

by

Richard D. Reid

Dissertation submitted to the Faculty of the

Virginia Polytechnic Institute and State University

in partial fulfillment of the requirements for the degree of

Doctor of Philosophy

in

Chemistry

APPROVED:

John C. Schug, Chairman

James W. Viers

George S. Sanzone

Harold M. Bell

Brian E. Hanson

December 19, 1986

Blacksburg, Virginia

Feynman-Dyson Perturbation Theory Applied to Model Linear Polyenes

by

Richard D. Reid

John C. Schug, Chairman

Chemistry

(ABSTRACT)

In the work described in this thesis, the Feynman-Dyson perturbation theory, developed from quantum field theory, was employed in semiempirical calculations on *trans* - polyacetylene. A variety of soliton-like excited states of the molecule were studied by the PPP-UHF-RPA method. The results of this study provide useful information on the nature of these states, which are thought to account for the unique electrical conduction properties of *trans* - polyacetylene and similar conducting polymers.

Feynman-Dyson perturbation theory was also used to extend Hartree-Fock theory by the inclusion of time-independent second-order self-energy insertions. The results of calculations on polyenes show that consideration of this approach is warranted, as the contribution of the second-order terms is significant.

The computer program, written during the course of the research reported here, is discussed as well.

Acknowledgements

I gratefully acknowledge the aid and direction given to me by my research professor, Dr. Schug, during the course of this research. I am also indebted to Dr. T. K. Lee in the Physics Department here at V.P.I. and S. U. for his helpful discussions on Feynman-Dyson perturbation theory and to Dr J. W. Viers for his assistance in the use of the computing facilities here. This work was supported in part by the Philip Morris Research Center in Richmond, Virginia. I would like to thank _____ and _____ at the the Philip Morris Research Center for their aid in the work on polyacetylene. Finally, I dedicate this work to my wonderful wife, _____, without whom life would be empty and to my mother and father, whose support in all my endeavors has made getting to this point easy.

Table of Contents

1.0	Introduction	1
2.0	The Feynman-Dyson Perturbation Expansion	3
3.0	Self-Energy and Polarization Insertion	9
3.1	The Self-Energy	9
3.2	The Polarization Insertion	11
4.0	Previous Experimental and Theoretical Results on TPA	23
5.0	Electron Screening and the RPA	29
6.0	Calculational Details	47
7.0	Solutions To The Solitary Wave Equation	51
8.0	PPP-UHF-RPA Results for TPA	53

8.1	TPA Ground State	53
8.2	Neutral Solitons	54
8.3	Charged Solitons	55
8.4	Polarons	56
8.5	Conclusions from the PPP-UHF-RPA Study of TPA	57
9.0	Theory of the Extended UHF-TISOSE Method	69
9.1	Relation to Hartree-Fock Theory	70
9.2	Extension of Hartree-Fock Theory with the TISOSE Terms	71
9.3	Results of the Extended PPP-UHF-RPA-TISOSE Calculations on TPA	73
10.0	Description of the Computer Code	76
	Appendix A. Derivation of Equation 46a	80
	Appendix B. Computer Program	85
	References	120
	Vita	125

List of Illustrations

Figure 1. a) Typical connected diagram b) typical disconnected	7
Figure 2. Feynman-Dyson expansion of the exact interacting particle	8
Figure 3. Typical self-energy insertion	12
Figure 4. Self-energy expansion of the exact Green function for the	13
Figure 5. a) Typical proper self-energy insertion.	14
Figure 6. Proper self-energy expansion of the self-energy.	15
Figure 7. Proper self-energy expansion of the exact Green function	16
Figure 8. Typical polarization part	18
Figure 9. Effective interaction	19
Figure 10. a) Typical proper polarization part.	20
Figure 11. Dyson equation for the effective interaction	21
Figure 12. RPA polarization insertion	22
Figure 13. Peierls distortion	27
Figure 14. Neutral and charged domain wall defects. The arrows	28
Figure 15. Proper polarization parts.	36
Figure 16. RPA effective interaction.	37
Figure 17. Hartree-Fock approximation to the exact interacting particle	38
Figure 18. SCF-Hartree-Fock approximation to the exact interacting	39
Figure 19. RPA effective interaction with the bare Green function	40
Figure 20. RPA polarization insertion with the bare Green function	41
Figure 21. Effective interaction at site 1	42

Figure 22. bond alternation pattern	43
Figure 23. Interaction potential at site 1	44
Figure 24. Cooper and Linderberg effective interaction.	45
Figure 25. Vertex part	46
Figure 26. Bond alternation pattern for a 57 membered chain containing	59
Figure 27. Spin distribution for a 57 membered chain containing	60
Figure 28. Bond alternation pattern for a 57 membered chain	61
Figure 29. Bond alternation pattern for a 57 membered chain containing	62
Figure 30. Charge density distribution for a 57 membered chain	63
Figure 31. Charge density distribution for a 57 membered chain containing	64
Figure 32. Bond alternation pattern for a 40 membered chain	65
Figure 33. Bond alternation pattern for a 40 membered chain containing	66
Figure 34. Charge density distribution for a 40 membered chain	67
Figure 35. Charge density distribution for a 40 membered chain containing	68
Figure 36. TISOSE insertions	75
Figure 37. Complete Feynman diagram for self-energy insertion "2a".	84

1.0 Introduction

The pioneering work of Feynman (1) and Dyson (2) led to the development of the quantum field theory used in solid state physics. Although the general theory can be applied to the quantum description of any many particle system, it has seen only limited use in molecular orbital studies.

The Feynman-Dyson perturbation treatment, which can be developed by application of quantum field theory to the many-particle Schrodinger equation, has been used extensively for the calculation of excitation energies in relatively small conjugated systems (3). However, this approach is also useful in the calculation of the topological and electronic properties of ground and excited states of all molecular systems.

In the work reported here, the Feynman-Dyson field-theoretical perturbation treatment has been applied, at various levels, to the ground state and several exotic excited states of the linear polyene, *trans* - polyacetylene (TPA). The results of this study show that the field-theoretical approach can be successfully applied to such systems when more simple-minded approaches fail.

The first phase of this research involved the application of the random phase approximation (RPA) (4-7), to the semi-empirical Pariser-Pople-Parr (8,9)-unrestricted Hartree-Fock (10,11) (PPP-UHF) treatment of TPA states. The RPA involves the inclusion of some important terms

in the Feynman-Dyson perturbation expansion to screen the electron-electron interactions in many-electron systems.

The Hartree-Fock theory (the first-order approximation in Feynman-Dyson perturbation theory), was extended in the second phase of the research by the addition of time independent second-order self-energy terms (TISOSE approach). The TISOSE extended UHF method was used to examine the kink soliton-like excitation in TPA. This phase of the study included the development of matrix forms of the second-order perturbation terms which were suitable for use in PPP-UHF calculations.

In addition to a discussion of the theory and results of the two main research topics, this report also includes a general discussion of the development of the Feynman-Dyson perturbation expansion from quantum-field theory and a description of the computer code used in the calculations performed in this work.

2.0 The Feynman-Dyson Perturbation Expansion

Molecules and atoms can be viewed as a collection of many interacting particles. In principle, the Schrodinger equation provides a means of obtaining a wave function which contains all possible information about a system of interacting particles. However, the solution of this equation is impossible directly. Application of quantum-field theory, using Green functions, provides a way to obtain a great deal of information (total ground state energy and excitation energies, for example), and to obtain approximations for other types of information (such as electronic structures), from approximate wave functions.

Beginning with the exact Green function for the non-interacting Schrodinger equation, it is possible to obtain an approximation to the exact Green function for an interacting system by application of Feynman-Dyson perturbation theory.

The Schrodinger equation for a system of non-interacting particles has the field-theoretical form
(12)

$$\hat{H}_0 \Psi_0(\vec{x}) = E_0 \Psi_0(\vec{x}) \tag{1}$$

where $\Psi_0(\vec{x})$, is the wave function of the non-interacting system, E_0 is the energy of the system and \hat{H}_0 is the Hamiltonian operator. For a system of non-interacting electrons in an atom or molecule, within the Born-Oppenheimer approximation (12)

$$\hat{H}_0 = \int d^3x \hat{\psi}^\dagger(\vec{x})_\alpha \left[\frac{-\hbar^2}{8m\pi^2} \nabla^2 + U(\vec{x}) \right] \hat{\psi}(\vec{x})_\alpha. \quad (2)$$

In equation 2, $U(\vec{x})$, is a static external potential which destroys spatial uniformity and m is the particle (electron), mass. The field-operators, $\hat{\psi}^\dagger(\vec{x})_\alpha$ and $\hat{\psi}(\vec{x})_\alpha$, in equation 2 are defined as (12)

$$\hat{\psi}(\vec{x})_\alpha \equiv \sum_k \psi_k(\vec{x})_\alpha c_k \quad (3a)$$

$$\hat{\psi}^\dagger(\vec{x})_\alpha \equiv \sum_k \psi_k(\vec{x})_\alpha c_k^\dagger \quad (3b)$$

where $\psi(\vec{x})_\alpha$ is the single particle two component wave function ($\alpha = 1,2$), and the sum is over the complete set of single particle quantum numbers. In equation 3, $c_k^\dagger(c_k)$ is the particle creation (destruction) operator, that is $c_k^\dagger(c_k)$ creates (destroys) a particle with the set of quantum numbers k .

The exact Green function for equation 1 is (12)

$$iG^0(x,x') = \sum_j \varphi_j^0(\vec{x}) \varphi_j^0(\vec{x}')^\dagger \exp\left\{ \frac{-i\varepsilon_j^0(t-t')}{\hbar/2\pi} \right\} [\Theta(t-t')\Theta(\varepsilon_j^0 - \varepsilon_F^0) - \Theta(t'-t)\Theta(\varepsilon_F^0 - \varepsilon_j^0)] \quad (4)$$

where $\Theta(x-y)$ is the step function and $x \equiv (\vec{x}, t)$. In equation 4, $\varphi_j^0(\vec{x})$ and ε_j^0 are the eigenfunctions and eigenvalues of \hat{H}_0

$$\left[-\frac{\hbar^2}{8m\pi^2} \nabla^2 + U(\vec{x}) \right] \varphi_j^0(\vec{x}) = \varepsilon_j^0 \varphi_j^0(\vec{x}). \quad (5)$$

The single particle eigenfunctions, $\varphi_j^0(\vec{x})$, form a basis for the field operators defined in equation 3.

The Schrodinger equation for a system of interacting electrons in an atom or molecule has the form

$$\hat{H}\Psi(\vec{x}) = E\Psi(\vec{x}) \quad (6)$$

where $\Psi(\vec{x})$ is the wave function for the interacting particle system and E is the corresponding total energy. The Hamiltonian operator for this system can be separated into interacting and non-interacting parts

$$\hat{H} = \hat{H}_0 + \hat{H}_1 \quad (7)$$

where \hat{H}_0 is given by equation 2 and

$$\hat{H}_1 = \frac{1}{2} \int d^3x d^3x' \hat{\psi}^\dagger(\vec{x})_\alpha \hat{\psi}^\dagger(\vec{x}')_\beta V(\vec{x} - \vec{x}') \hat{\psi}(\vec{x})_\alpha \hat{\psi}(\vec{x}')_\beta. \quad (8)$$

The interparticle interaction potential, $V(\vec{x} - \vec{x}')$, may be assumed to be spin independent.

If \hat{H}_1 is treated as a perturbation to \hat{H}_0 , then a perturbation expansion of the exact Green function for equation 6 can be developed (1,2,12). The terms in the expansion have been shown (13,14) to correspond exactly to the infinite set of connected Feynman diagrams. The general rules for creating and analyzing all n^{th} order diagrams are (12) :

1. Draw all topologically distinct connected diagrams with n particle interaction lines and $2n + 1$ directed Green function (particle) lines.
2. Label each vertex with a space-time point, x_i .
3. A solid line represents the non-interacting (bare) Green function, $G_{\alpha\beta}^0(x,y)$, running from y to x.
4. A wavy line represents the interparticle interaction,

$$U(x,y)_{\lambda\lambda',\mu\mu'} = V(x,y)_{\lambda\lambda',\mu\mu'}\delta(t_x - t_y).$$

5. All internal variables are integrated over space and time.
6. There is a spin matrix product for each continuous fermion line.
7. A factor of $(-1)^F$ is assigned to each diagram, where F is the number of closed fermion loops.
8. A factor of $(2\pi i/\hbar)^n$ is assigned to each n^{th} order term.
9. A Green function with equal time variables is interpreted as $G_{\alpha\beta}^0(\vec{x}, t, \vec{y}, t^+)$

The Greek subscripts are fermion spin indices and a connected diagram is one in which all interaction and particle lines are somehow connected to the rest of the diagram. Figure 1a shows a typical connected diagram and figure 1b shows a typical disconnected diagram. The diagrammatic representation of the Feynman-Dyson perturbation expansion is shown through second order in figure 2.

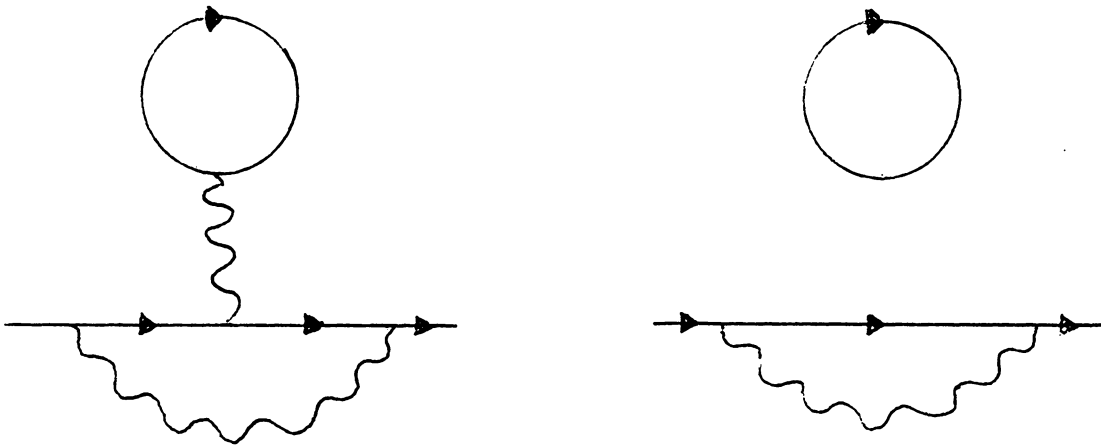


Figure 1. a) Typical connected diagram b) typical disconnected diagram

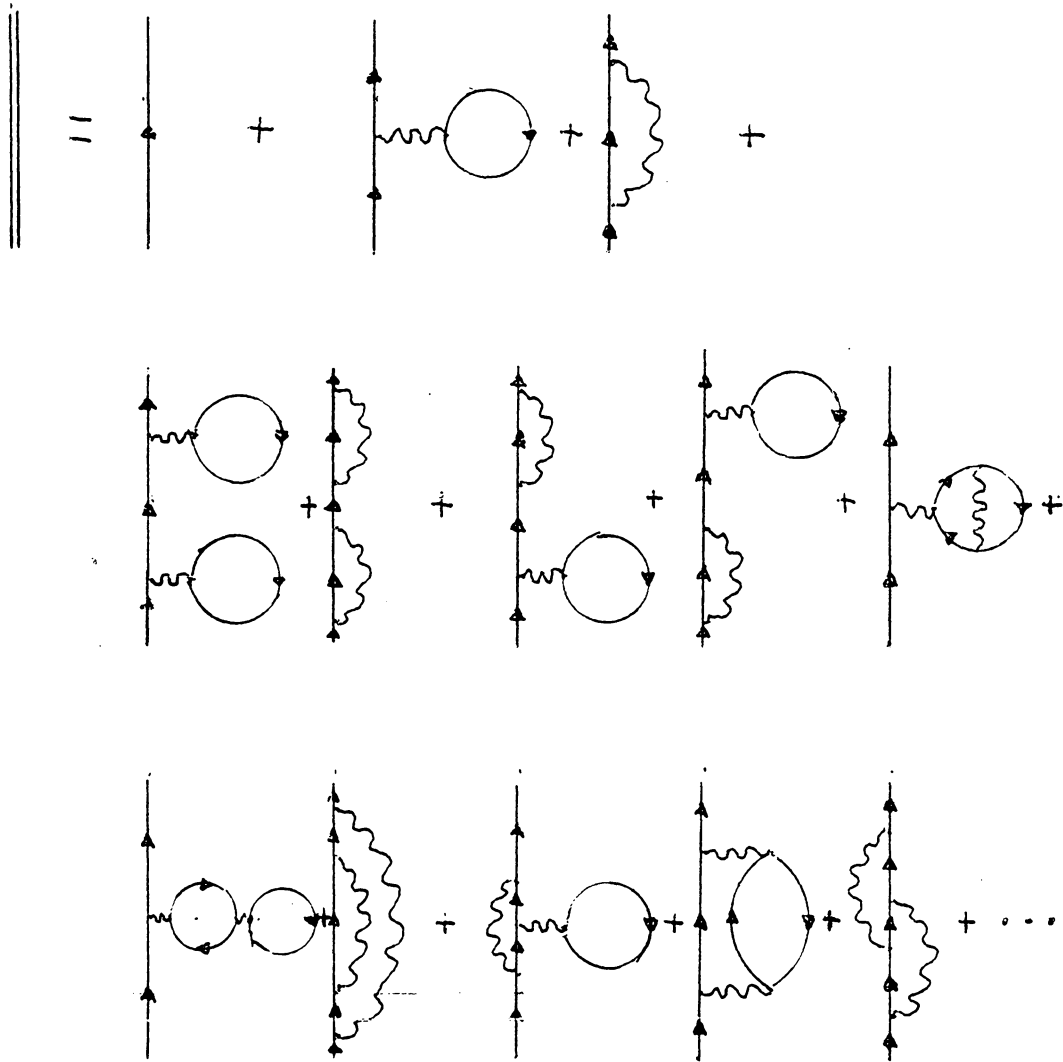


Figure 2. Feynman-Dyson expansion of the exact interacting particle Green function

3.0 Self-Energy and Polarization Insertion

Representing the terms in the perturbation expansion by Feynman diagrams enables one to notice certain distinct contributions to each term. Two such contributions are the self-energy insertion and the polarization part. Analysis of the perturbation terms with respect to these contributions leads to Dyson's equation.

3.1 *The Self-Energy*

Examination of figure 2 shows that the exact interacting Green function is the sum of the bare Green function and connected diagrams with a bare Green function coming in and another going out. This observation leads to the definition of the self-energy insertion, which is defined as a part on a diagram connected to the rest of the diagram by one particle line coming in and one particle line going out. For example, the boxed-off portion of figure 3 is a typical self-energy insertion.

Defining the self-energy as the sum of the infinite set of self-energy insertions, the compact analytical expression for the interacting system Green function is obtained

$$G_{\alpha\beta}(x,y) = G_{\alpha\beta}^0(x,y) + \int d^4x_1 d^4x'_1 G_{\alpha\lambda}^0(x,x_1) \Sigma_{\lambda\mu}(x_1, x'_1) G_{\mu\beta}^0(x'_1, y) \quad (9)$$

where $\Sigma_{\lambda\mu}(x_1, x'_1)$ is the self-energy. Equation 9 is represented by the Feynman diagram in figure 4, where the double cross-hatched bubble represents the self-energy.

A self-energy insertion may be further classified as proper or improper. A proper self-energy insertion is one which cannot be separated into two pieces by cutting a single particle line. A proper self-energy insertion is illustrated in figure 5a, while the self-energy insertion in figure 5b is improper. The proper self-energy is the sum of the infinite set of proper self-energy insertions and is denoted by $\Sigma_{\alpha\beta}^*(x,y)$. The sum of all possible repetitions of the proper self-energy is equivalent to the self-energy. This is represented analytically by

$$\Sigma(x_1, x'_1) = \Sigma^*(x_1, x'_1) + \int d^4x_2 d^4x'_2 \Sigma^*(x_1, x_2) G^0(x_2, x'_2) \Sigma^*(x'_2, x'_1) + \dots \quad (10)$$

and is represented diagrammatically as shown in figure 6, where the cross-hatched bubble represents the proper self-energy. In equation 10, the spin indices have been repressed.

Insertion of equation 10 in equation 9 yields the expression for the interacting system Green function in terms of the proper self-energy

$$G(x,y) = G^0(x,y) + \int d^4x_1 d^4x'_1 G^0(x,x_1) \Sigma^*(x_1, x'_1) G^0(x'_1, y) + \int d^4x_1 d^4x'_1 d^4x_2 d^4x'_2 G^0(x,x_1) \Sigma^*(x_1, x'_1) G^0(x'_1, x_2) \Sigma^*(x_2, x'_2) G^0(x'_2, y) + \dots, \quad (11)$$

where the spin indices have been suppressed. Equation 11 can be formally summed (2), yielding Dyson's equation

$$G_{\alpha\beta}(x,y) = G_{\alpha\beta}^0(x,y) + \int d^4x_1 d^4x'_1 G_{\alpha\lambda}^0(x,x_1) \Sigma_{\lambda\mu}^*(x_1, x'_1) G_{\mu\beta}(x'_1, y) \quad (12)$$

The Feynman diagrams of equations 11 and 12 are given in figure 7.

Dyson's equation allows the practical iterative summation of an infinite class of perturbation terms. This feature will be discussed later in terms of self consistent Hartree-Fock theory and its extension by the inclusion of the time independent second-order self-energy insertions.

3.2 *The Polarization Insertion*

Another class of contribution to each diagram is observed upon the examination of the inter-particle interaction part of the diagrams in figure 2. Each interaction is the sum of the bare interaction and all connected diagram parts with particle interaction lines coming in and out. This leads to the definition of a polarization part. A typical polarization part is illustrated by the boxed-off part of figure 8. The polarization insertion, $\Pi(x - y)_{\mu\nu, \eta\lambda}$, is defined as the sum of the infinite set of polarization parts. This definition allows for the calculation of an effective interaction, $U(x - y)_{\alpha\beta, \rho\tau}$, in terms of the bare interaction, $U_0(x - y)_{\alpha\beta, \rho\tau}$, and the polarization insertion

$$U(x - y)_{\alpha\beta, \rho\tau} = U_0(x - y)_{\alpha\beta, \rho\tau} + U_0(x - y)_{\alpha\beta, \mu\nu} \Pi(x - y)_{\mu\nu, \eta\lambda} U_0(x - y)_{\eta\lambda, \rho\tau} \quad (13)$$

Figure 9 shows the diagram corresponding to equation 13. The heavy wavy line represents the effective interaction and the bubble with the double cross-hatched box represents the polarization insertion.

Defining a proper polarization part as one which cannot be separated into two pieces by cutting a bare interaction line allows the introduction of the proper polarization insertion, $\Pi^*(x - y)_{\mu\nu, \eta\lambda}$, suitably defined as the sum of the infinite set of proper polarization parts. Figure 10a shows a proper polarization part and 10b shows an improper polarization part. An analysis similar to that for the self-energy insertion yields Dyson's equation for the effective interaction

$$U(x - y) = U_0(x - y) + U_0(x - y) \Pi^*(x - y) U(x - y) \quad (14)$$

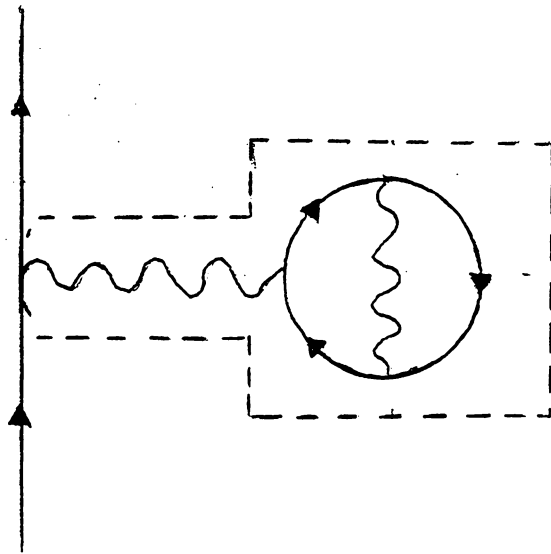


Figure 3. Typical self-energy insertion

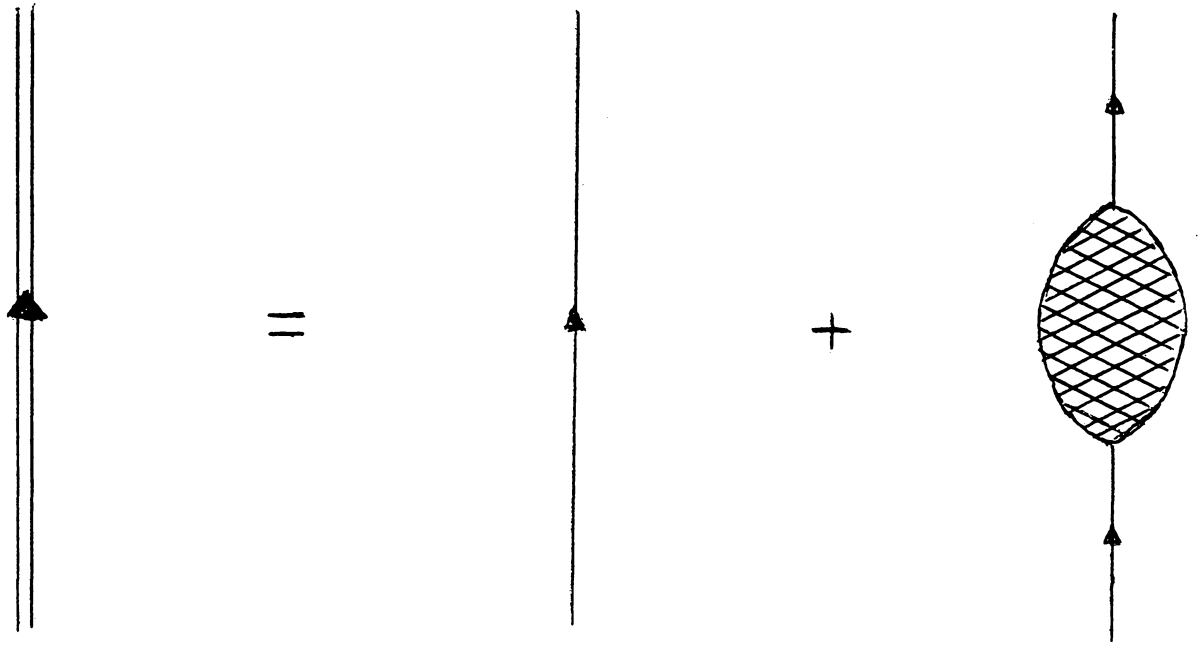


Figure 4. Self-energy expansion of the exact Green function for the interacting particle system.

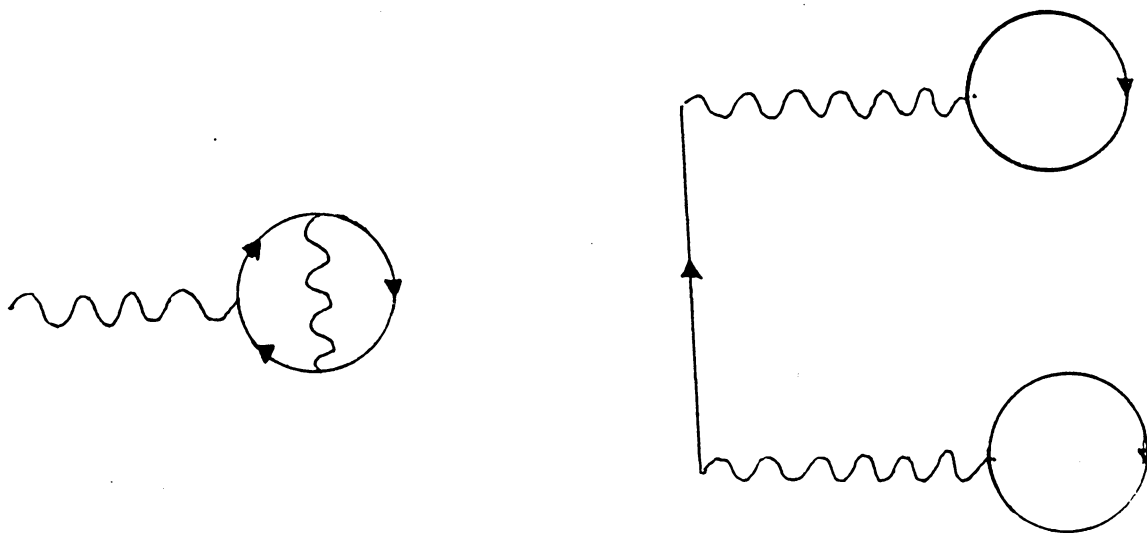


Figure 5. a) Typical proper self-energy insertion. b) Typical improper self-energy insertion.

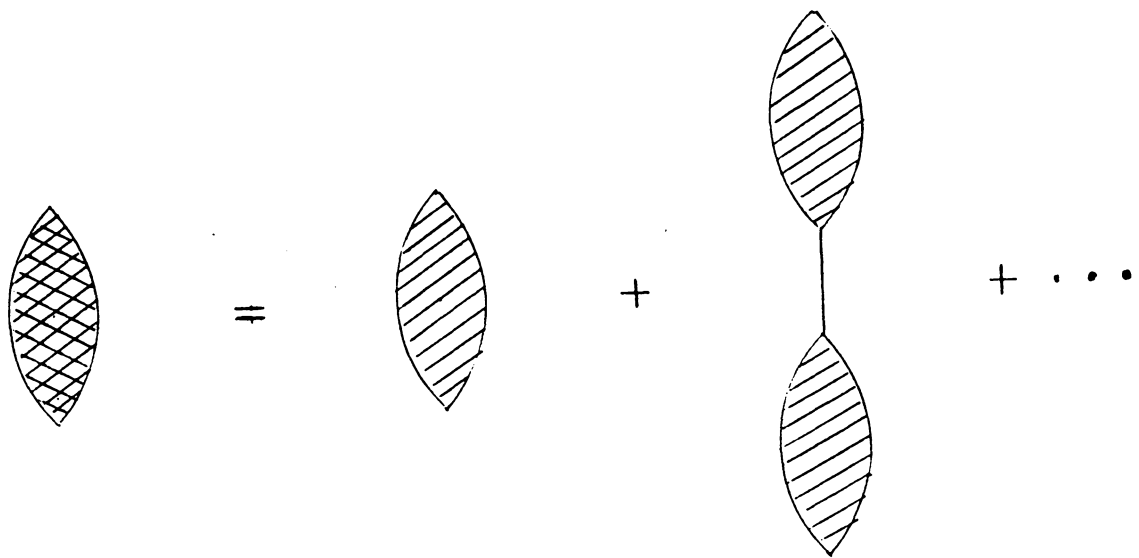


Figure 6. Proper self-energy expansion of the self-energy.

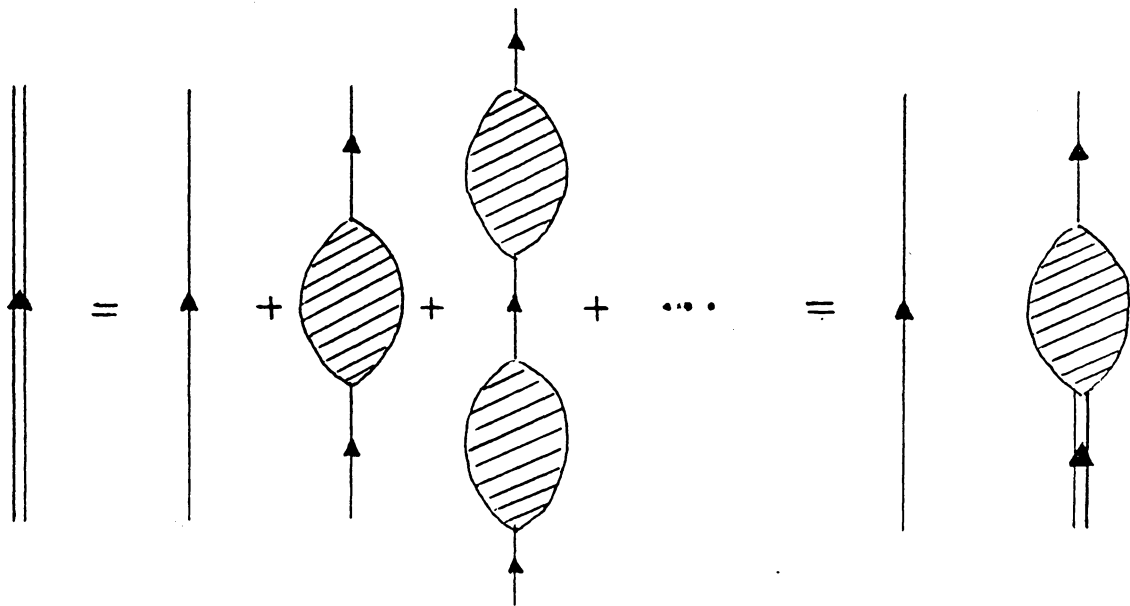


Figure 7. Proper self-energy expansion of the exact Green function of the interacting particle system.

where the spin indices have been repressed. The Feynman representation of equation 14 is given in figure 11.

Dyson's equation for the effective interparticle interaction again allows for the iterative summation of an infinite set of terms of a given class. In particular, if the only proper polarization part retained is the zero-order term, the polarization insertion becomes a sum of ring diagrams. This is the well-known random phase approximation (RPA) (4-7) and is shown in figure 12. The RPA will be discussed in more detail in the section on electron screening.

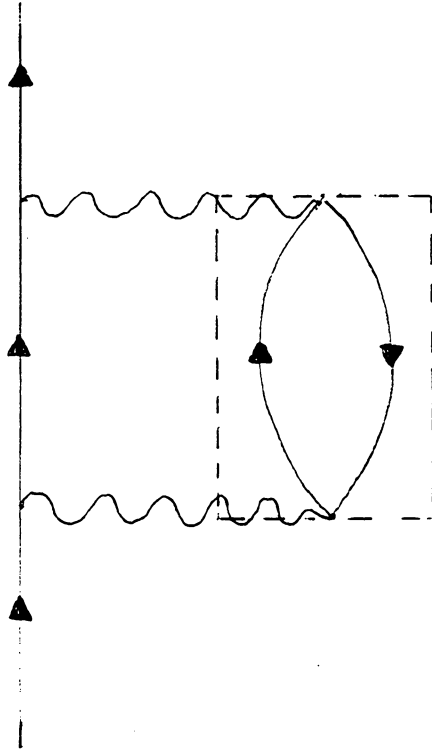


Figure 8. Typical polarization part

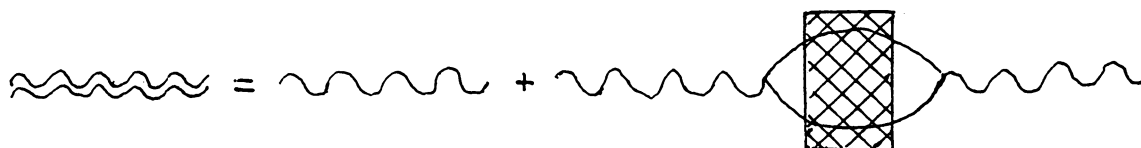


Figure 9. Effective interaction



a



b

Figure 10. a) Typical proper polarization part. b) Typical improper polarization part.

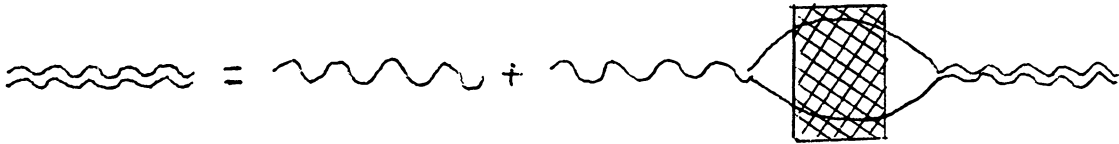


Figure 11. Dyson equation for the effective interaction

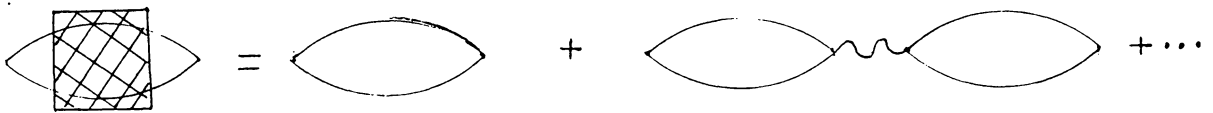


Figure 12. RPA polarization insertion

4.0 Previous Experimental and Theoretical Results on TPA

The simplest example of a class of organic semiconductors is *trans* – polyacetylene (TPA). A great deal of theoretical (15-21) interest in TPA has been generated because of its relative molecular simplicity and because of the large increase in conductivity exhibited upon chemical doping with electron donor or acceptor species (22). It has been suggested (15,16,23,24) that electrical conduction occurs in doped TPA through the formation of a highly mobile domain wall. This domain wall can be well described as a topological kink soliton-like excitation (15,16,25). Existence of the soliton-like state has been strongly supported both experimentally (26-28) and theoretically (15-20).

Pristine TPA is obtained by thermal treatment of a *cis* – polyacetylene/ *trans* – polyacetylene mixture, causing the *cis* – oriented molecules to isomerize to the energetically more favorable *trans*-configuration (22). Theoretical (29-31) and experimental (32-34) results show that TPA undergoes a Peierls distortion (35), in which pairs of atoms move toward each other. This yields a dimerized ground state and a gap between the valence and conduction bands. This distortion can occur in two directions, so that there are two isoenergetic configurations (or phases), possible for the ground state of TPA. The Peierls distortions leading to each configuration are illustrated in figure 13.

The Peierls dimerized ground state for TPA has received strong experimental support in studies by Fincher, et al. (32), Yannoni and Clarke (33) and Duijvestijn, et al. (34). Fincher and co-workers performed an X-ray scattering study of stretch oriented TPA films and found a symmetry-breaking dimerization distortion of $u_0 \cong 0.03\text{\AA}$. The parameter u_0 is the distance each carbon atom moves in one direction toward its neighbor in the Peierls distortion. Yannoni and Clarke and Duijvestijn and co-workers undertook NMR studies of TPA. In both studies it was determined that TPA was indeed dimerized. Yannoni and Clarke's nutation-NMR experiment yielded single and double bond lengths of 1.44Å and 1.36Å, while the double nuclear polarization-cross polarization experiment performed by Duijvestijn and co-workers yielded bond lengths of $1.45 \pm 0.01\text{\AA}$ and $1.38 \pm 0.01\text{\AA}$.

The existence of the dimerized ground state in infinite chain polyenes had been theoretically predicted (29,30) before a model system such as polyacetylene existed. More recently, Kirtman and co-workers (31) performed a minimal basis set *ab initio* study of polyacetylene. Their theoretical experiment confirmed that TPA existed in a dimerized ground state.

A domain wall defect will be present on a TPA chain if a structural transition from a region of one phase to a region of the opposite phase occurs. This defect can arise during the *cis/trans* isomerization process. This occurrence phenomenon is supported experimentally by the observance of random *cis* – linkages remnant in TPA samples (36). the domain wall defect can also arise after electron transfer to or from dopant species (22). This effect has been observed experimentally by Ikehata and co-workers (27), who measured the magnetic susceptibility of doped-TPA samples as a function of dopant concentration and found the charge carriers to be spinless, a feature consistent with the predicted electronic structure of the charged domain wall defects.

The domain wall defect is characterized by a geometric defect centered at the domain wall, since symmetry requires equivalent bonds adjacent to the boundary, and by an unpaired electron centered at the domain wall due to an interruption in the normal bonding pattern. In a charge-neutral chain,

the unpaired electron will occupy an orbital approximately mid-way (energetically), between the valence and conduction bands. In charged chains, this defect orbital will be empty (cation) or doubly-occupied (anion), so that the net spin in the charged systems will be zero. The neutral and charged defects are shown in a stylized manner in figure 14, where the arrows represent electrons. In real chains the defects extend over several carbon atoms.

The presence of paramagnetic sites in undoped TPA has been confirmed by electron and nuclear magnetic resonance experiments (37-41). Motionally narrowed EPR lines (37,38,40) and the observation of the Overhauser effect in NMR experiments (39,41) demonstrate the existence of delocalized paramagnetic sites, explained as rapidly diffusing domain wall defects (39,42). Localized paramagnetic sites have been observed in NMR experiments, as evidenced by the observation of the solid-state effect. The presence of localized sites, explained as domain wall defects trapped by oxygen impurities, is also required in order to reconcile EPR and NMR results for the defect diffusion rate (39).

Further experimental evidence for the existence of soliton-like domain wall defects in TPA has been produced in the work of Mele and Rice (26) and Suzuki and co-workers (28). Mele and Rice used group theory to predict the vibrational modes for a TPA chain containing a soliton-like defect and found the IR spectra of lightly doped-TPA samples fit their predictions quite well. Suzuki and co-workers performed an optical absorption study on lightly doped-TPA samples and observed peaks corresponding to the mid-gap to conduction band transition as well as the valence band to conduction band transition.

TPA films are generally doped by exposure of the films to vapor containing the dopant molecules or electrochemically in solutions containing the dopant molecules using TPA films as electrodes. The most commonly used acceptor dopants include halogens (Cl, Br and I) and arsenic pentafluoride (AsF_5) (43). Donor dopants which have been investigated include the sodium ion (Na^+) and ammonia (NH_3) (43).

The conductivity of pristine TPA is $4.4 \times 10^{-5} \Omega^{-1} \text{cm}^{-1}$ (43). The conductivity of TPA doped with the optimum amount of AsF_5 has been measured at $4.0 \times 10^2 \Omega^{-1} \text{cm}^{-1}$ (43), so that an increase in conductivity of seven orders of magnitude can be obtained by doping pure TPA. A conductivity range of eleven orders of magnitude has been achieved for TPA by doping with ammonia and subsequent compensation doping with arsenic pentafluoride (43).

Experiments (44) have shown that polaron defects develop upon light doping. As the dopant concentration increases, pairs of polarons decay into kink-antikink pairs.

A number of theoretical investigations (15-21) of soliton-like excitations in TPA have been conducted. The first such investigation was conducted by Su, Schrieffer and Heeger (SSH) (15,16), who employed a semi-empirical approach using a tight-binding (Huckel type), Hamiltonian. The SSH Hamiltonian included electron-phonon interactions for the pi-valence electrons and a quadratic bonding function for the sigma valence electrons. In the SSH study a wave function corresponding to the solitary wave solution from ϕ^4 theory (45,46) was assumed. A Green function technique was employed to find the wave function parameters which minimized the defect state formation energy. Kivelson and Heim (17) examined the effect of adding a constant on-site Coulomb term (U) to the SSH Hamiltonian in a UHF study where the linear polyene was modeled as a ring with periodic boundaries. Subbaswamy and Grabowski (18) added both on-site and nearest-neighbor off-site Coulomb terms (U and V, respectively) to the SSH Hamiltonian in a SCF UHF study of chains ranging from 61 to 101 carbon atoms. These investigators examined the magnitude of the on-site term and the nearest-neighbor to on-site term ratio to achieve the best agreement with experimentally measured dimerization distortion, band gap and negative to positive spin density ratio. Hirsch and Grabowski (19) performed a similar experiment using a Monte Carlo simulation technique on chains of 25 carbon atoms with periodic boundaries. Boudreaux, Chance, Bredas and Silbey (BCBS) (20) used the all valence electron MNDO method (45) to examine the ground state and various soliton-like defects on linear polyenes ranging in size from $C_{17}H_{19}$ to $C_{41}H_{43}$ and performed complete geometry optimizations on these systems.

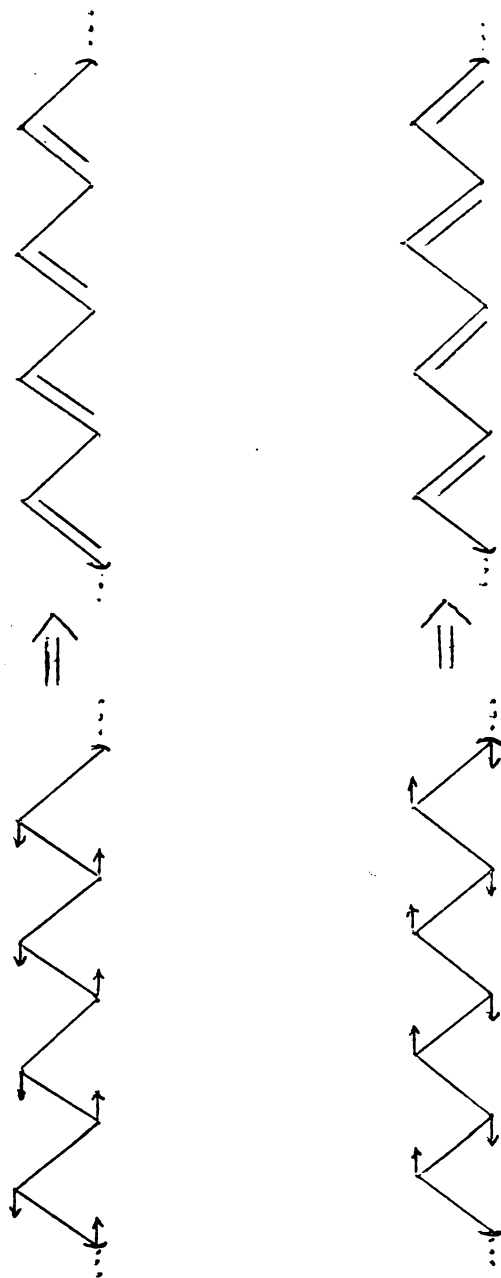


Figure 13. Peierls distortion

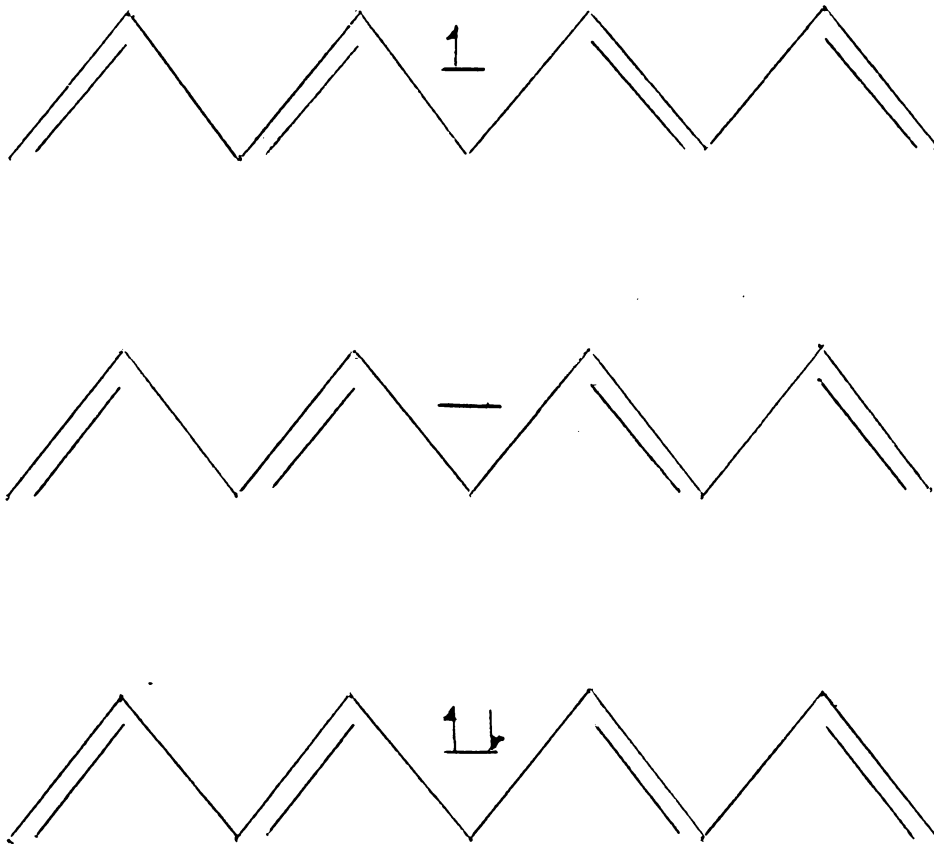


Figure 14. Neutral and charged domain wall defects. The arrows represent electrons.

5.0 Electron Screening and the RPA

It has long been known (48) that two-electron interactions in atoms and molecules are influenced by the presence of other electrons in the system. In pi-molecular orbital calculations, such as those performed within the PPP approximation, the two- electron interactions are modeled by suitable potential functions (49). Electron screening effects are implicitly included in these functions, as they are parametrized to give results which are consistent with experiment. However, most commonly used potential functions were parametrized in calculations on relatively small conjugated systems, and do not adequately account for the screening present in larger systems.

This shortcoming of common potential functions was exhibited quite clearly by Fukutome and Sasai (21), who examined the Mataga-Nishimoto (50) and Ohno (51) potentials in a semi-empirical UHF study of the ground state of TPA. Those authors found that the ratio between the on-site and off-site repulsion integrals was a major factor in determining if a dimerized ground state would arise. Particularly, the ratio of the nearest-neighbor and on-site repulsion integrals should be near 0.68 in order to realize the dimerized ground state. In order to obtain a potential with the required nearest-neighbor to on-site repulsion integral ratio, they screened the Ohno potential with a constant dielectric factor of 0.5 and screened the off-site terms with an exponential factor, $\exp\{-r_{mn}/2.683\text{\AA}\}$. Using this screened potential they found a difference between adjacent bond lengths of $0.140 \pm 0.02\text{\AA}$ in the ground state of TPA.

Subbaswamy and Grabowski and Hirsch and Grabowski found that a nearest-neighbor to on-site repulsion integral ratio of 0.5 gave the best agreement with experimentally measured values for dimerization, band gap and ratio of negative to positive spins.

Mazumdar and Campbell (52) studied the effects of long range Coulomb interactions in a one-dimensional half-filled band, with particular interest in the ground state of TPA. These authors found that, for downwardly convex potentials (53), the broken symmetry bond-order wave (BOW) state would be the ground state if

$$\sum_j V_{2j+1} < \frac{1}{2}U + \sum_j V_{2j} , \quad (15)$$

otherwise, a charge density wave (CDW) ground state would result. The inequality (15) is satisfied by the potentials employed in the TPA studies mentioned previously (18-20)

Several years prior to the work reported by Fukutome and Sasai, Gutfreund and Little (6,7) noted the necessity of accounting for electron screening effects in calculations involving large conjugated systems. These authors developed a general scheme for obtaining a screened, or effective, potential which was based on the random phase approximation (RPA). Their approach was similar to that commonly used to include screening effects in the electron gas model (12).

A simple model of the electrons in a metallic system is the electron gas. This model is further simplified by placing the electrons in a uniformly distributed positive field so that charge neutrality is ensured. For a spin and time independent bare electron interaction potential, the Dyson equation for the effective particle interaction in an electron gas is

$$V(r_i, r_j) = V^0(r_i, r_j) + \sum_k \sum_l V^0(r_i, r_k) \Pi^*(r_k, r_l) V(r_l, r_j) \quad (16)$$

where $V^0(r_i, r_j)$ is the bare interaction between electrons on sites i and j , $V(r_i, r_j)$ is the effective interaction between electrons on sites i and j and $\Pi^*(r_k, r_l)$ is the proper polarization insertion. The

proper polarization parts, which are summed to yield the proper polarization insertion, are shown through first order in figure 15.

The RPA is made by retaining only the zero-order proper polarization part, so that the RPA effective interaction is

$$V(r_i, r_j) = V^o(r_i, r_j) + \sum_k \sum_l V^o(r_i, r_k) \Pi^o(r_k, r_l) V(r_l, r_j) \quad (17)$$

where $\Pi^o(r_k, r_l)$ is the zero-order proper polarization at site k due to site l. The RPA effective interaction is shown in figure 16.

If the electron interactions are assumed to be frequency independent, the zero-order proper polarization is given by (6,12)

$$\Pi^o(r_k, r_l) = 2i \int_0^\infty \left(\frac{d\omega}{2\pi} \right) G^o(r_k, r_l, \omega) G^o(r_l, r_k, \omega) \quad (18)$$

where $G^o(r_k, r_l, \omega)$ is the Fourier transformed bare single particle Green function and has the form (12)

$$G^o(r_k, r_l, \omega) = \sum_i \frac{\varphi_i(r_k) \varphi_i(r_l)}{\omega - \varepsilon_i \hbar^{-1} + i\eta} + \sum_\alpha \frac{\varphi_\alpha(r_k) \varphi_\alpha(r_l)}{\omega - \varepsilon_\alpha \hbar^{-1} - i\eta} \quad (19)$$

for occupied molecular orbitals, $\varphi_\alpha(r_k)$, with orbital energies, ε_α and unoccupied molecular orbitals, $\varphi_i(r_l)$, with orbital energies ε_i , where the molecular orbitals and molecular energies are the eigenvectors and eigenvalues obtained through diagonalization of a Huckel-type Hamiltonian. In 19,

$$\lim_{\eta \rightarrow 0^+} e^{i\omega\eta} \equiv \lim_{t' \rightarrow t^+} e^{i\omega(t'-t)}$$

and the limit $\eta \rightarrow 0^+$ is implicit and is required to ensure convergence of the time integration.

Evaluating the integral in equation 18 by performing a contour integration, expressing the molecular orbitals as linear combinations of atomic orbitals (LCAO approximation) and assuming no explicit geometry dependence for the LCAO expansion coefficients, the following form is obtained

$$\Pi_{kl}^{\circ} \equiv \Pi^{\circ}(r_{k,r,l}) = -2 \sum_i \sum_{\alpha} \sum_{\lambda} \frac{c_{ki}^{\lambda} c_{li}^{\lambda} c_{k\alpha}^{\lambda} c_{l\alpha}^{\lambda}}{\epsilon_i^{\lambda} - \epsilon_{\alpha}^{\lambda}} \quad (20)$$

where $\{c_{k\alpha}^{\lambda}\}$ and $\{c_{ki}^{\lambda}\}$ are sets of expansion coefficients in the LCAO approximation and the sum over λ accounts for different electron spins. For closed shell systems this reduces to the atom-atom polarizability expression obtained by Coulson and Longuet-Higgins (54).

If the electron-electron interaction is assumed to be spin independent, equation 17 can be solved to give an expression for the effective interaction in terms of the bare interaction and the zero-order proper polarization (12). The PPP approximation allows the use of a matrix notation for expressing the two electron interaction. Using this notation and solving equation 17, the following expression for the effective interaction is obtained (6,12)

$$\mathbf{V} = \mathbf{V}^{\circ}(\mathbf{I} - \mathbf{\Pi} \mathbf{V}^{\circ})^{-1} \quad (21)$$

where \mathbf{I} is the identity matrix, V_{ij}° is the bare interaction between electrons on sites i and j , V_{ij} is the effective interaction between electrons on sites i and j , Π_{ij} is the polarization at site i due to site j and all matrices are $N \times N$ for N atomic sites.

In Gutfreund and Little's calculational scheme the polarization matrix is calculated using the orbital coefficients and energies obtained from an initial Huckel treatment of the system. Then this polarization matrix is used in equation 21 to find an effective interaction matrix which is used in the SCF procedure. In our calculations, use of the Huckel orbital coefficients and orbital energies in calculating the polarization matrix yielded results for the ground state of TPA which were not consistent with experimental results. The major inconsistency of the results was the lack of dimerization, with a difference between adjacent bonds in the center of the system of 0.008Å. The

nearest-neighbor to on-site repulsion integral ratio has an average value of 0.45, so a dimerized ground state would not be expected, according to Fukutome and Sasai's criteria.

This problem can be rectified by using the orbital coefficients and orbital energies obtained from the SCF procedure to calculate the polarization matrix. This approach was also employed by Terasaka and co-workers (55) in the calculation of excitation energies in cyclic and linear polyenes. The SCF-RPA scheme requires that the effective interaction be calculated iteratively within the SCF procedure and is thus more time consuming, however this does solve the problems of short range overscreening and long range antiscreening and is necessary in order to achieve agreement with experiment. The average value for the repulsion integral ratio for the potential obtained from this scheme was 0.69, which is sufficiently close to the critical value of 0.68 reported by Fukutome and Sasai.

Examination of this potential in terms of Mazumdar and Campbell's inequality, (equation 15), shows that the BOW ground state should be expected, as the potential is downward convex and the inequality is met. Interestingly, the inequality in 15 holds only for interactions at sites away from the ends of the molecule. However, this should be expected since the Mazumdar-Campbell relationship was developed for an infinite system modeled by a finite system with periodic boundaries.

Use of the SCF orbital coefficients and orbital energies is equivalent to the inclusion of higher order polarization terms. This can be shown clearly using diagrams. In equation 17, the bare Green function is replaced by the SCF-Hartree-Fock approximation to the exact Green function. The HF approximation to the exact Green function is shown diagrammatically in figure 17. Iterations within the SCF procedure yield the SCF-HF approximation to the exact Green function which is represented by the diagram in figure 18. Replacement of the bare Green function lines in figure 16 yields the diagram in figure 19, where the heavy bubble can be expanded as shown in figure 20. These diagrams can be identified as higher order polarization terms.

Figure 21 shows the effective interaction at site 1 (V_{1j}), for a system containing 40 carbon atoms. The asterisks represent the values obtained when the bare Green function was used to calculate the polarization matrix and the circles represent the values obtained by using the SCF-HF approximation to the exact Green function to calculate the polarization matrix. The bond alternation patterns resulting from both approaches are plotted in figure 22.

A comparison of the bare Ohno potential, the Ohno potential screened as suggested by Fukutome and Sasai, and the Ohno potential screened by our modification of Gutfreund and Little's technique is made in figure 23. The calculated differences in adjacent bonds in the ground state of TPA (ΔR_∞), which result when these potentials are used are 0.021Å, 0.140Å and 0.087Å respectively.

Cooper and Linderberg (56) developed a technique for the inclusion of screening effects in which polarization terms containing exchange interactions were included. According to their scheme, the effective interaction is calculated iteratively using the following equations

$$V_{rs} = V_{rs}^{\circ} + \sum_t \sum_u V_{rt} (\sum_p \sum_q \Pi_{u,pq}^{\circ} \Gamma_{pq,t}) V_{us}^{\circ} \quad (22a)$$

$$\Gamma_{pq,t} = \delta_{pt} \delta_{qt} - \left(\frac{1}{2}\right) V_{pq} \sum_u \sum_v \Pi_{pq,uv}^{\circ} \Gamma_{uv,t} \quad (22b)$$

Here, V_{rs} is the effective interaction between electrons at sites r and s , V_{rs}° is the bare interaction between electrons at sites r and s , $\Pi_{u,pq}^{\circ}$ and $\Pi_{pq,uv}^{\circ}$ are the zero-order mutual atom-bond and bond-bond polarizabilities respectively and $\Gamma_{pq,t}$ represents the so called "vertex parts" which are terms that when multiplied with the zero-order proper polarization term yield a series of higher order polarization terms.

Equation 22a can be expressed as the diagram shown in figure 24. The shaded area in the bubble represents the vertex part, which is shown diagrammatically in figure 25.

Cooper and Linderberg reported excitation energies and screened repulsion integral values for butadiene and azulene. When an attempt was made to repeat their calculations, it was found that, in order to match their results, the orbital coefficients and orbital energies from the SCF procedure had to be used to calculate the polarizabilities in equations 22a and 22b and that only one iteration per SCF cycle of equation 22b could be made so that

$$\Gamma_{pq,t} \equiv \delta_{pt}\delta_{qt} . \quad (23)$$

The screened potential calculated in this manner is exactly that calculated according to the SCF-RPA scheme. This can be seen by replacing the vertex part in equation 22a with the first approximation to the vertex part given in equation 23. This yields equation 24,

$$V_{rs} = V_{rs}^{\circ} + \sum_t \sum_u V_{rt} \Pi_{u,t}^{\circ} V_{us}^{\circ} , \quad (24)$$

which is equivalent to equation 17. It should be noted that when equations 22a and 22b were used iteratively until the screened potential had converged, the values for all on-site and off-site interactions were essentially the same. This was true when either the bare Green function or the SCF-HF approximation to the exact Green function was used.

The inclusion of polarization terms containing exchange interactions is important in the calculation of excitation energies, particularly the energies of triplet excitations. However, we found that including the diagonal part of the lowest order polarization term containing an exchange interaction (represented by the fourth diagram in figure 15) had little effect on the electronic or topological structure of the singlet and doublet ground states studied. Gutfreund and Little point out (6) that the diagonal part of this term gives the major contribution to the polarization, thus it can be concluded that it is not essential that this or higher order polarization terms with exchange interactions be included in these calculations.

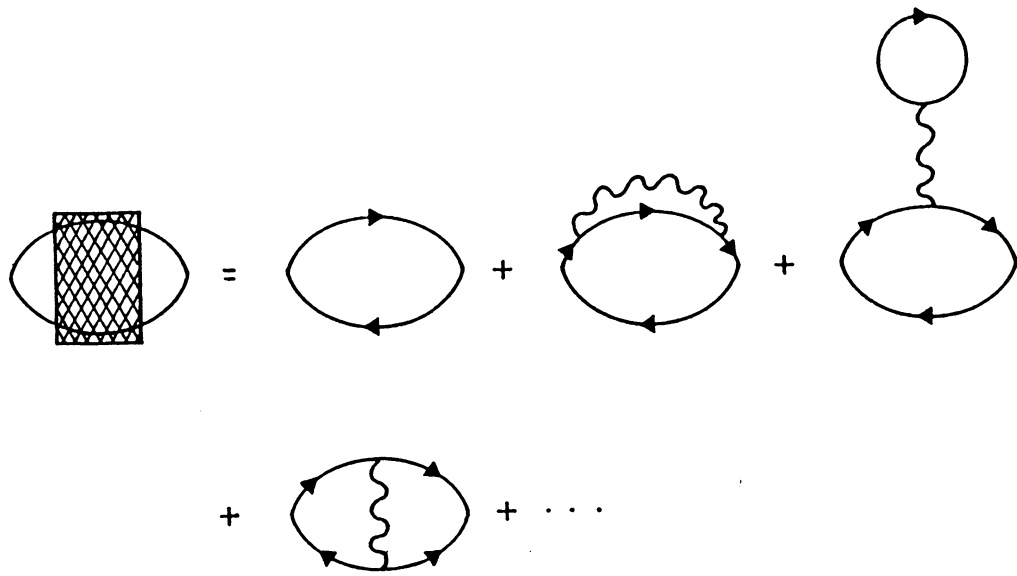


Figure 15. Proper polarization parts.

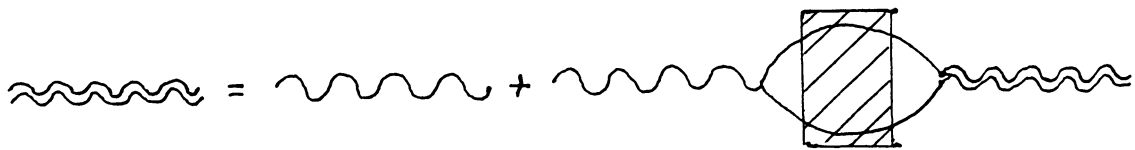


Figure 16. RPA effective interaction.

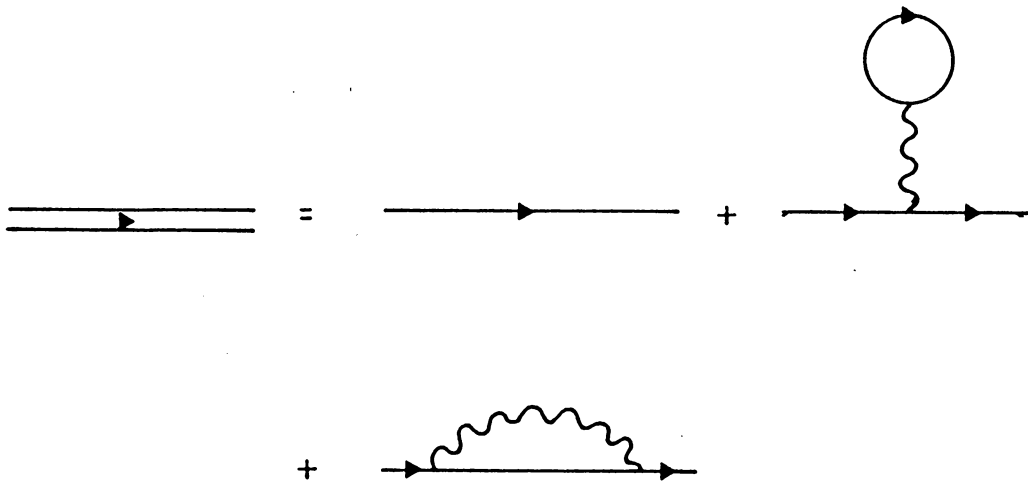


Figure 17. Hartree-Fock approximation to the exact interacting particle system Green function

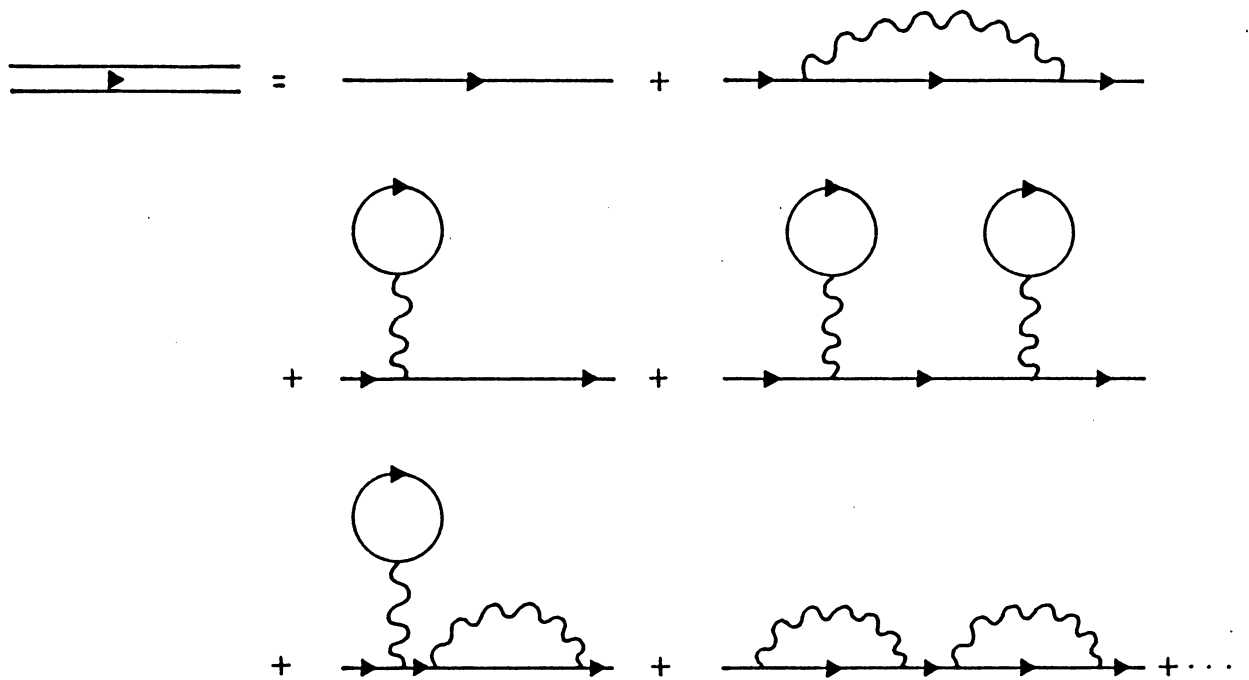


Figure 18. SCF-Hartree-Fock approximation to the exact interacting particle system Green function

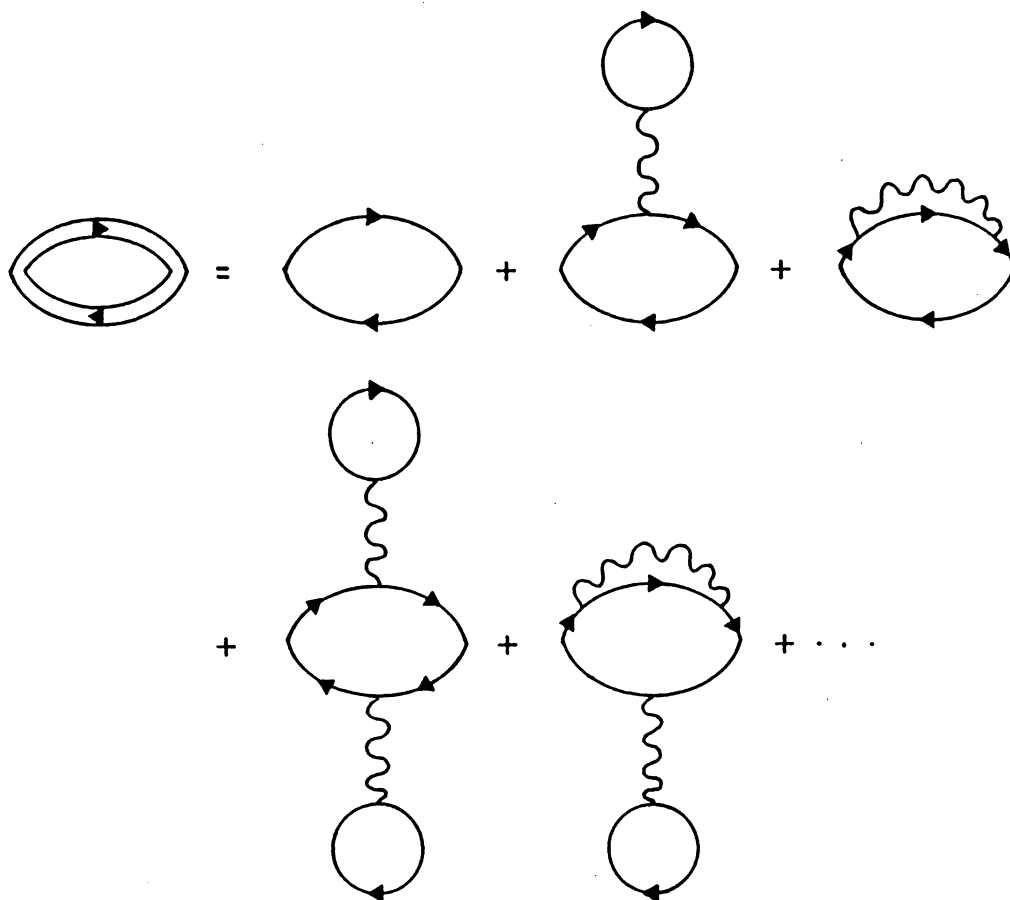


Figure 19. RPA effective interaction with the bare Green function replaced by the SCF-Hartree-Fock approximation to the exact interacting particle system Green function

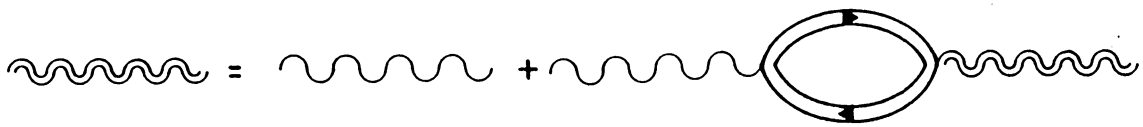


Figure 20. RPA polarization insertion with the bare Green function replaced by the SCF-Hartree-Fock approximation to the exact interacting particle system Green function

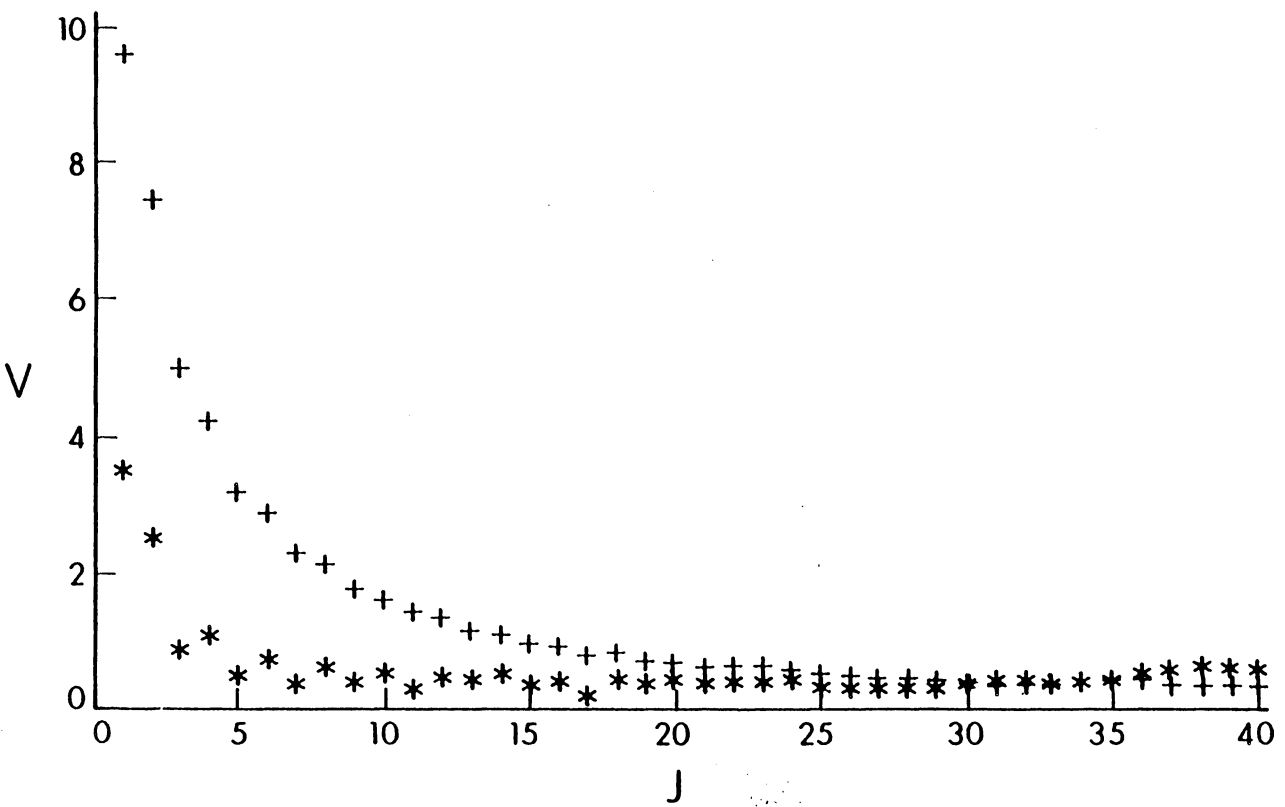


Figure 21. Effective interaction at site 1 for a 40 carbon chain. Asterisks are for RPA and plusses for SCF-RPA.

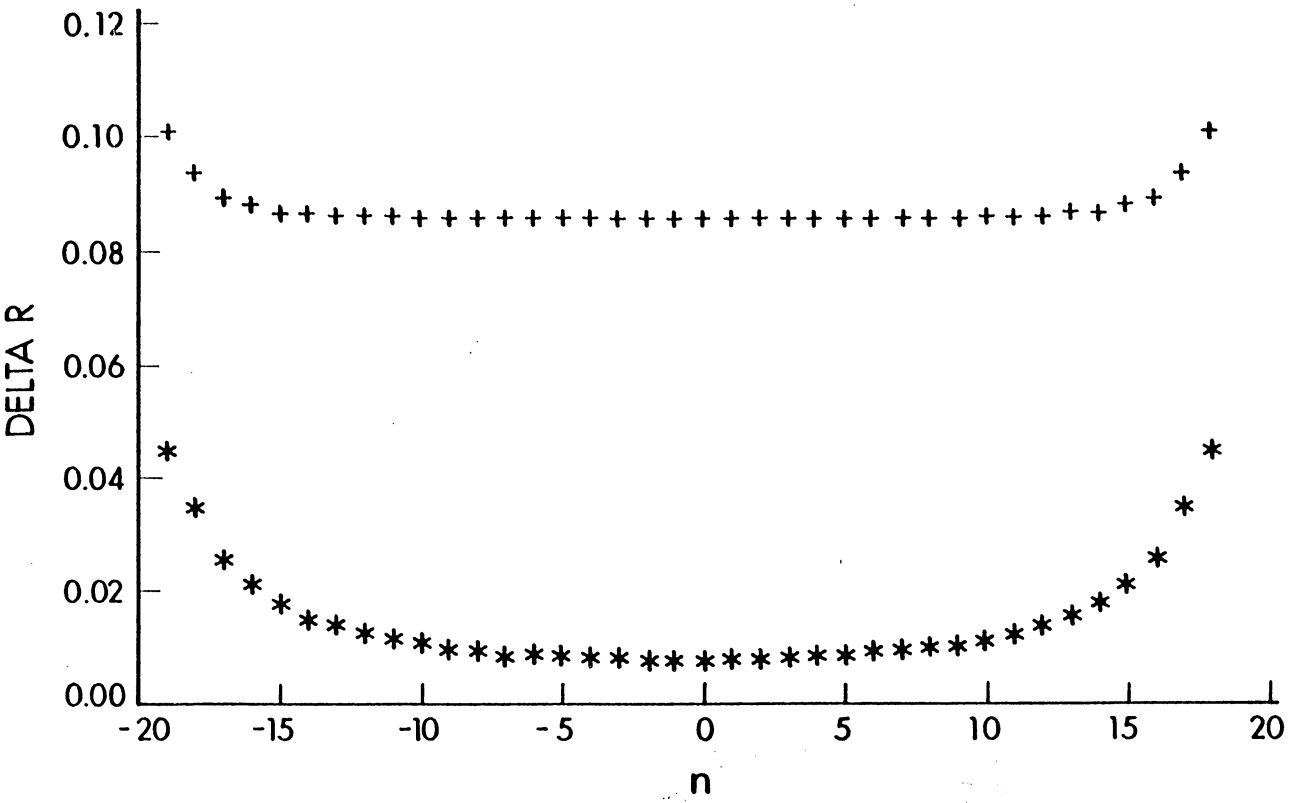


Figure 22. bond alternation pattern for a 40 carbon chain. Asterisks are result with RPA screening and pluses are result with SCF-RPA screening.

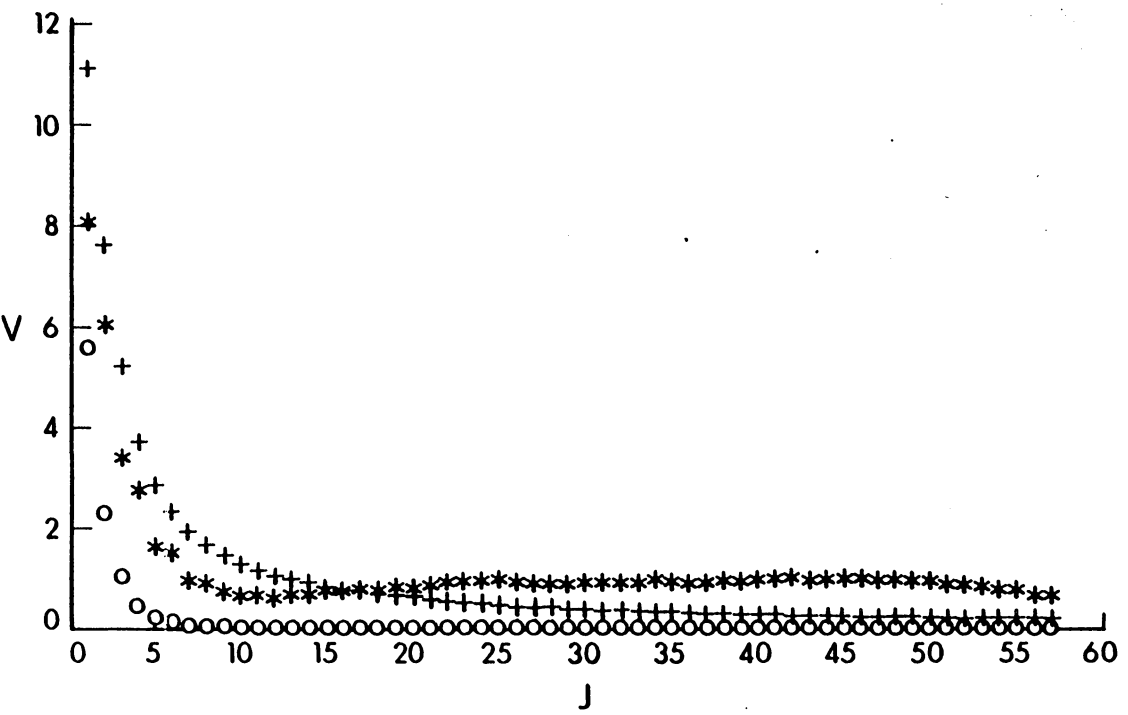


Figure 23. Interaction potential at site 1 where: pluses-bare Ohno Asterisks-SCF-RPA screened Ohno and circles-Fukutome-Sasai screened Ohno.



Figure 24. Cooper and Linderberg effective interaction.

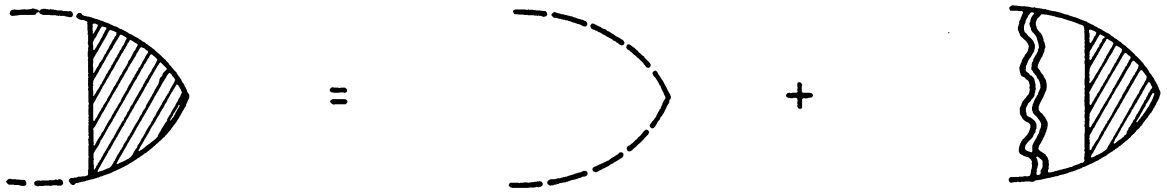


Figure 25. Vertex part

6.0 Computational Details

In the initial stages of the study of soliton-like excitations in TPA, the quantum chemical force field (QCFF) method of Warshel and Karplus (57) was used. Use of this approach proved unsuccessful in modeling the kink soliton-like state because of the electron interaction potential employed. However, results of these calculations showed the TPA ground state to be essentially planar and that the C-C-C bond angles were close to 120°. Further, values of 122° and 123° have been found experimentally (34) for the C-C-C bond angles in TPA. Results of the QCFF studies of polyenes with and without attached hydrogen atoms showed that the presence of the hydrogen atoms had no significant effect on the pi-electronic structure or carbon-backbone geometry. As a result of these findings, the systems studied by the PPP-UHF-RPA method consisted only of planar carbon skeletons, with bond angles fixed at 120°.

The pi orbitals in the conjugated system were handled using the PPP Hamiltonian within the UHF approximation. The resonance (transfer) integrals, $\beta(r_{ij})$, were chosen to have the standard exponential distance dependence (47)

$$\beta(r_{ij}) = \beta^0 \exp\{\delta(r^0 - r_{ij})\} \quad (25)$$

where the constants β° , δ and r° have the values suggested by Schulten, Ohmine and Karplus (58) of $-2.0419eV$, 1.2518\AA^{-1} and 1.536\AA respectively. The repulsion integrals, $V^0(r_i, r_j)$, were given by the bare Ohno interaction potential, screened as described earlier. The distance dependence of the bare interaction is given by

$$V^0(r_i, r_j) = \gamma^\circ [1 + (\frac{r_{ij}}{a^\circ})^2]^{-1/2}. \quad (26)$$

The values $\gamma^\circ = 11.13eV$ and $a^\circ = 1.2935\text{\AA}$ were used.

The energy contribution of the sigma valence electrons was calculated by using a Morse bonding potential (57)

$$E_\sigma = \sum_{i=1}^n E_{\sigma,i} = \sum_{i=1}^n D [\exp\{-2\alpha(q_i - r^\circ)\} - 2 \exp\{-\alpha(q_i - r^\circ)\}] \quad (27)$$

where $D = 87.95 \text{ kcal mol}^{-1}$, $\alpha = 1.7562 \text{\AA}^{-1}$, $r^\circ = 1.5265\text{\AA}$, n is the number of sigma bonds and $q_i \equiv r_{i,i+1}$.

Optimization of the energy as a function of bond lengths was carried out using the method of steepest descents. According to the method of steepest descents, the shift of the functional parameters is chosen so that the value of the function approaches an optimum value along the path of steepest descent. The analytical expression for the bond shifts in this work was

$$r_i^{new} = r_i^{old} - S \left(\frac{dE^{TOTAL}}{dr_i} \right) \quad (28)$$

where the step size, S , is

$$S = a \left(\frac{1}{n} \sum_i \frac{dE^{TOTAL}}{dr_i} \right) \quad (29)$$

for n bonds. In equation 29, a is 0.75 times its value in the previous iteration if the energy was lowered by the previous bond shift and 1.2 times its previous value if the energy went up in the

preceding iteration. The initial value of α is 0.002. S has the dimensions of length² over energy and a has the dimensions of length³ over energy².

The first derivatives of all energy functions with respect to bond length were found analytically. The derivative of the energy contribution of the i^{th} sigma bond with respect to bond i (where bond i is the bond between sites i and $i + 1$) was calculated according to

$$\frac{dE_{\sigma,i}}{dq_i} = -2D\alpha[\exp\{-2\alpha(q_i - r^\circ)\} - \exp\{-\alpha(q_i - r^\circ)\}]. \quad (30)$$

The energy derivatives of the pi functions were calculated assuming no explicit distance dependence in the molecular orbitals. Thus, the first derivative of the one-electron contribution to the pi energy, E_π^1 , with respect to bond i was approximated as

$$\frac{\partial E_\pi^1}{\partial q_i} = -2\delta\beta^\circ \exp\{\delta(r^\circ - q_i)\} P_{i,i+1} \quad (31)$$

where \mathbf{P} is the total density matrix. The first derivative of the two-electron contribution to the pi energy, E_π^2 with respect to bond i was approximated by

$$\frac{\partial E_\pi^2}{\partial q_i} = \sum_k \sum_{l=k} \mathbf{V}'_{kl} \mathbf{A}_{kl} \quad (32)$$

where the kl^{th} element of \mathbf{V}' is

$$\mathbf{V}'_{kl} = [(\mathbf{I} + \mathbf{V}^\circ \mathbf{\Pi})(\mathbf{V}^{\circ\prime})(\mathbf{I} - \mathbf{V}^\circ \mathbf{\Pi})^{-1}]_{kl}. \quad (33)$$

Here, the kl^{th} element of $\mathbf{V}^{\circ\prime}$ is

$$\mathbf{V}^{\circ\prime}_{kl} = -\gamma^\circ \left(\frac{r_{kl}}{a^\circ}\right) \left[1 + \left(\frac{r_{kl}}{a^\circ}\right)^2\right]^{-3/2} \frac{dr_{kl}}{dq_i}. \quad (34)$$

In (32), the matrix \mathbf{A} is a sum of density matrix products so that the kl^{th} element is given by

$$A_{kl} = -\frac{1}{2}[\mathbf{P}_{kk}^{\alpha}\mathbf{P}_{ll}^{\alpha} - (\mathbf{P}_{kl}^{\alpha})^2 + \mathbf{P}_{kk}^{\beta}\mathbf{P}_{ll}^{\beta} - (\mathbf{P}_{kl}^{\beta})^2 + \mathbf{P}_{kk}^{\alpha}\mathbf{P}_{ll}^{\beta} + \mathbf{P}_{ll}^{\alpha}\mathbf{P}_{kk}^{\beta} - (\mathbf{P}_{kk}^{\alpha} + \mathbf{P}_{ll}^{\alpha} + \mathbf{P}_{kk}^{\beta} + \mathbf{P}_{ll}^{\beta} - Z_k Z_l)] \quad (35)$$

where \mathbf{P}^{α} and \mathbf{P}^{β} are the alpha and beta density matrices and Z_k is the charge on atom k. Equation 33 can be derived directly from equation 21 and equation 32 is obtained by examination of the standard PPP-UHF pi energy expression.

It is well known that the UHF theory yields orbitals which are not pure spin eigenfunctions (59). To remedy this, Harriman spin projection (60) was used and all spin densities reported here are those of the pure doublet spin states.

7.0 Solutions To The Solitary Wave Equation

The work of Goldstone and Jackiw (46) in the quantization of non-linear waves yields the ϕ^4 -field theory which is derived for a one-dimensional kink such as that observed in TPA. Further, the continuum model of TPA can be shown to be in direct correspondence with the model developed by Goldstone and Jackiw which leads to the ϕ^4 -field theory wave equation.

One solution to the ϕ^4 -field theory solitary wave equation (45,46)

$$\phi_{xx} - \phi_{tt} = \pm (\phi - \phi^3) \quad (36)$$

is the kink soliton. The wave function for a TPA chain containing the kink soliton-like domain wall defect should consequently have the form (25)

$$\psi(n) = N_0 \text{sech}(n/l') \quad (37)$$

where $N_0 = (1/2) l'^{-1/2}$, n is the carbon number away from the defect center and l' is approximately half of the defect extent in terms of carbon-carbon bond units. From equation 37, the spin distribution for this defect state is found to be proportional to $\text{sech}^2(n/l')$.

The bond length alternation pattern for a TPA chain segment containing a domain wall defect has the form (15,25)

$$\Delta R_n = \Delta R_\infty \tanh(n/l) \quad (38)$$

where $\Delta R_n = (-1)^n(r_{n+1} - r_n)$. Here, ΔR_∞ is the difference between the lengths of adjacent bonds in regions of normal bond alternation and l is approximately half of the geometric defect extent in terms of C-C bond units.

Another solution to the ϕ^4 -field theory solitary wave equation which is useful in the description of TPA defect states is the 2-soliton solution. This solution models the polaron defect in TPA, which is described as a local deviation from one of possible dimerized ground states. The bond alternation pattern of the soliton-like polaron state has the form (20,25)

$$\Delta R_n = \Delta R_\infty [1 - \alpha \operatorname{sech}^2(n/l)] \quad (39)$$

where α is a measure of the defect amplitude and l is approximately the half width, in C-C bond units, of the topological defect.

8.0 PPP-UHF-RPA Results for TPA

8.1 TPA Ground State

As described previously, TPA can exist in one of two isoenergetic dimerized configurations in the ground state. In this study, the ground state was modeled by even membered carbon chains of 26, 40, 60 and 74 atoms. The proper C_{2n} molecular symmetry was ensured during the SCF and spin projection procedures by symmetrizing the appropriate orbitals during diagonalization.

These calculations yielded a single bond length of 1.456Å and a double bond length of 1.369Å, so that $\Delta R_\infty = 0.087\text{Å}$. This value is in good agreement with the experimental (34) value of $0.07 \pm 0.01\text{Å}$. Suhai (61) applied second-order Moller-Plesset perturbation theory in an *ab initio* study on the ground state of TPA and found $\Delta R_\infty = 0.085\text{Å}$, so that the result of the present study is in good agreement with the current best theoretical result as well.

The MNDO treatment of BCBS yielded a value of $\Delta R_\infty = 0.106\text{Å}$, while SSH found a value of $\Delta R_\infty = 0.146\text{Å}$.

It should be noted that the results of the studies on the effects of adding Coulomb repulsion terms to the SSH Hamiltonian performed by Kivelson and Heim (17), Subbaswamy and Grabowski (18) and Hirsch and Grabowski (19) should be modified in light of the smaller dimerization distortion found experimentally.

8.2 *Neutral Solitons*

A neutral soliton defect on a TPA chain was modeled by inserting a carbon radical into a $4N$ even membered carbon chain, creating an odd membered chain of $4N + 1$ carbon atoms. Calculations on systems ranging from 33 to 73 carbon atoms yielded values of $l = 14$ for the geometric defect and $l' = 8$ for the electronic defect. A projected spin density ratio of -0.25 ± 0.01 was found, in good agreement with the value -0.33 ± 0.02 reported by Thomann and coworkers (38,62).

Figures 26 and 27 illustrate the bond alternation pattern and spin density distribution for a 57 carbon atom chain containing a neutral soliton defect. In figure 27 the asterisks represent the spin densities calculated from the spin-projected pure-doublet wave function and the pluses represent the spin densities calculated from the unprojected wave function. This comparison clearly shows the necessity of obtaining wave functions which are pure spin eigenfunctions in UHF studies.

In their theoretical investigation SSH found the values $l = l' = 7$ for TPA containing a neutral soliton defect. Kivelson and Heim, Subbaswamy and Grabowski and Hirsch and Grabowski found defects which were roughly of the same extent as those reported by SSH and BCBS reported values of $l = 3$ and $l' = 5$ for the geometric and electronic defects. It is interesting to note that the extent of the neutral geometric defect in TPA we find is much broader than that reported elsewhere, which is consistent with the smaller dimerization found for the ground state. The electronic defect, as

evidenced by the spin density distribution, is only slightly broader than that previously reported. Further, there is a qualitative difference in the relative extents of the geometric and electronic defects. SSH, Kivelson and Heim, Subbaswamy and Grabowski and Hirsch and Grabowski found both defects to be of the same extent, BCBS found the electronic defect to be broader than the geometric defect, while we found the geometric defect to be broader than the electronic defect. It is clear that the difference lies in the way in which the two-electron interactions were handled in each study.

8.3 Charged Solitons

The large change in the conductivity of TPA samples upon doping (22) prompts interest in systems containing charged soliton-like domain wall defects. As pointed out by BCBS, the approach employed by SSH does not allow a distinction to be made between neutral and charged solitons. This is due to the fact that in their treatment the soliton level is at the Fermi energy and is therefore a non-interacting state. Thus, changing the occupation of this level to create charged solitons would not cause the change in energy and distribution of electron density which are necessary to have a change in geometry and spin distribution. The addition of two-electron terms shifts the soliton energy level from mid-gap, allowing a distinction to be made between charged and neutral soliton defects.

Systems containing charged soliton defects were modeled by removing an electron from the highest occupied molecular orbital to create a cationic soliton or adding an electron to the lowest unoccupied molecular orbital to create an anionic soliton.

The bond alternation patterns for cationic and anionic soliton defects on 57 carbon atom chains are shown in figures 28 and 29. The carbon chain containing the positively charged defect has a

bond alternation pattern which fits $\tanh(n/13)$ with $l = 13$. The geometric defect on the chain containing the negative defect is more compact, with $l = 10$. These results are in qualitative agreement with those reported by BCBS who found $l = 5$ and $l < 3$ for chains containing positive and negative defects respectively.

Both charged systems exhibit damped charge density waves (DCDW), with positive to negative oscillations of charge density from site to site. The distribution of charge density for the charged defect states are shown in figures 30 (cation) and 31 (anion). The charge densities fit a curve which is proportional to $\text{sech}^2(n/l')$. In this study the DCDW for the system containing the positive defect fit the hyperbolic secant curve with $l' = 15$ and the DCDW for the system containing the negative defect fit with $l' = 10$. Thus, the DCDW is slightly more diffuse than the geometric defect on the chain containing the cationic soliton, while the DCDW is of the same dimension as the geometric defect on the chain containing the anionic soliton. This result is greatly different from that reported by BCBS who found DCDW's which were much more diffuse than the topological defects in both charged systems, with an identical value of $l' = 8$ for chains containing either a cationic or anionic defect.

8.4 Polarons

The polaron defect will arise if an electron is gained or lost from a perfectly dimerized chain, and is thought to account for conduction in doped TPA and other organic semiconductors (22,63). Chains containing positively and negatively charged polarons were modeled as 40 membered polyene radicals with C_{2h} symmetry.

The bond alternation pattern for 40 membered chains containing positive and negative polaron defects are represented in figures 32 and 33, respectively. The solid lines represent

$\Delta R_{\infty}[1 - \alpha \text{sech}^2(n/l)]$ with $l = 14$ and $\alpha = 0.96$ for the positive polaron and $l = 10$ and $\alpha = 1.42$ for the negative polaron. Values of $l = 9$ and $\alpha = 0.51$ (positive polaron) and $l = 7$ and $\alpha = 0.69$ (negative polaron) were reported by BCBS.

The distribution of charge density (lattice polarization) in a system containing a positive polaron defect is shown in figure 34. Figure 35 shows the lattice polarization for a 40 carbon chain containing a negative polaron defect. The features of both curves are in qualitative agreement with those reported by BCBS, however both curves are more diffuse than the BCBS curves. This is reasonable in light of the difference in the extent of lattice distortion reported here as compared to that reported by BCBS. and is consistent with the results obtained for other defect states.

8.5 *Conclusions from the PPP-UHF-RPA Study of TPA*

The results found in this study present defects which are much more diffuse than those previously reported. However, the qualitative characteristics of the defect states are in agreement with experiment and with those predicted in other theoretical studies. While it is currently impossible to measure the extent of the geometric defect experimentally and the exact extent of the electronic defect is unclear due to the possibility of soliton diffusion (39,42), such quantities as the measured ground state dimerization and ratio of negative to positive spin density can be used as a way of comparing the results of theoretical studies. It can be seen that the results of this study are in better agreement with the experimentally measured degree of ground state dimerization and ratio of negative to positive spin density on chains containing domain wall defects than results reported in the other studies mentioned.

While the model employed by SSH, and modified by others (17-19) was useful in characterizing the neutral soliton defect in TPA and the MNDO treatment of BCBS yielded results on this and

other defect states of interest in TPA, the use of UHF theory and the explicit consideration of electron screening effects are necessary steps in the better understanding of soliton defects in TPA.

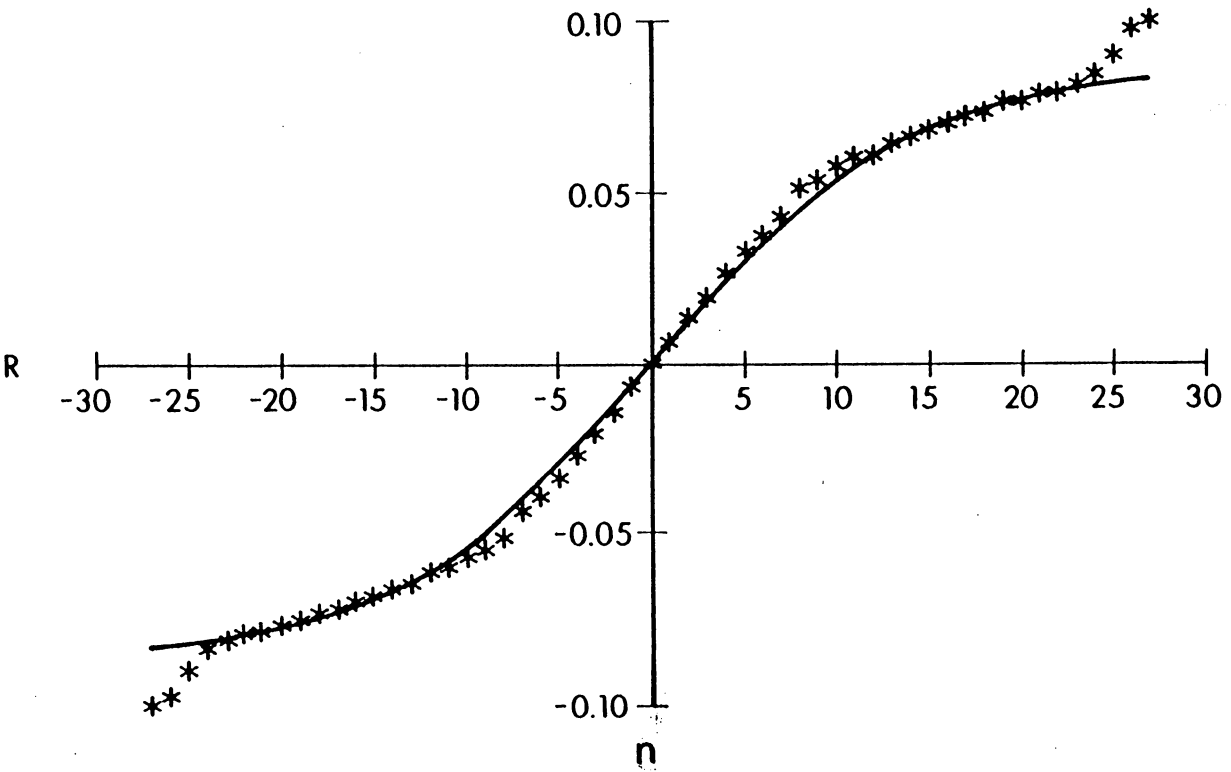


Figure 26. Bond alternation pattern for a 57 membered chain containing a neutral soliton. The solid line represents $0.087 \tanh(u/14)$.

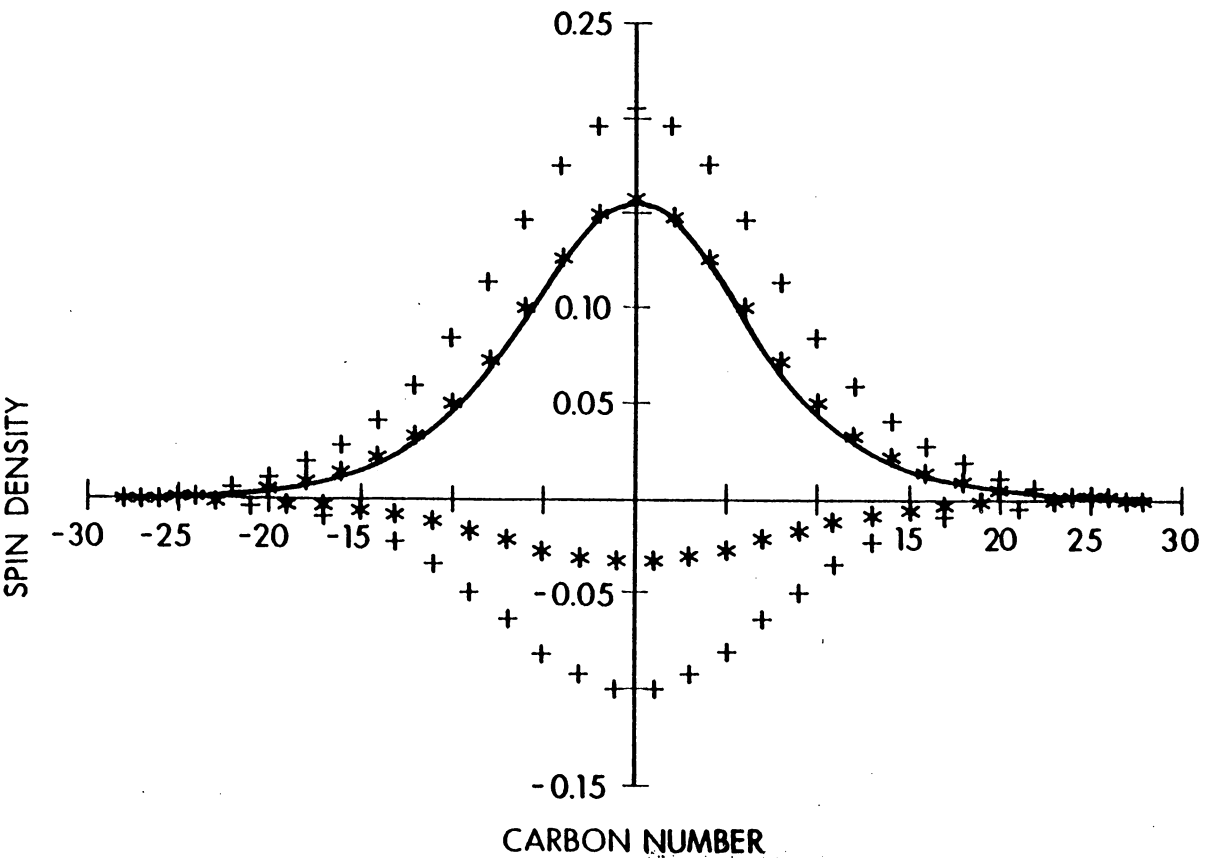


Figure 27. Spin distribution for a 57 membered chain containing a neutral soliton. The solid line represents $0.156 \text{sech}^2(\pi/8)$, the asterisks represent the projected spin densities and the pluses represent the unprojected spin densities.

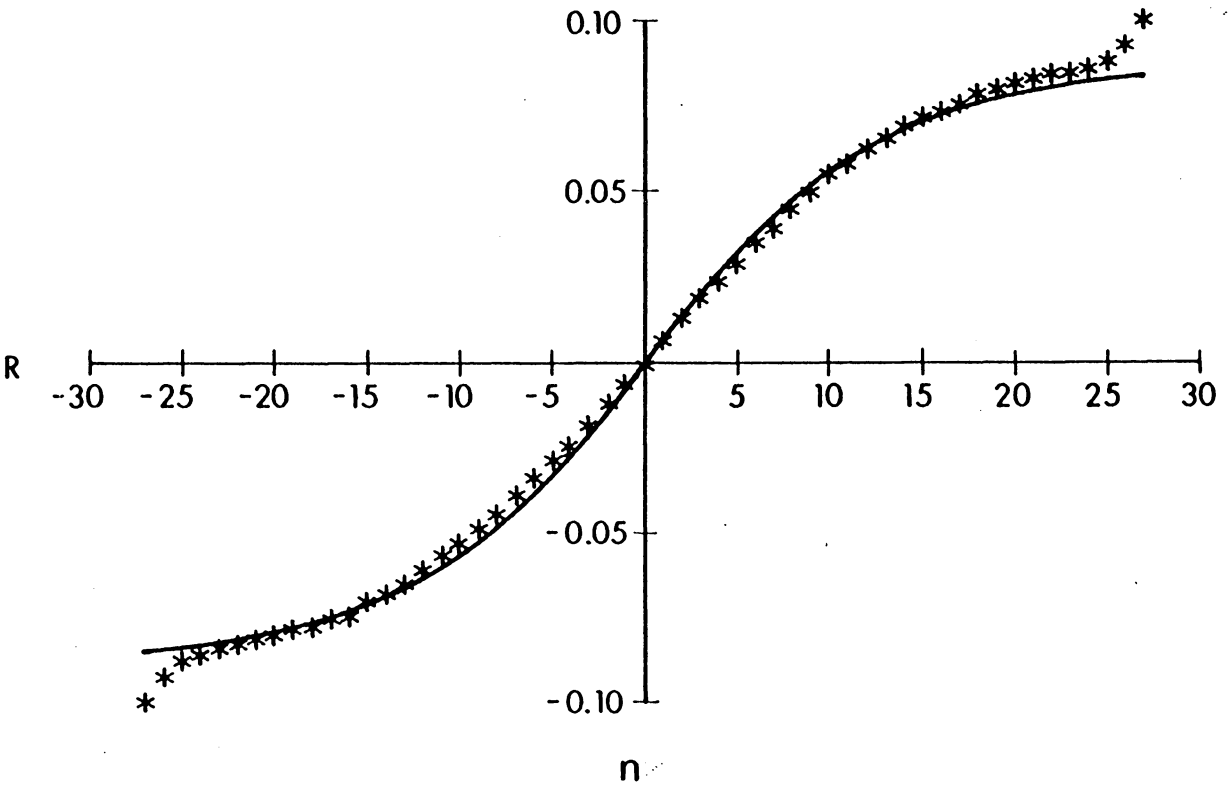


Figure 28. Bond alternation pattern for a 57 membered chain containing a positive soliton. The solid line represents $0.087 \tanh(n/13)$.

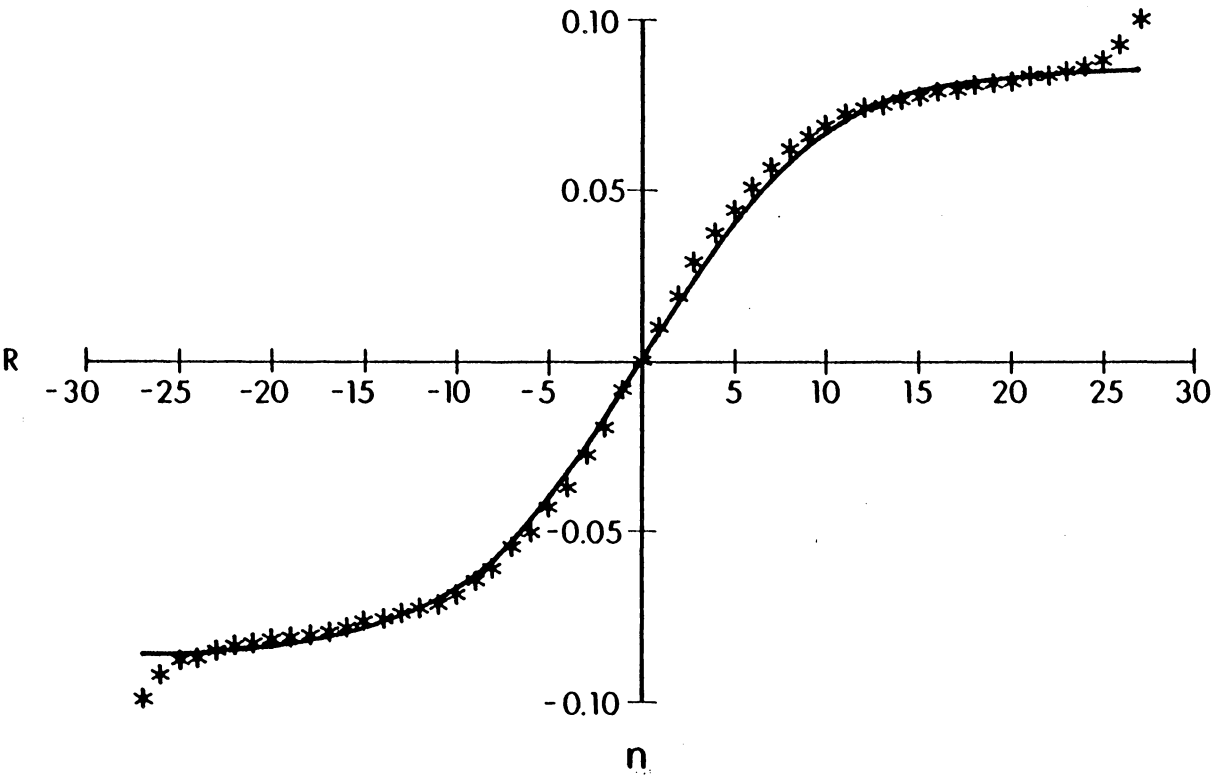


Figure 29. Bond alternation pattern for a 57 membered chain containing a negative soliton. The solid line represents $0.087 \tanh(n/10)$.

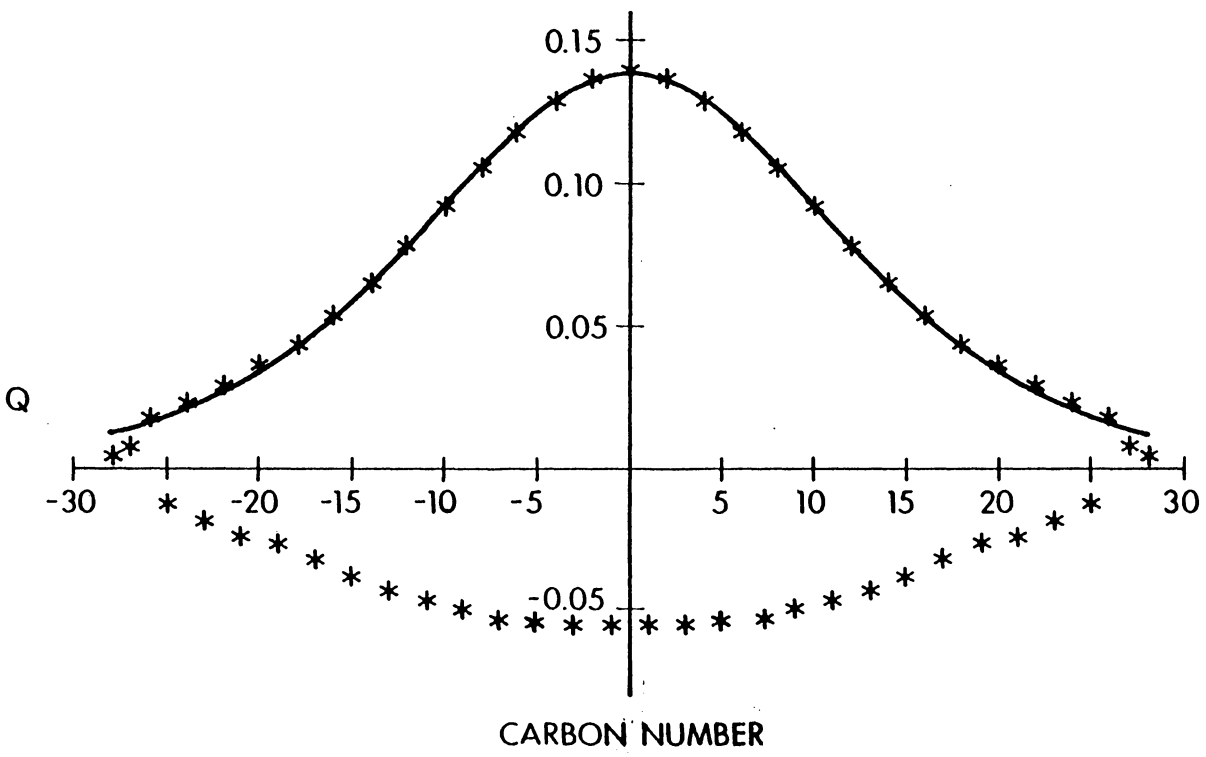


Figure 30. Charge density distribution for a 57 membered chain containing a positive soliton. The solid line represents $0.139\text{sech}^2(n/15)$.

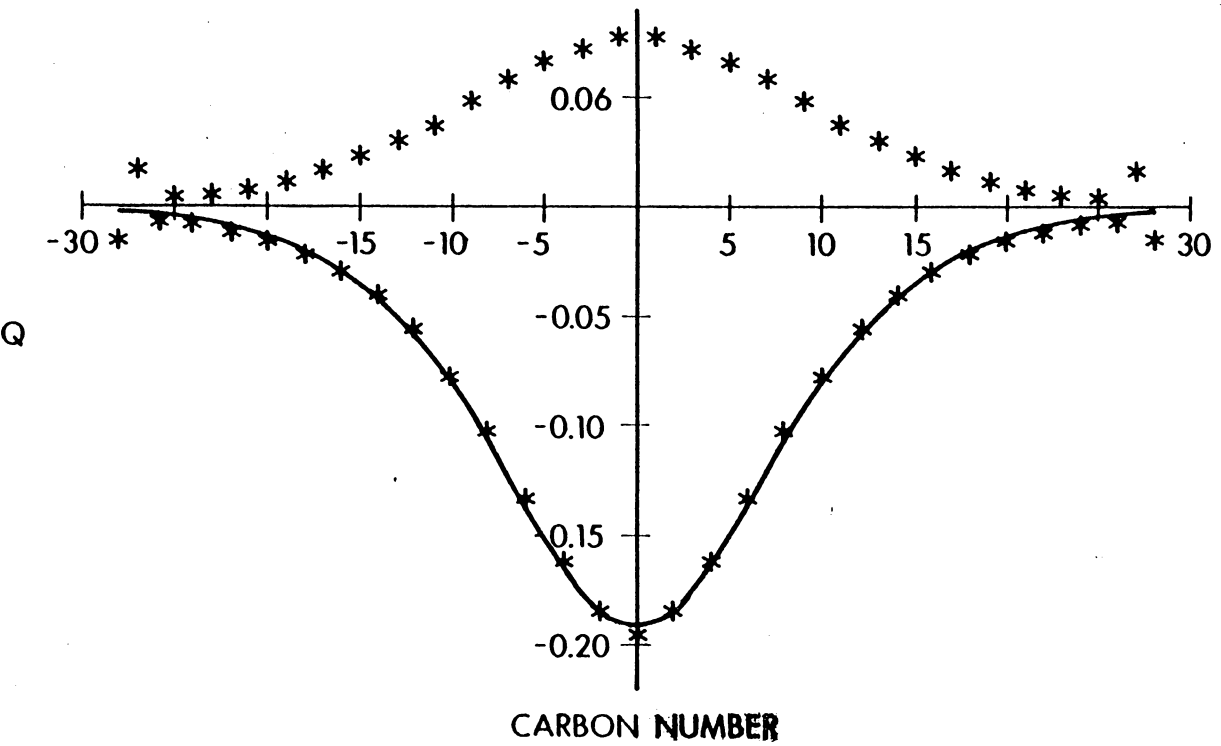


Figure 31. Charge density distribution for a 57 membered chain containing a negative soliton. The solid line represents $0.192\sec^2(\pi/10)$.

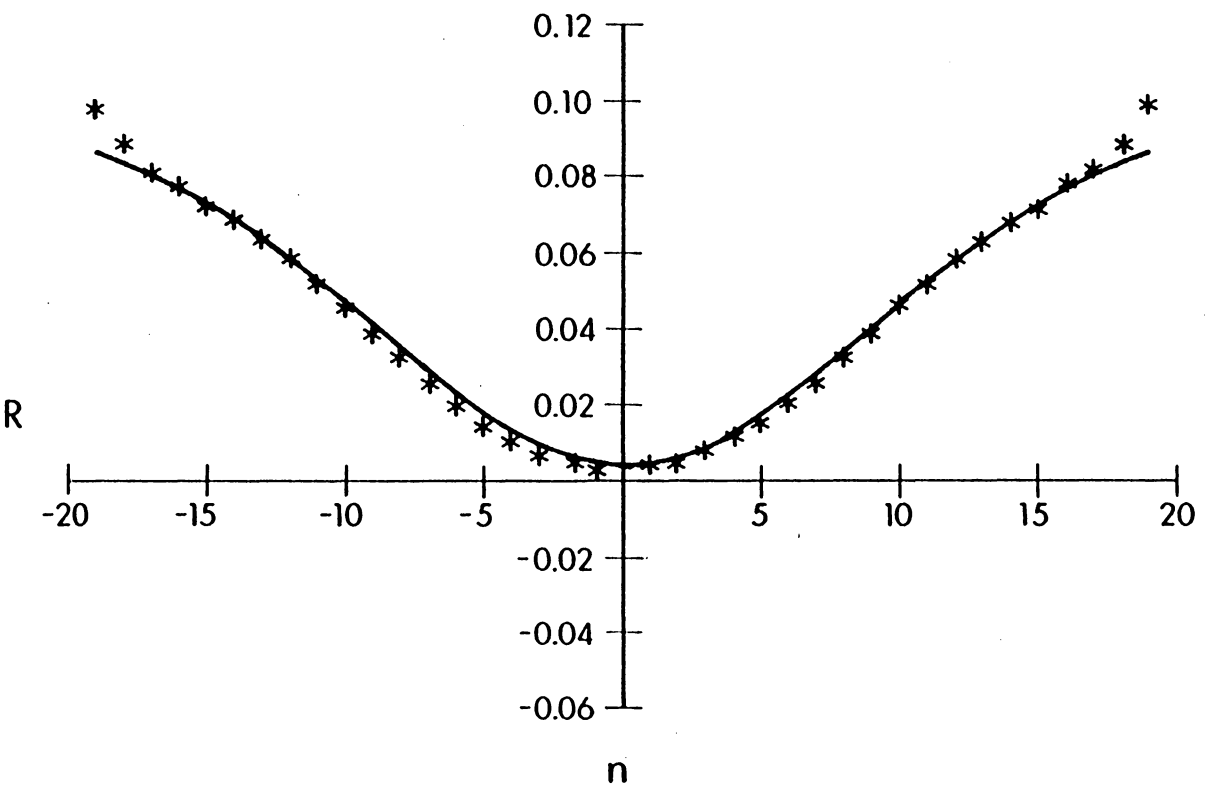


Figure 32. Bond alternation pattern for a 40 membered chain containing a positive polaron. The solid line represents $0.087|1 - 0.89\text{sech}^2(n/14)|$.

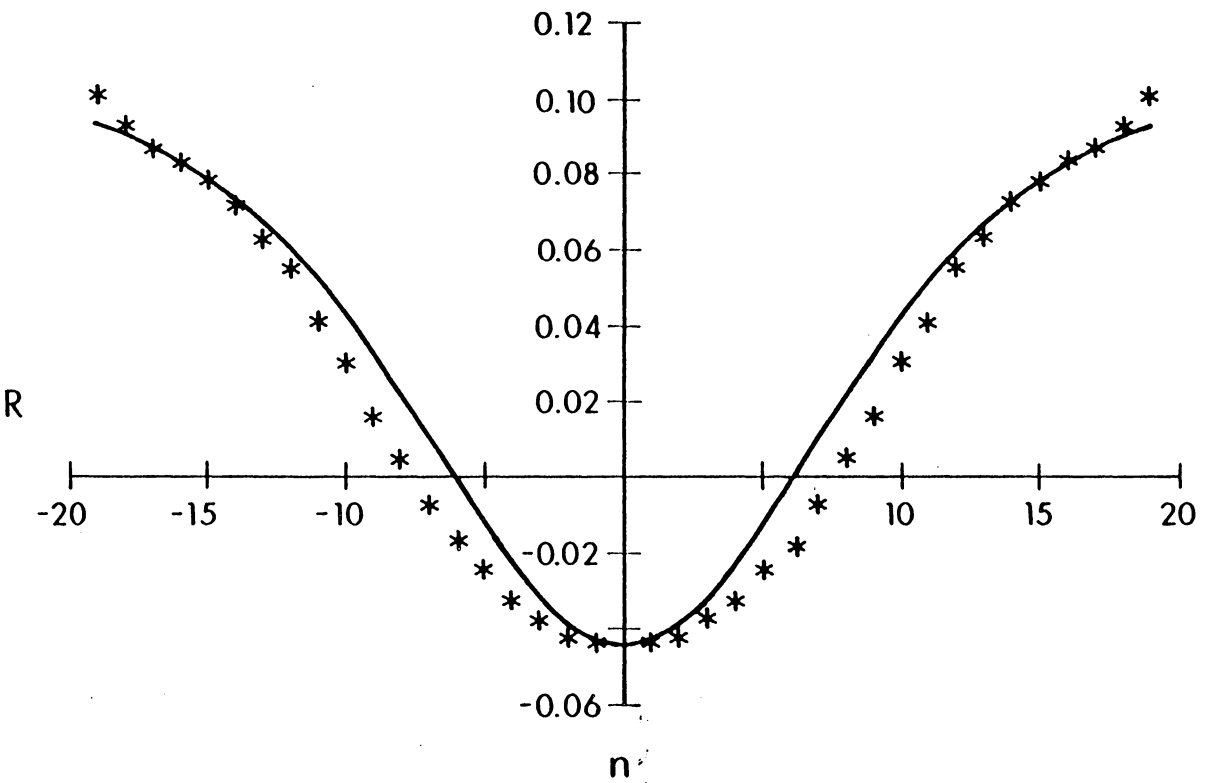


Figure 33. Bond alternation pattern for a 40 membered chain containing a negative polaron. The solid line represents $0.087[1 - 1.42\text{sech}^2(\pi/10)]$.

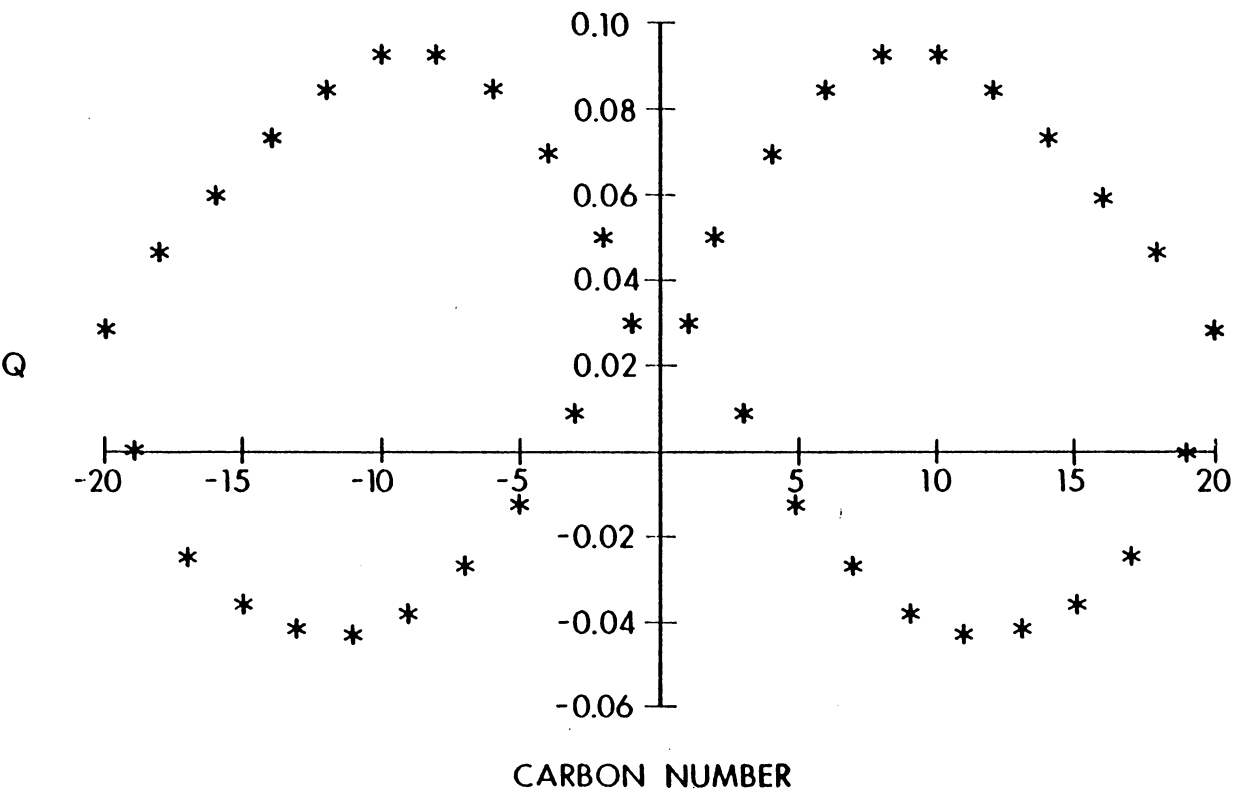


Figure 34. Charge density distribution for a 40 membered chain containing a positive polaron.

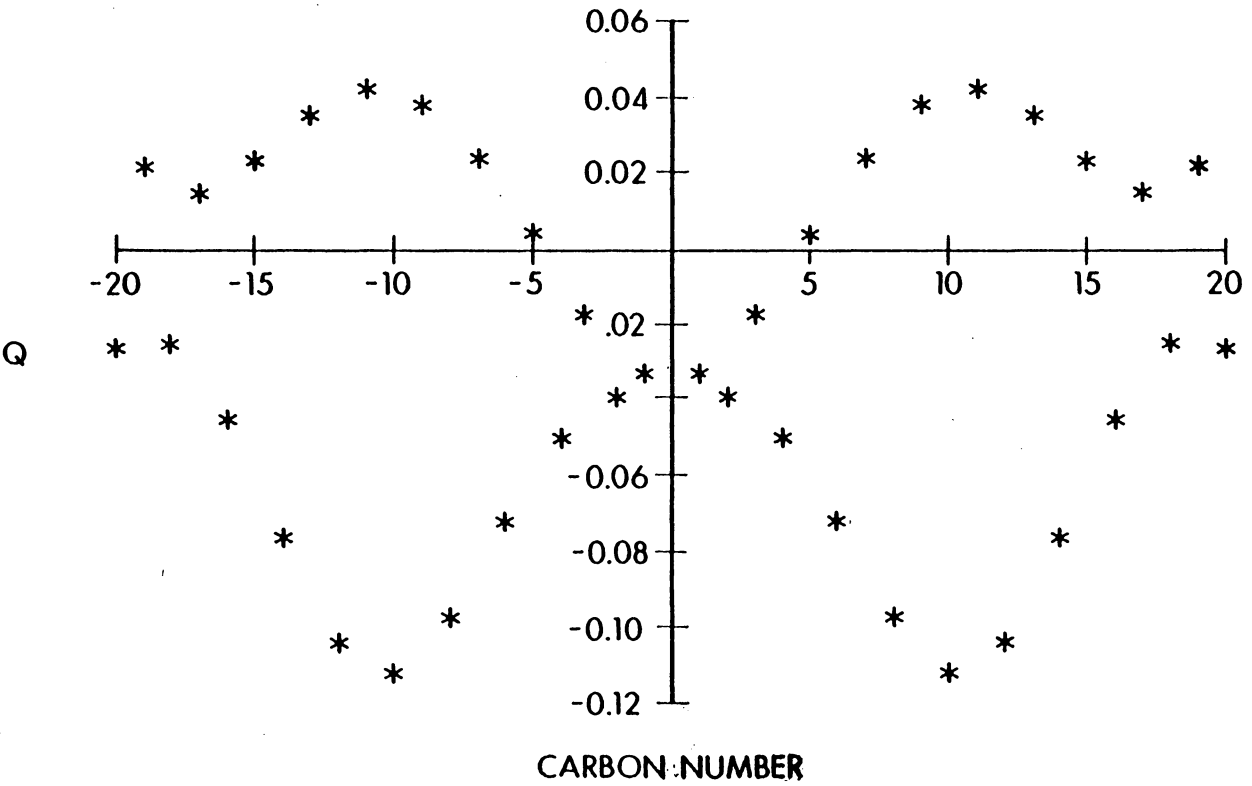


Figure 35. Charge density distribution for a 40 membered chain containing a negative polaron.

9.0 Theory of the Extended UHF-TISOSE

Method

Although the form of the exact interacting particle system Green function is unknown, this function can be assumed to have the same form as the bare Green function if the proper self-energy is time independent (12). Making this assumption, it is possible (12) to develop a Schrodinger-like equation for the single particle wave functions of the interacting particle system

$$\left[\frac{-\hbar^2}{8m\pi^2} \nabla_1^2 + U(\vec{x}) \right] \phi_j(\vec{x}_1) + \int d^3x_2 \hbar/2\pi \Sigma^*(x_1, x_2) \phi_j(\vec{x}_2) = \epsilon_j \phi_j(\vec{x}_1) \quad (40)$$

where $\Sigma^*(x_1, x_2)$ is the time-independent self energy and $\phi_j(\vec{x}_1)$ and ϵ_j are the orbitals and orbital energies of the interacting particle system.

9.1 Relation to Hartree-Fock Theory

The first-order approximation in the self-energy Feynman-Dyson perturbation expansion of the exact interacting particle system Green function is the retention of the first-order proper self-energy insertions, so that $\Sigma^*(x,y) \equiv {}_1\Sigma^*(x,y)$. The Feynman diagram for this approximation is shown in figure 17. The analysis of these diagrams according to Feynman's rules yields

$${}_{1a}\Sigma^*(x_1, x_2) = - (2\pi i/\hbar)\delta(x_1 - x_2) \sum_{\mu, \mu'} \int d^4x_3 U(x_1 - x_3) G_{\mu\mu'}^0 \quad (41a)$$

$${}_{1b}\Sigma^*(x_1, x_2) = (2\pi i/\hbar) \sum_{\lambda, \mu'} U(x_1 - x_3) G_{\lambda\mu'}^0 \quad (41b)$$

These are simplified to

$${}_{1a}\Sigma^*(x_1, x_2) = (\hbar/2\pi)^{-1} \delta(x_1 - x_2) \sum_{\mu} \sum_j^{occ} \int d^3x_3 V(\vec{x}_1 - \vec{x}_3) \varphi_j^{0\mu}(\vec{x}_1) \varphi_j^{0\mu}(\vec{x}_3)^* \quad (42a)$$

$${}_{1b}\Sigma^*(x_1, x_2) = - (\hbar/2\pi)^{-1} V(\vec{x}_1 - \vec{x}_3) \sum_j^{occ} \varphi_j^{0\lambda}(\vec{x}_1) \varphi_j^{0\mu}(\vec{x}_2)^* \quad (42b)$$

Inserting these into equation 40 yields

$$\left[\frac{-\hbar^2}{8m\pi^2} \nabla_1^2 + U(\vec{x}) \right] \varphi_j(\vec{x}_1) + \int d^3x_2 \varphi_k(\vec{x}_2) V(\vec{x}_1 - \vec{x}_2) \varphi_k(\vec{x}_2) \varphi_j(\vec{x}_1) + \int d^3x_2 \varphi_k(\vec{x}_2) V(\vec{x}_1 - \vec{x}_2) \varphi_j(\vec{x}_2) \varphi_k(\vec{x}_1) = \epsilon_j \varphi_j(\vec{x}_1). \quad (43)$$

The second term on the left hand side of equation 43 is the Hartree-Fock Coulomb operator, while the third term is the Hartree-Fock exchange operator, so that the first order approximation in the self-energy Feynman-Dyson perturbation theory is the Hartree-Fock approximation.

9.2 Extension of Hartree-Fock Theory with the TISOSE

Terms

If the self-energy expansion for the interacting system Green function is made with the total proper self-energy replaced by the first-order approximation, then the SCF-HF theory develops. This is shown diagrammatically in figure 18.

The next order of approximation to the exact Green function for the interacting particle system which is consistent with the assumptions leading to equation 40 is the inclusion of the time-independent second-order self energy insertions. The Feynman diagrams for the four time-independent second-order self-energy insertions are shown in figure 36.

The analysis of these diagrams by the Feynman rules yields

$$\Sigma_{2a}^*(x_1, x_2) = - (2\pi \frac{i}{\hbar})^2 \delta(x_1 - x_2) \sum_{\mu, \mu'} \sum_{\sigma, \sigma'} \sum_{\tau, \tau'} \int d^4x_3 d^4x_4 d^4x_5 \quad (44a)$$

$$V(x_1 - x_3)_{\lambda\lambda', \mu\mu'} V(x_4 - x_5)_{\sigma\sigma', \tau\tau'} G_{\mu\sigma}^0(x_3, x_4) G_{\sigma'\tau'}^0(x_4, x_5) G_{\tau\mu'}^0(x_5, x_3)$$

$$\Sigma_{2b}^*(x_1, x_2) = (2\pi \frac{i}{\hbar})^2 \delta(x_1 - x_2) \sum_{\mu, \mu'} \sum_{\sigma, \sigma'} \sum_{\tau, \tau'} \int d^4x_3 d^4x_4 d^4x_5 \quad (44b)$$

$$V(x_1 - x_3)_{\lambda\lambda', \mu\mu'} V(x_4 - x_5)_{\sigma\sigma', \tau\tau'} G_{\sigma\tau}^0(x_3, x_4) G_{\tau'\sigma'}^0(x_4, x_3) G_{\mu\mu'}^0(x_5, x_5)$$

$$\Sigma_{2c}^*(x_1, x_2) = (2\pi \frac{i}{\hbar})^2 \sum_{\lambda, \lambda'} \sum_{\mu, \mu'} \sum_{\sigma, \sigma'} \sum_{\tau, \tau'} \int d^4x_3 d^4x_4 \quad (44c)$$

$$V(x_1 - x_2)_{\lambda\lambda', \mu\mu'} V(x_3 - x_4)_{\sigma\sigma', \tau\tau'} G_{\lambda\tau'}^0(x_1, x_3) G_{\tau\sigma}^0(x_3, x_4) G_{\sigma'\mu'}^0(x_4, x_2)$$

$$\Sigma_{2d}^*(x_1, x_2) = - (2\pi \frac{i}{\hbar})^2 \sum_{\lambda, \lambda'} \sum_{\mu, \mu'} \sum_{\sigma, \sigma'} \sum_{\tau, \tau'} \int d^4x_3 d^4x_4 \quad (44d)$$

$$V(x_1 - x_2)_{\lambda\lambda', \mu\mu'} V(x_3 - x_4)_{\sigma\sigma', \tau\tau'} G_{\lambda\sigma'}^0(x_1, x_3) G_{\sigma\mu'}^0(x_3, x_2) G_{\tau\tau'}^0(x_4, x_4)$$

Performing the appropriate contour integrations, assuming the bare Green function to be diagonal in spin, making the zero differential overlap approximation (ZDO), expressing molecular or-

bitals as linear combinations of atomic orbitals (LCAO approximation) and assuming that the interparticle potential has the spin independent form

$$V(x - x')_{\lambda\lambda', \mu\mu'} = V(\vec{x} - \vec{x}')\delta(t - t')\delta_{\lambda\lambda'}\delta_{\mu\mu'} \quad (45)$$

yields matrix elements appropriate for use in the PPP-UHF treatment of pi-valence electrons. The derivation of equation 46a from equation 44a is given in the appendix. The second-order matrix elements are

$${}_{2a}S_{uv}^{\alpha, \beta} = \begin{cases} -2\sum_{\sigma} \sum_r \sum_s \sum_t \sum_l \sum_m^p \sum^h P_{rs}^{\sigma} \gamma_{rs} \gamma_{ut} c_{rl}^{\sigma} c_{sm}^{\sigma} c_{il}^{\sigma} c_{tm}^{\sigma} (\epsilon_l^{\sigma} - \epsilon_m^{\sigma})^{-1} & (u = v) \\ 0 & (u \neq v) \end{cases} \quad (46a)$$

$${}_{2b}S_{uv}^{\alpha, \beta} = \begin{cases} -2\sum_{\sigma} \sum_r \sum_s \sum_t \sum_l \sum_m^p \sum^h P_{ss}^{\sigma} \gamma_{ur} \gamma_{st} c_{rl}^{\sigma} c_{rm}^{\sigma} c_{il}^{\sigma} c_{tm}^{\sigma} (\epsilon_l^{\sigma} - \epsilon_m^{\sigma})^{-1} & (u = v) \\ 0 & (u \neq v) \end{cases} \quad (46b)$$

$${}_{2c}S_{uv}^{\sigma} = 2\sum_r \sum_s \sum_l \sum_m^p \sum^h P_{rs}^{\sigma} \gamma_{rs} \gamma_{uv} c_{rl}^{\sigma} c_{sm}^{\sigma} c_{ul}^{\sigma} c_{vm}^{\sigma} (\epsilon_l^{\sigma} - \epsilon_m^{\sigma})^{-1} \quad (46c)$$

$${}_{2d}S_{uv}^{\sigma} = -\sum_r \sum_s \sum_l \sum_m^p \sum^h P_{rr}^T \gamma_{rs} \gamma_{uv} c_{sl}^{\sigma} c_{sm}^{\sigma} (c_{ul}^{\sigma} c_{vm}^{\sigma} + c_{vl}^{\sigma} c_{um}^{\sigma}) (\epsilon_l^{\sigma} - \epsilon_m^{\sigma})^{-1} \quad (46d)$$

In equation 46, σ represents particle spin, $\mathbf{P}^{\alpha}(\mathbf{P}^{\beta})$, is the alpha (beta), density matrix, \mathbf{P}^T is the total density matrix, γ is the matrix of two-electron repulsion integrals and $\{c^{\alpha}\}$ and $\{\epsilon^{\alpha}\}$ ($\{c^{\beta}\}$ and $\{\epsilon^{\beta}\}$) are the sets of eigenvectors and eigenvalues of the modified Fock matrices

$$\mathbf{F}^{\alpha'} = \mathbf{F}_{UHF}^{\alpha} + \mathbf{S}^{\alpha} \quad (47a)$$

$$\mathbf{F}^{\beta'} = \mathbf{F}_{UHF}^{\beta} + \mathbf{S}^{\beta} \quad (47b)$$

The matrix \mathbf{S}^{σ} in equation 47 may be any of the matrices defined in equation 15, or the sum of them.

9.3 Results of the Extended PPP-UHF-RPA-TISOSE

Calculations on TPA

The pi-valence electrons of the linear polyenes studied were treated using the PPP-UHF Hamiltonian, with the time-independent second-order perturbation terms added.

In this preliminary study, the effects of the time-independent second-order perturbation terms on calculations involving the polyene radicals *trans* - C_9H_{11} and *trans* - $C_{17}H_{19}$ were examined, and were modeled as planar carbon skeletons with fixed bond angles. The matrix elements in equation 46 were added either individually, or as a sum, to the PPP-UHF treatment, as indicated in equation 47.

The results for the change in pi-energy, ΔE_π , and the total negative to total positive spin density ratio, ρ^-/ρ^+ , are given in table 1. The pi-energy difference is defined as

$$\Delta E_\pi = E_\pi^{UHF+SO} - E_\pi^{UHF} \quad (48)$$

where E_π^{UHF} is the pi-energy calculated when only the first-order self-energy terms are included (Hartree-Fock approximation), and E_π^{UHF+SO} is the pi-energy calculated when one, or all, of the time independent second-order self-energy terms is included.

The results of this study show that important many-body contributions can be included in simple pi-orbital calculations by the use of the field theory familiar to solid state physicists. Further, the time independent second-order self-energy terms considered here have been shown to contribute significantly to the electronic structure and energy of the systems studied.

Table 1

C-9 Results-

	$E^\pi(kcal/mol)$	ΔE_π	ρ^-/ρ^+
UHF	-393.01	0	0.5668
2-A	-393.01	0	0.5668
2-B	-51.28	341.72	0.2544
2-C	-381.62	11.39	0.7000
2-D	-337.16	55.93	0.4212
ALL	-102.04	290.97	0.3115

C-17 Results-

	$E^\pi(kcal/mol)$	ΔE_π	ρ^-/ρ^+
UHF	-786.36	0	0.6956
2-A	-786.3	0	0.6956
2-B	-305.47	480.89	0.5108
2-C	-753.83	32.53	0.8216
2-D	-116.42	669.94	0.5427
ALL	106.55	894.91	0.7872
RPA	-886.49	-100.13	0.4700

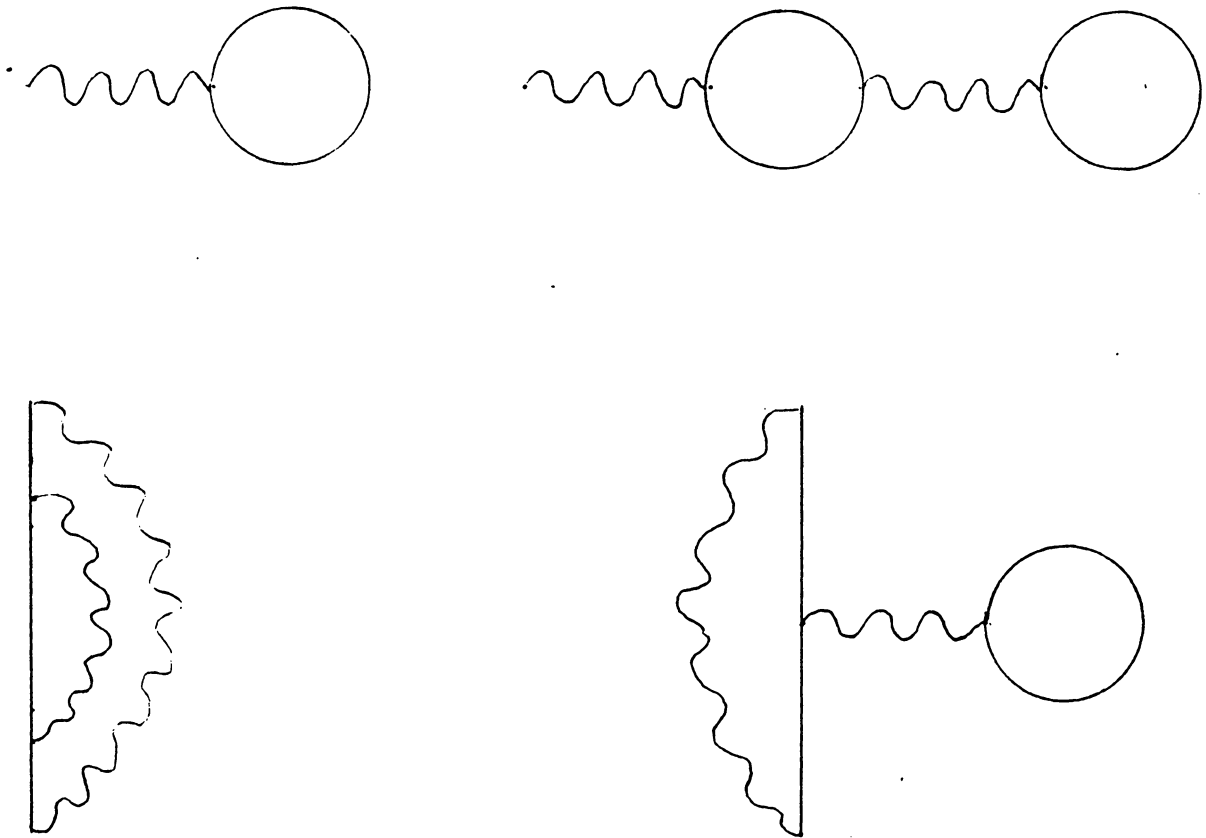


Figure 36. TISOSE insertions

10.0 Description of the Computer Code

The calculations performed in this research were carried out using a computer program written specifically for the PPP-UHF treatment of polyenes. The program was compiled and executed on the VM1 system at V. P. I. and S. U.

The main program reads in the number of atoms in the system, the net charge on the system, the net electronic spin in the system and the number of iteration cycles to be carried out. Switches controlling the type of calculation are also input as data. The program is able to perform standard PPP-UHF calculations, as well as the PPP-UHF-RPA procedure and the extended PPP-UHF-TISOSE procedure. The initial bond lengths of the system to be studied are the final data required.

The main program also sets up matrices to symmetrize- antisymmetrize the calculated molecular orbitals, so that the proper molecular symmetry is assured, calls the energy function controlling routine MOLECU, controls the optimization procedure STEEPD and prints the initial and final geometry and energy contributions.

A brief description of the main subroutines follows:

BFUNC2- Calculates the sigma bonding energy and sigma bonding energy derivative contributions for each sigma bond according to the Morse bonding function, equation 25 and the corresponding derivative equation 26. BFUNC2 is called by BONDP.

VPHI- Sets-up the diagonal elements of the one-electron Hamiltonian matrix using the SOK parametrized form of the standard PPP expression, equation 23, and calculates the one-electron pi-energy derivative contribution for each bond according to equation 27. VPHI is called by BONDP.

BONDP- Calculates the length of each bond from the Cartesian coordinates of the bonded atoms. It also calls the routines BFUNC2 and VPHI. BONDP is called by MOLECU

STEEPD- Calculates bond shifts leading to minimization according to the steepest descents method. STEEPD is called by the main program.

MOLECU- Controls the calculation of all energy and energy derivative contributions. It also performs an initial Huckel treatment of the system for input into the SCF procedure. It is called by the main program.

SCF- Performs the SCF UHF procedure. It calls routines which set-up and diagonalize the alpha and beta Fock matrices used in the calculation of the pi-energy contribution. It may also call routines which calculate the RPA effective interparticle interaction according to equation 21 or set up the second-order self-energy matrices defined by equation 46. This routine controls the output of all information about the pi-valence electrons, including density matrices, charge and spin distributions and molecular orbitals and energies. SCF is called by MOLECU.

SN2A-SN2D- Set up the matrix elements defined by equation 46. These routines are called by SCF, when required.

SYDI- Diagonalizes the Fock matrices so that the molecular orbitals have the proper symmetry. It uses the external diagonalization routine RS from the EISPAK package of eigensystem routines. SYDI is called by SCF.

PROJ- Performs Harriman spin projection on the UHF orbitals to find the spin distribution and pi-energy of pure spin eigenfunctions. PROJ is called by SCF.

DENA- Calculates the alpha and beta density matrices. DENA is called by SCF.

UHFOCK- Sets up the alpha and beta Fock matrices in the UHF and UHF-RPA procedures or the modified Fock matrices (according to equation 36) if the extended UHF-TISOSE procedure is used. UHFOCK is called by SCF.

SYMNAT- Diagonalization routine which produces natural orbitals for spin projection. The orbitals are constrained to have the proper symmetry. This routine also uses the EISPAK routine RS. SYMNAT is called by PROJ.

SYMCOR- Diagonalization routine which produces beta-corresponding orbitals for spin projection. The orbitals are constrained to have the proper symmetry. This routine also uses the EISPAK routine RS. SYMNAT is called by PROJ.

VEFF- Calculates the RPA effective particle interaction according to equation 21. This routine uses the external LINPAK routines DGECO and DGEDI to find the matrix inverse in equation 21. VEFF is called by SCF.

VZERO- Calculates the Ohno (50) bare interaction according to equation (24). It may be called by MOLECU or VEFF, as required.

VPRIME- Calculates the two-electron pi-energy derivative contribution of each bond according to equation (28). It is called by MOLECU.

In addition to the main program and these nineteen subroutines, there are twelve other subroutines and three functions. A listing of the program is included (see appendix), for reference.

Appendix A. Derivation of Equation 46a

Figure 39 shows the complete Feynman diagram of the second-order self energy insertion "2a".

Starting with equation 45a

$$\begin{aligned} \Sigma_{2a}^*(x_1, x_2) = & - (2\pi \frac{i}{\hbar})^2 \delta(x_1 - x_2) \sum_{\mu, \mu'} \sum_{\sigma, \sigma'} \sum_{\tau, \tau'} \int d^4x_3 d^4x_4 d^4x_5 \\ & U(x_1 - x_3)_{\lambda\lambda', \mu\mu'} U(x_4 - x_5)_{\sigma\sigma', \tau\tau'} G_{\mu\sigma}^0(x_3, x_4) G_{\sigma'\tau'}^0(x_4, x_5) G_{\tau\mu'}^0(x_5, x_3) \end{aligned} \quad (A1)$$

we first assume the interparticle interaction to be spin and time independent so that

$$\begin{aligned} \Sigma_{2a}^*(x_1, x_2) = & - (2\pi \frac{i}{\hbar})^2 \delta(x_1 - x_2) \sum_{\mu, \mu'} \sum_{\sigma, \sigma'} \sum_{\tau, \tau'} \int d^4x_3 d^4x_4 d^4x_5 \\ & V(\vec{x}_1 - \vec{x}_3) \delta(t_1 - t_3) \delta_{\lambda\lambda'} \delta_{\mu\mu'} V(\vec{x}_4 - \vec{x}_5) \delta(t_4 - t_5) \delta_{\sigma\sigma'} \delta_{\tau\tau'} \\ & G_{\mu\sigma}^0(x_3, x_4) G_{\sigma'\tau'}^0(x_4, x_5) G_{\tau\mu'}^0(x_5, x_3). \end{aligned} \quad (A2)$$

Then, assuming the bare Green function to be diagonal in spin and simplifying yields

$$\begin{aligned} \Sigma_{2a}^*(x_1, x_2) = & - (2\pi \frac{i}{\hbar})^2 \delta(x_1 - x_2) \sum_{\mu} \int d^4x_3 d^4x_4 d^4x_5 \\ & V(\vec{x}_1 - \vec{x}_3) \delta(t_1 - t_3) V(\vec{x}_4 - \vec{x}_5) \delta(t_4 - t_5) \\ & G_{\mu\mu}^0(x_3, x_4) G_{\mu\mu}^0(x_4, x_5) G_{\mu\mu}^0(x_5, x_3). \end{aligned} \quad (A3)$$

Performing the t_3 and t_5 time integrations yields

$$\Sigma_{2a}^*(x_1, x_2) = - (2\pi \frac{i}{h})^2 \delta(x_1 - x_2) \sum_{\mu} \int d^3 x_3 d^3 x_5 d^4 x_4 V(\vec{x}_1 - \vec{x}_3) V(\vec{x}_4 - \vec{x}_5) G^0(\vec{x}_3, t_1, \vec{x}_4, t_4) G^0(\vec{x}_4, t_4, \vec{x}_5, t_4) G^0(\vec{x}_5, t_4, \vec{x}_3, t_1) \quad (A4)$$

It is now advantageous to Fourier transform the time component of the Green functions

$$\Sigma_{2a}^*(x_1, x_2) = - (2\pi \frac{i}{h})^2 \delta(x_1 - x_2) \sum_{\mu} \int d^3 x_3 d^3 x_5 d^4 x_4 \frac{d\omega_1}{2\pi} \frac{d\omega_2}{2\pi} \frac{d\omega_3}{2\pi} V(\vec{x}_1 - \vec{x}_3) V(\vec{x}_4 - \vec{x}_5) e^{i\omega_1(t_1 - t_4)} G^0(\vec{x}_3, \vec{x}_4, \omega_1) e^{i\omega_2 \eta} G^0(\vec{x}_4, \vec{x}_5, \omega_2) e^{-i\omega_3(t_1 - t_4)} G^0(\vec{x}_5, \vec{x}_3, \omega_3) \quad (A5)$$

which simplifies to

$$\Sigma_{2a}^*(x_1, x_2) = - (2\pi \frac{i}{h})^2 \delta(x_1 - x_2) \sum_{\mu} \int d^3 x_3 d^3 x_5 d^3 x_4 \frac{d\omega_1}{2\pi} \frac{d\omega_2}{2\pi} V(\vec{x}_1 - \vec{x}_3) V(\vec{x}_4 - \vec{x}_5) e^{i\omega_2 \eta} G^0(\vec{x}_4, \vec{x}_5, \omega_2) e^{i\omega_1 \eta'} G^0(\vec{x}_3, \vec{x}_4, \omega_1) G^0(\vec{x}_5, \vec{x}_3, \omega_1) \quad (A6)$$

Inserting the Fourier transformed bare Green function

$$G^0(x, y) = \sum_k \left[\frac{\Theta(\epsilon_F - \epsilon_k)}{\omega - \epsilon_k 2\pi/h + i\eta} + \frac{\Theta(\epsilon_k - \epsilon_F)}{\omega - \epsilon_k 2\pi/h - i\eta} \right] \varphi_k(\vec{x}) \varphi_k(\vec{y}) \quad (A7)$$

into (A6) yields

$$\Sigma_{2a}^*(x_1, x_2) = - (2\pi \frac{i}{h})^2 \delta(x_1 - x_2) \sum_{\mu} \sum_j \sum_k \sum_l \int d^3 x_3, x_5, x_4 \frac{d\omega_1}{2\pi} \frac{d\omega_2}{2\pi} V(\vec{x}_1 - \vec{x}_3) V(\vec{x}_4 - \vec{x}_5) e^{i\omega_2 \eta} \left[\frac{\Theta(\epsilon_F - \epsilon_j)}{\omega_2 - \epsilon_j 2\pi/h + i\eta} + \frac{\Theta(\epsilon_j - \epsilon_F)}{\omega_2 - \epsilon_j 2\pi/h - i\eta} \right] \varphi_j(\vec{x}_4) \varphi_j(\vec{x}_5) e^{i\omega_1 \eta'} \left[\frac{\Theta(\epsilon_F - \epsilon_k)}{\omega_1 - \epsilon_k 2\pi/h + i\eta'} + \frac{\Theta(\epsilon_k - \epsilon_F)}{\omega_1 - \epsilon_k 2\pi/h - i\eta'} \right] \left[\frac{\Theta(\epsilon_F - \epsilon_l)}{\omega_1 - \epsilon_l 2\pi/h + i\eta'} + \frac{\Theta(\epsilon_l - \epsilon_F)}{\omega_1 - \epsilon_l 2\pi/h - i\eta'} \right] \varphi_k(\vec{x}_3) \varphi_l(\vec{x}_4) \varphi_k(\vec{x}_5) \varphi_l(\vec{x}_3) \quad (A8)$$

Using the integration contour in figure 41, the following expression in terms of the interparticle interaction and the molecular orbitals and orbital energies is obtained

$$\begin{aligned} \Sigma_{2a}^*(x_1, x_2) = & - (2\pi/\hbar)\delta(x_1 - x_2)\sum_{\mu}^{\text{occ}}\sum_j^{\text{occ}}\sum_k^{\text{occ}}\sum_l^{\text{unocc}}\int d^3x_3, x_5, x_4 \\ & V(\vec{x}_1 - \vec{x}_3)V(\vec{x}_4 - \vec{x}_5)\varphi_j(\vec{x}_4)\varphi_l(\vec{x}_5) \\ & [\varphi_k(\vec{x}_3)\varphi_k(\vec{x}_4)\varphi_k(\vec{x}_5)\varphi_l(\vec{x}_3) + \varphi_k(\vec{x}_4)\varphi_l(\vec{x}_3)\varphi_k(\vec{x}_3)\varphi_l(\vec{x}_5)](\varepsilon_l - \varepsilon_k)^{-1} \end{aligned} \quad (A9)$$

Inserting this into the Schrodinger-like equation

$$\begin{aligned} \left[-\frac{\hbar^2}{8mn^2}\nabla_1^2 + U(\vec{x}_1) \right]\varphi_j(\vec{x}_1) + \\ \int d^3x_2 (h/2\pi)\Sigma^*(\vec{x}_1, \vec{x}_2)\varphi_j(\vec{x}_2) = \varepsilon_j\varphi_j(\vec{x}_1), \end{aligned} \quad (A10)$$

yields

$$\begin{aligned} f(\vec{x}_1)\varphi_j(\vec{x}_1) - \sum_{\mu}^{\text{occ}}\sum_k^{\text{occ}}\sum_l^{\text{unocc}}\sum_m^{\text{unocc}}\int d^3x_3, x_5, x_4 V(\vec{x}_1 - \vec{x}_3)V(\vec{x}_4 - \vec{x}_5) \\ \varphi_k(\vec{x}_4)\varphi_k(\vec{x}_5)[\varphi_l(\vec{x}_3)\varphi_m(\vec{x}_4)\varphi_l(\vec{x}_5)\varphi_m(\vec{x}_3) + \varphi_l(\vec{x}_4)\varphi_m(\vec{x}_3)\varphi_l(\vec{x}_3)\varphi_m(\vec{x}_5)] \\ (\varepsilon_l - \varepsilon_k)^{-1}\varphi_j(\vec{x}_1) = \varepsilon_j\varphi_j(\vec{x}_1) \end{aligned} \quad (A11)$$

where $f(\vec{x}_1)$ is the one-electron Fock operator. This allows the definition of a new operator defined from

$$f(\vec{x}_1)\varphi_j(\vec{x}_1) + S(\vec{x}_1)\varphi_j(\vec{x}_1) = \varepsilon_j\varphi_j(\vec{x}_1). \quad (A12)$$

The matrix representation of $S(\vec{x}_1)$ in the atomic orbital basis is

$$S_{uv} = \int d^3x_1 \chi_u^*(\vec{x}_1)S(\vec{x}_1)\chi_v(\vec{x}_1) \quad (A13)$$

Inserting $S(\vec{x}_1)$ from (A10) and assuming all orbitals are real yields

$$\begin{aligned} S_{uv} = \sum_{\mu}^{\text{occ}}\sum_k^{\text{occ}}\sum_l^{\text{unocc}}\sum_m^{\text{unocc}}\int d^3x_1 x_3, x_5, x_4 \chi_u(\vec{x}_1)V(\vec{x}_1 - \vec{x}_3)V(\vec{x}_4 - \vec{x}_5) \\ \varphi_k(\vec{x}_4)\varphi_k(\vec{x}_5)[\varphi_l(\vec{x}_3)\varphi_m(\vec{x}_4)\varphi_l(\vec{x}_5)\varphi_m(\vec{x}_3) + \varphi_l(\vec{x}_4)\varphi_m(\vec{x}_3)\varphi_l(\vec{x}_3)\varphi_m(\vec{x}_5)](\varepsilon_l - \varepsilon_k)^{-1}\chi_v(\vec{x}_1). \end{aligned} \quad (A14)$$

Expanding the molecular orbitals in the atomic orbital basis (LCAO approximation) gives

$$\begin{aligned}
S_{uv} = & -2 \sum_{\mu} \sum_k^{occ} \sum_l^{occ} \sum_m^{unocc} \sum_r \sum_s \sum_t \sum_c \sum_b \sum_w \int d^3 x_1 x_3, x_5, x_4 V(\vec{x}_1 - \vec{x}_3) V(\vec{x}_4 - \vec{x}_5) \chi_u(\vec{x}_1) \\
& c_{rk} c_{sk} c_{tl} c_{cl} c_{bm} c_{wm} \chi_r(\vec{x}_4) \chi_s(\vec{x}_5) \\
& \chi_t(\vec{x}_3) \chi_c(\vec{x}_4) \chi_b(\vec{x}_5) \chi_w(\vec{x}_3) (\epsilon_l - \epsilon_k)^{-1} \chi_v(\vec{x}_1).
\end{aligned} \tag{A15}$$

Using chemists notation for the two-electron integral, this becomes

$$\begin{aligned}
S_{uv} = & -2 \sum_{\mu} \sum_k^{occ} \sum_l^{occ} \sum_m^{unocc} \sum_r \sum_s \sum_t \sum_c \sum_b \sum_w \sum_c c_{rk} c_{sk} c_{tl} \\
& c_{cl} c_{bm} c_{wm} (uv|tw)(rc|sb) (\epsilon_l - \epsilon_k)^{-1}
\end{aligned} \tag{A16}$$

Making the zero-differential overlap approximation:

$$(uv|tw) \equiv (uv|tw) \delta_{uv} \delta_{tw} \equiv \gamma_{ut}$$

yields

$$\begin{aligned}
S_{uv} = & -2 \sum_{\mu} \sum_k^{occ} \sum_l^{occ} \sum_m^{unocc} \sum_r \sum_s \sum_t \sum_c c_{rk} c_{sk} c_{tl} c_{cl} c_{bm} c_{wm} \gamma_{ut} \gamma_{rs} (\epsilon_l - \epsilon_k)^{-1} & (u = v) \\
& 0 & (u \neq v)
\end{aligned} \tag{A17}$$

finally, using the density matrix definition

$$P_{uv}^{\sigma} = \sum_j c_{uj}^{\sigma} c_{vj}^{\sigma}$$

yields the form of equation 46a

$$\begin{aligned}
2a S_{uv}^{\alpha, \beta} = & -2 \sum_{\sigma} \sum_r \sum_s \sum_t \sum_l^p \sum_m^h P_{rs}^{\sigma} \gamma_{rs} \gamma_{ut} c_{rl}^{\sigma} c_{sm}^{\sigma} c_{tl}^{\sigma} c_{tm}^{\sigma} (\epsilon_l^{\sigma} - \epsilon_m^{\sigma})^{-1} & (u = v) \\
& 0 & (u \neq v)
\end{aligned} \tag{A18}$$

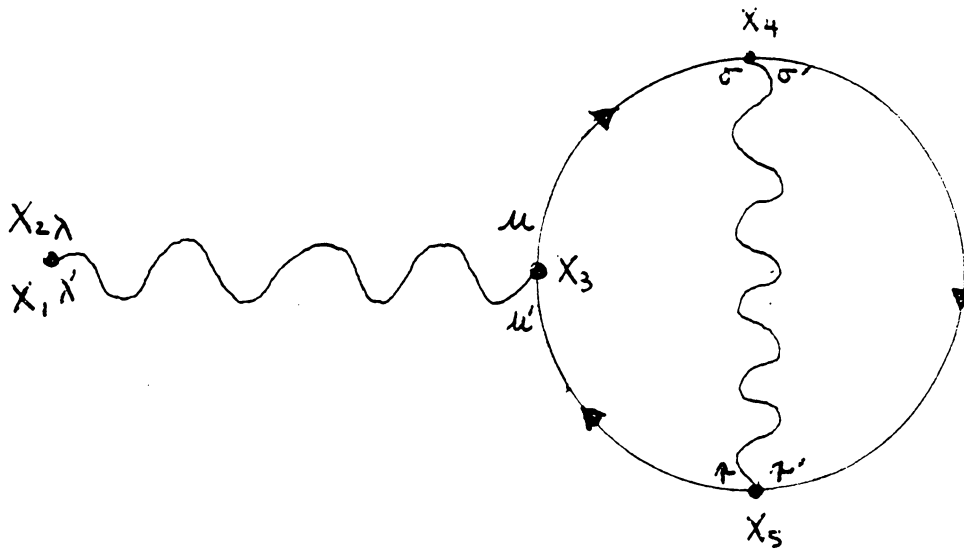


Figure 37. Complete Feynman diagram for self-energy insertion "2a".

Appendix B. Computer Program

```
C   PPP-UHF WITH RPA AND TISOSE C   SUBROUTINE CONF
IMPLICIT REAL*8 (A-H,P-Z)
REAL*8 LENGTH
CHARACTER OCH(60),OSYMB
COMMON/ISEC/ISOA,ISOB,ISOC,ISOD,IDMP
COMMON/HH/H(60,60),R(60,60),PT(60,60),Z(60)
COMMON/MAT/BMAT(60,60),GMAT(60,60),HCORM(60,60)
COMMON/FINAL/B(60),X(180),AL(60),NC(60)
COMMON/CONTRO/NATOM,NBOND,NAP,NAO,NAT3
COMMON/ENSTOR/ENS(20),STEPS(20),ITH
COMMON/UHF/PA(60,60),PB(60,60)
COMMON/PII/JCHG,NALPH,NBET,NPIE,JSPIN,JUHF
COMMON/SW/ISW,IPR,ISCR
COMMON/SYM/S(60,60),ST(60,60),NSM(2),NOCC(2)
COMMON/DER/D1(60),D2(60),D3(60),VOP(60,60),D(60)
COMMON/EXCI/IEX
COMMON/SELF/DMP1,DMP2
DIMENSION ITITLE(10)
DIMENSION DX(3)
DATA OSYMB/'A'/ C   IEX = 1
   IEX = 0
PI = 3.141592635898D0
DMP1 = 70.D0
DMP2 = 0.D0
DO 10 I = 1,60
  OCH(I) = OSYMB
10 NC(I) = I
  CALL ERRSET(207,256,-1,1,1,209)
  READ 9, (ITITLE(I),I = 1,10)
  PRINT 19, (ITITLE(I),I = 1,10)
  ISW = 1
  READ (5,29) NATOM
  NAP = NATOM
  NBOND = NAP-1
```

```

NAT3 = 3*NATOM
DO 20 I = 1, NATOM
20 Z(I) = 1.D0 C...FORM S = SYMM. TRANSFORMATION.
CALL INIT (S)
KOC = MOD(NAP,2)
IF (KOC .EQ. 0) GO TO 40 C...ODD SYSTEM
NSMS = (NAP + 1)/2
NSMA = (NAP - 1)/2
NSM(1) = NSMS
NSM(2) = NSMA
KOC = MOD(NSMS,2)
IF (KOC .EQ. 0) GO TO 50
NOC1 = (NSMS + 1)/2
GO TO 55
50 CONTINUE
NOC1 = NSMS/2
55 CONTINUE
KOC = MOD(NSMA,2)
IF (KOC .EQ. 0) GO TO 60
NOC2 = (NSMA + 1)/2
GO TO 65
60 CONTINUE
NOC2 = NSMA/2
65 CONTINUE
NOCC(1) = NOC1
NOCC(2) = NOC2
CN = 1.D0/DSQRT(2.D0)
NSMSM = NSMS - 1
DO 70 K = 1, NSMSM
KA = NAP + 1 - K
I1 = K
IS = NAP + 1 - I1
S(I1, K) = CN
S(IS, K) = CN
S(I1, KA) = CN
70 S(IS, KA) = -CN
S(NSMS, NSMS) = 1.D0
GO TO 80
40 CONTINUE C...EVEN SYSTEM
NO2 = NAP/2
NSM(1) = NO2
NSM(2) = NO2
IOC = MOD(NO2,2)
IF (IOC .EQ. 0) GO TO 90
NOC1 = (NO2 + 1)/2
NOC2 = (NO2 - 1)/2
GO TO 95
90 NOC1 = NO2/2
NOC2 = NO2/2
95 CONTINUE
NOCC(1) = NOC1
NOCC(2) = NOC2
CN = 1.D0/DSQRT(2.D0)
DO 100 K = 1, NO2
KA = NAP + 1 - K
I1 = K

```

```

IS = NAP + 1 - I1
S(I1,K) = CN
S(IS,K) = CN
S(I1,KA) = CN
100 S(IS,KA) = -CN
80 CONTINUE
DO 110 I = 1, NAP
DO 110 J = 1, NAP
110 ST(I,J) = S(J,I) C..
PRINT 49, NAP, NSM(1), NOCC(1), NSM(2), NOCC(2)
READ (5,29) NSTEEP, INEW, JCHG, JSPIN, ISCR
READ (5,29) ISOA, ISOB, ISOC, ISOD, IDMP C
DO 6098 I = 1, NBOND
6098 READ(5,6099) B(I)
6099 FORMAT(F12.5)
AL60 = DACOS(0.5D0)
DO 6000 I = 1, NBOND
AL(I) = 0.D0
IK = 2*(I/2)
6000 IF(IK.EQ.I) AL(I) = AL60
CALL CART(B,X,AL,NAT3,NATOM)
CALL ALPH(X,AL,NBOND)
DO 207 I = 1, NAP
READ (5,69) (PA(I,J), J = 1, NAP)
207 CONTINUE
DO 217 I = 1, NAP
READ (5,69) (PB(I,J), J = 1, NAP)
217 CONTINUE C CC
NPIE = NAP - JCHG
NALPH = (NPIE + JSPIN)/2
NBET = (NPIE - JSPIN)/2
NTOT = NALPH + NBET
WRITE(6,79) NTOT, NPIE, NALPH, NBET
IF(NTOT .NE. NPIE) STOP
NAO = NALPH CC
PRINT 89, NATOM C
IPR = 1
CALL MOLECU(1,1,E,50,EB,EPI,EDCOR,OCH,ESOD)
IPR = 0
IF(NSTEEP.LT.1) GO TO 150 C C STEEPEST DESCENT MINIMIZATION C
DO 160 ITH = 1, NSTEEP
CALL MOLECU(1,1,E,75,EB,EPI,EDCOR,OCH,ESOD)
PRINT 99
IF(ITH.GT.1) GO TO 170 C
PRINT 109
PRINT 119, (ITITLE(I), I = 1, 9) C
PRINT 129, E, EDCOR, EB, EPI, ESOD
CALL INTERO (NBOND, B, D)
IPR = 0
170 CONTINUE
CALL STEEPD(NBOND, D, B, E, STEP)
CALL CART(B,X,AL,NAT3,NATOM)
DO 180 IAT = 1, NATOM
180 WRITE(7,39) (X((IAT-1)*3 + J), J = 1, 3)
160 CONTINUE C
150 CONTINUE

```

```

IF (NSTEEP .EQ. 0) ITH = 1
IPR = 1
CALL MOLECU(-1,1,E,70,EB,EPI,EDCOR,OCH,ESOD) C      DO 190 I=1,NAP C
WRITE (7,59) (R(I,J),J=1,NAP)
190 CONTINUE
DO 200 I=1,NAP
WRITE (7,69) (PA(I,J),J=1,NAP)
200 CONTINUE
DO 210 I=1,NAP
WRITE (7,69) (PB(I,J),J=1,NAP)
210 CONTINUE
IPR = 0
EFIN = E
PRINT 139
PRINT 119,(ITITLE(I),I=1,9)
CALL INTERO (NBOND,B,D)
PRINT 129,E,EDCOR,EB,EPI,ESOD
PRINT 149
DO 220 I=1,NSTEEP
PRINT 159,I,ENS(I),STEPS(I)
220 CONTINUE C C
RETURN C
9 FORMAT(20A4)
19 FORMAT(1H1,20A4)
29 FORMAT(9I5)
39 FORMAT(3F8.4)
49 FORMAT(/,3X,'NAP=' ,I3,' NS=' ,I3,' NSO=' ,I3,' NA=' ,I3,' NAO=' ,I3)
59 FORMAT (8F10.6)
69 FORMAT (8F10.8)
79 FORMAT(/,3X,'NTOT=' ,I4,' NPIE=' ,I4,' NALPH=' ,I4,' NBET=' ,I4)
89 FORMAT ( 30X, 18HNUMBER OF ATOMS = ,I6)
99 FORMAT(//)
109 FORMAT (1H1 , 6X , 30H I N I T I A L R E S U L T S , / 6X , 30H
*-----, /// )
119 FORMAT(24X,18A4)
129 FORMAT (4(/),10X, 19H TOTAL ENERGY = ,F20.10, ' KCAL'
* ,/,1X,'DIAGONAL CORE CONTRIBUTION = ',F20.10,' KCAL'
* ,/ 5X , 25H BOND CONTRIBUTION = , F20.10, ' KCAL'
* ,/,4X,' PI CONTRIBUTION = ',F20.10,' KCAL'
* ,/,2X,'SECOND ORDER CONTRIBUTION = ',F20.10,' KCAL',/)
139 FORMAT (1H1 , 5X , 26H F I N A L R E S U L T S , / 7X , 25H----
*-----, /// )
149 FORMAT(/,10X,'ITERATION HISTORY',/,5X,'ITER',5X,'ENERGY',10X,'STEP
*',/)
159 FORMAT(5X,I4,2(F15.6,1X))
END C-----
SUBROUTINE BFUNC2(I1,J1,BI,F,DF)
IMPLICIT REAL*8 (A-H,P-Z) C MORSE TYPE BOND ENERGY FUNCTION C
CB1 = 87.948D0
BO1 = 1.52645D0
CA = 1.7562D0
DR = BI-BO1
A2 = DEXP(-1.D0*CA*DR)
A1 = A2**2
F = CB1*(A1-2.D0*A2)
DF = -CB1*CA*(2.D0*A1-2.D0*A2)

```

```

RETURN
END C-----
SUBROUTINE VPHI(I1,J1,D,H,BI,DX)
IMPLICIT REAL*8 (A-H,P-Z) C   THIS SUBROUTINE BUILDS THE MATRIX EL-
EMENTS OF H WHICH ARE OF C   THE PPP FORM BETA0*EXP(DELTA*X), WITH
SOK PARAMETRIZATION.
DIMENSION D(1),H(60,60)
DIMENSION DB(60),DX(1)
COMMON/FINAL/B(60),X(180),AL(60),NC(60)
COMMON/CONTRO/NATOM,NBOND,NAP,NAO,NAT3
COMMON/MAT/BMAT(60,60),GMAT(60,60),HCORM(60,60)
COMMON/PII/JCHG,NALPH,NBET,NPIE,JSPIN,JUHF   C.....SET   CONSTANTS
C.....SOK PARAMETERS
B0 = -2.0419D0
DEL = 1.2518D0
R0 = 1.536D0
CON = 23.062D0 C
DR1 = R0-BI
BEXP = DEXP(DEL*DR1)
VBB = B0*BEXP
PCON = 2.D0*BMAT(I1,J1)
VPB = CON*PCON
H(I1,J1) = H(I1,J1) + VBB
H(J1,I1) = H(I1,J1)
I3 = (I1-1)*3
J3 = (J1-1)*3
DVPBDB = -DEL*VBB
DF = DVPBDB*VPB C           CALL DFBON(DX,DB,BI,AL,I1,J1) C           CALL
DBD(I1,J1,DF,DB,D,NBOND)
D(I1) = DF
RETURN
END C-----
FUNCTION LENGTH(DX)
IMPLICIT REAL*8 (A-H,P-Z) C   THIS FUNCTION EQUALS THE LENGTH OF
VECTOR DX
DIMENSION DX(3)
REAL*8 LENGTH C
S = 0.0D0
DO 10 I = 1, 3
10  S = S + DX(I) * DX(I)
LENGTH = DSQRT(S)
RETURN
END C-----
SUBROUTINE BONDP(E,H)
IMPLICIT REAL*8 (A-H,P-Z) C C   THIS SUBROUTINE COMPUTES THE BOND
CONTRIBUTIONS TO E , D AND DD C
COMMON/FINAL/B(60),X(180),AL(60),NC(60)
COMMON/DER/D(60),DR(60),DV(60),VOP(60,60),DT(60)
COMMON/CONTRO/NATOM,NBOND,NAP,NAO,NAT3
DIMENSION H(60,60)
DIMENSION DB(60),DX(3)
REAL*8 LENGTH C
DO 10 I1 = 1,NBOND
J1 = I1 + 1
I3 = (I1-1)*3
J3 = (J1-1)*3

```

```

DO 20 J = 1,3
20  DX(J)=X(J3+J)-X(I3+J) C
    BI = LENGTH(DX)
    B(I1) = BI
    CALL DFBON(DX,DB,BI,AL,I1,J1) C C...CALL BOND ENERGY FUNCTION
    CALL BFUNC2(I1,J1,BI,F,DF) C C...ADD DIAGONAL CONTRBUTIONS TO
H-MATRIX
    CALL VPHI(I1,J1,DV,H,BI,DX) C    PACK 1ST DERIVATIVE VECTOR D AND
TOTAL ENERGY E
    E = E + F C
    D(I1) = DF C
10  CONTINUE C
    RETURN
END C-----
SUBROUTINE DFBON (X,DB,R,AL,I,J)
IMPLICIT REAL*8 (A-H,P-Z) C    THIS SUBROUTINE RETURNS THE 1ST AND
2ND DERIVATIVES OF R(I,J) C
DIMENSION X(3),DB(1),AL(1) C C    1ST DERIVATIVES C C
R1 = 1.0D0/R
R3 = R1**3
I1 = I-1
M = J-I
DO 10 K = 1,M
10  DB(K) = R1*(X(1)*DCOS(AL(I1 + K)) + X(2)*DSIN(AL(I1 + K)))
    RETURN
END C-----
SUBROUTINE DBD(I3,J3,DF,DB,D,NB)
IMPLICIT REAL*8 (A-H,P-Z) C    CONSTRUCTION OF THE D VECTOR AND THE
DD MATRIX FOR ATOM PAIR C
DIMENSION D(1),DB(1) C C    PACK 1ST DERIVATIVES VECTOR D
I1 = I3-1
M = J3-I3
DO 10 K = 1,M
    DBX = DB(K)*DF
10  D(I1 + K) = D(I1 + K) + DBX
    RETURN
END C-----
SUBROUTINE INTERO (NB,B,D)
IMPLICIT REAL*8 (A-H,P-Z)
COMMON/CONTRO/NATOM,NBOND,NAP,NAO,NAT3 C C    THIS SUBROUTINE
PRINTS OUT THE INTERNAL COORDINATES C
DIMENSION B(1),D(1) C
PRINT 9
PRINT 19
DO 10 I = 1 , NB
    I1 = I-1
    IF(I1) 20,20,30
30  DELR = B(I)-B(I1)
    GO TO 40
20  DELR = 0.0000D0
40  CONTINUE
    PRINT 29, B(I) ,DELR,D(I),I
10  CONTINUE C
    PRINT 19 C
    RETURN
9  FORMAT( 2X,'BOND LENGTHS',5X,'DELTA R',5X,'DERIVATIVE',3X,'BOND',

```

```

&/)
19 FORMAT( 1H )
29 FORMAT( 3(2X,F10.4),9X,I4)
END C-----
SUBROUTINE STEEPD (N,D,B,E,STEP)
IMPLICIT REAL*8 (A-H,P-Z) C STEEPD CALCULATES THE BOND SHIFTS US-
ING THE METHOD OF C STEEPEST DESCENT
COMMON/ENSTOR/ENS(20),STEPS(20),ITH
DIMENSION D(1),B(1) C
ENS(ITH) = E
IF(ITH.NE.1) GO TO 10 C
STEP = 0.002D0
GO TO 40 C
10 CONTINUE
IF ( ENS ( ITH ) - ENS( ITH - 1 ) ) 30, 20, 20 C
20 CONTINUE
STEP = 0.75D0*STEP
GO TO 40 C
30 CONTINUE
STEP = STEP * 1.2D0
40 CONTINUE
STEPS( ITH ) = STEP
S = 0.0D0
DO 50 I = 1, N
50 S = S + D( I ) * D( I ) C
S = S/N
S = DSQRT( S )
S = STEP/S
DO 60 I = 1, N
60 B( I ) = B( I ) - S * D( I )
RETURN
END C-----
SUBROUTINE MOLECU(IHF,ISF,E,MXIT,EB,EPI,EDCOR,OCH,ESOD) C THIS
SUBROUTINE CALLS ALL THE ENERGY FUNCTIONS
IMPLICIT REAL*8 (A-H,P-Z)
CHARACTER OCH(60)
COMMON/UHF/PA(60,60),PB(60,60)
COMMON/PII/JCHG,NALPH,NBET,NPIE,JSPIN,JUHF
COMMON/SW/ISW,IPR,ISCR
COMMON/POL/RI(60,60),P(60,60)
COMMON/DER/DBND(60),DREP(60),DVPH(60),VOP(60,60),D(60)
COMMON/HH/H(60,60),R(60,60),PT(60,60),Z(60)
COMMON/MAT/BMAT(60,60),GMAT(60,60),HCORM(60,60)
COMMON/FINAL/B(60),X(180),AL(60),NC(60)
COMMON/CONTRO/NATOM,NBOND,NAP,NAO,NAT3
COMMON/SCR/S1(60,60),S2(60,60),S3(60,60),S4(60)
COMMON/EIS/FV1(60),FV2(60),MATZ
DATA CON/23.062D0/
DATA ALPHA1/-11.13D0/
DATA ZERO/0.D0/
MATZ = 1
E = ZERO
EB = ZERO
EPI = ZERO
EDCOR = ZERO
DMAX = 1.D-05

```

```

KMAX = 3 C
DO 10 I = 1, NBOND
  DBND(I) = ZERO
  DREP(I) = ZERO
  DVPH(I) = ZERO
  IF (DABS(D(I)) .GT. DMAX) DMAX = DABS(D(I))
10  D(I) = ZERO
  IF (DMAX .LT. 10.D0) KMAX = 5
  IF (IHF .NE. 0 ) GO TO 20 C...DO A HUCKEL CALCULATION
  CALL INIT (S1)
  DO 30 I = 1, NAP
    IM1 = I-1
    S1(I,IM1) = -2.3848D0
    S1(IM1,I) = -2.3848D0
    S1(I,I) = -9.81D0
30  CONTINUE
  CALL RS(60, NAP, S1, S4, MATZ, S2, FV1, FV2, IERR)
  CALL DENA(S2, PA, NAP, NALPH, 1)
  CALL DENA(S2, PB, NAP, NBET, 2)
  DO 50 I = 1, NAP
    DO 60 J = 1, I
      BMAT(I,J) = PA(I,J) + PB(I,J)
      BMAT(J,I) = BMAT(I,J)
      GMAT(I,J) = 0.5D0*(PA(I,I)*PA(J,J)-PA(I,J)**2
X   + PB(I,I)*PB(J,J)-PB(I,J)**2
X   + PA(I,I)*PB(J,J) + PA(J,J)*PB(I,I)
X   -(PA(I,I) + PA(J,J) + PB(I,I) + PB(J,J)-Z(I)*Z(J)))
      GMAT(J,I) = GMAT(I,J)
60  CONTINUE
      GMAT(I,I) = ZERO
50  CONTINUE C   CALL VEFF(NAP, NBOND, 2)
      CALL VZERO(NAP, R, 0) C   IF (IPR .NE. 1 ) GO TO 20 C   WRITE (6,9) C   CALL
OUTPUT (S1, NAP, 2, NC, OCH)
20  CONTINUE
  IF (IHF .NE. 0) CALL VZERO(NAP, R, 0)
  DO 80 I = 1, NAP
    Z(I) = 1.D0
    DO 90 J = 1, NAP
      H(I,J) = ZERO
90  CONTINUE
      H(I,I) = ALPHA1
80  CONTINUE
      DO 100 I = 1, NAP
        EDCOR = EDCOR + CON*H(I,I)*(-Z(I))
100 CONTINUE
      CALL BONDP(EB, H)
      CALL SCF(IHF, ISF, MXIT, EPI, KMAX, OCH, ESOD)
      CALL VPRIME(NAP, NBOND)
      DO 110 IB = 1, NBOND
        D(IB) = DREP(IB) + DBND(IB) + DVPH(IB)
110 CONTINUE
      IF (IPR .NE. 1) GO TO 120
      PRINT 19
      DO 130 ID = 1, NBOND
        PRINT 29, ID, DBND(ID), DREP(ID), DVPH(ID), D(ID)
130 CONTINUE

```

```

120 CONTINUE
    E = EDCOR + EB + EPI + ESOD
    RETURN
9  FORMAT (//,3X,'UNMODIFIED REPULSION INTEGRAL MATRIX',//)
19  FORMAT(/,1X,'BOND',7X,'DBND',7X,'DREP',7X,'DVPHI',6X,'DTOT',/)
29  FORMAT(2X,14,2X,4(F10.3,2X))
39  FORMAT (//,3X,'F.S. SCREENED REPULSION INTEGRAL MATRIX',//)
    END C-----
    SUBROUTINE SCF(IHF,ISF,MXIT,EPI,KMAX,OCH,ESOD)
    IMPLICIT REAL*8 (A-H,P-Z)
    CHARACTER OCH(60)
    COMMON/ISEC/ISOA,ISOB,ISOC,ISOD,IDMP
    COMMON/MAT/BMAT(60,60),GMAT(60,60),HCORM(60,60)
    COMMON/FINAL/B(60),X(180),AL(60),NC(60)
    COMMON/CONTRO/NATOM,NBOND,NAP,NAO,NAT3
    COMMON/PII/JCHG,NALPH,NBET,NPIE,JSPIN,JUHF
    COMMON/SW/ISW,IPR,ISCR
    COMMON/UHF/PA(60,60),PB(60,60)
    COMMON/HH/H(60,60),R(60,60),PT(60,60),Z(60)
    COMMON/POL/RI(60,60),P(60,60)
    COMMON/EIG/V(60,60),EA(60),VB(60,60),EB(60)
    DIMENSION FB(60,60),FA(60,60),PP(60),SP(60),S(60,60),SB(60,60)
    DIMENSION A1(60,60),A2(60,60),S1(60)
    DATA CON/23.062D0/
    DATA ZERO/0.D0/
    IF(NAP.LE.1) GO TO 65
    MMS = 2
    IF (NALPH .EQ. NBET) MMS = 1
    CF = 1.D0
    KONT = 0
5  CONTINUE
    KONT = KONT + 1
    DO 10 I = 1,NAP
        DO 20 J = 1,I
            HCORM(I,J) = H(I,J)
            HCORM(J,I) = H(I,J)
20  CONTINUE
        X1 = ZERO
        DO 30 K = 1,NAP
            IF(K.NE.I) X1 = X1 + R(I,K)
30  CONTINUE
        HCORM(I,I) = HCORM(I,I) - X1
        S1(I) = ZERO
10  CONTINUE
    KOUNT = 1
15  CONTINUE C C...INITIALIZE ARRAYS AND ENERGIES C
    CALL INIT(S)
    CALL INIT(SB)
    CALL INIT(A1)
    CALL INIT(A2)
    ISND = 0
    EOLD = ETOT
    ETOT = ZERO
    ESOD = ZERO
    ESODA = ZERO
    ESODB = ZERO

```

```

DO 140 I= 1,NAP
S1(I)= ZERO
140 CONTINUE C..... C....
IF (KOUNT .LT. 2 ) GO TO 75
IF (ISOA.NE.0.OR.ISOB.NE.0) ISND= 1
IF (ISOC.NE.0.OR.ISOD.NE.0) ISND= 2
IF (ISOA.NE.0) CALL SN2A(R,NAP,S1)
IF (ISOB.NE.0) CALL SN2B(R,PT,NAP,S1)
IF (ISOC.NE.0) CALL SN2C(NAP,NALPH,S,V,EA,R,PA)
IF (ISOC.NE.0) CALL SN2C(NAP,NBET,SB,VB,EB,R,PB)
IF (ISOD.NE.0) CALL SN2D(NAP,NALPH,S,V,EA,R)
IF (ISOD.NE.0) CALL SN2D(NAP,NBET,SB,VB,EB,R)
DO 120 I= 1,NAP
S(I,I)= S(I,I)+ S1(I)
SB(I,I)= SB(I,I)+ S1(I)
120 CONTINUE
75 CONTINUE
DO 1 I= 1,NAP
DO 2 J= 1,I
PA1(I,J)= PA(I,J)
PA1(J,I)= PA(J,I)
PA2(I,J)= PB(I,J)
PA2(J,I)= PB(J,I)
2 CONTINUE
1 CONTINUE C C...ALPHA ORBITALS C
CALL UHFOCK(R,PA,PB,FA,NAP,S)
IF(ISND.NE.0.AND.IDMP .NE. 0) CALL EDAMP(V,FA,NAP,NALPH,A1,CF,1)
CALL SYDI(NAP,FA,V,EA,1)
CALL DENA(V,PA,NAP,NALPH,1) C C...BETA ORBITALS C
CALL UHFOCK(R,PB,PA,FB,NAP,SB)
IF(ISND.NE.0.AND.IDMP .NE. 0) CALL EDAMP(VB,FB,NAP,NBET,A2,CF,2)
CALL SYDI(NAP,FB,VB,EB,MMS)
CALL DENA(VB,PB,NAP,NBET,2)
115 CONTINUE C C..CALCULATE TOTAL DENSITY MATRIX C
DO 40 I= 1,NAP
DO 50 J= I,NAP
PT(I,J)= PA(I,J)+ PB(I,J)
PT(J,I)= PT(I,J)
BMAT(I,J)= PT(I,J)
BMAT(J,I)= BMAT(I,J)
50 CONTINUE
40 CONTINUE C C...CALCULATE SECOND ORDER SELF ENERGY CONTRIB-
UTION C
IF (ISND .EQ. 0) GO TO 125
CALL SECE(NAP,PA,S,ESODA)
CALL SECE(NAP,PB,SB,ESODB)
ESOD= -0.5D0*(ESODA+ ESODB)
WRITE (6,169) ESOD
125 CONTINUE C C..CALCULATE UHF ELECTRONIC ENERGY C
DO 60 I= 1,NAP
DO 70 J= 1,NAP
FA(I,J)= FA(I,J)-S(I,J)
FB(I,J)= FB(I,J)-SB(I,J)
ETOT= ETOT+ 0.5D0*(PT(J,I)*HCORM(I,J)+ PA(J,I)*(FA(I,J)-A1(I,J))
* + PB(J,I)*(FB(I,J)-A2(I,J)))
70 CONTINUE

```

```

60 CONTINUE
ETOT = ETOT + ESOD C C..TEST ENERGY FOR SCF CONVERGENCE C
IF (KOUNT .EQ. 1) EOLD = 2.D03
DEV = (ETOT - EOLD) / EOLD
IF (DABS(DEV) .LT. 5.D-06) GO TO 25
IF (KOUNT .GE. MXIT) GO TO 25
KOUNT = KOUNT + 1
2600 IF (KOUNT .LT. MXIT) GO TO 15
25 CONTINUE C C...TEST ENERGY FOR R-MATRIX CONVERGENCE C
IF (KONT .EQ. 1) EPAST = 2.D03
DEV1 = (EPAST - ETOT) / EPAST
IF (DABS(DEV1) .LT. 1.D-05) GO TO 85
IF (KONT .GE. KMAX) GO TO 85
IF (ISCR .NE. 0) CALL VEFF(NAP, NBOND, 1)
EPAST = ETOT
GO TO 5
85 CONTINUE C C...PERFORM SPIN PROJECTION C
CALL PROJ(HCORM, EPII, OCH, NC, R) C C...ADD Z(I)*Z(J)*R(I,J) TO PI ENERGY
C
EP = ZERO
DO 80 I = 2, NAP
  I1 = I - 1
  DO 90 J = 1, I1
    EP = EP + Z(I) * Z(J) * R(I, J)
90 CONTINUE
80 CONTINUE C C  EPI = CON * (ETOT - ESOD + EP)
EPI = CON * (EPII + EP)
ESOD = CON * ESOD C
PRINT 39, KOUNT, DEV C C  GO TO 451
452 IF (IPR .EQ. 0) GO TO 45 C C...PRINT DENSITY MATRICES, EIGENVECTORS AND
EIGENFUNCTIONS C C  WRITE(6, 179) C  CALL OUTPUT (S, NAP, 2, NC, OCH) C
WRITE(6, 189) C  CALL OUTPUT (SB, NAP, 2, NC, OCH)
  WRITE (6, 19)
  CALL OUTPUT (R, NAP, 2, NC, OCH) C  WRITE (6, 29) C  CALL OUTPUT
(H, NAP, 2, NC, OCH)
  PRINT 49
  CALL OUTPUT (PT, NAP, 2, NC, OCH)
  PRINT 59
  CALL OUTPUT (PA, NAP, 2, NC, OCH)
  PRINT 69
  CALL OUTPUT (PB, NAP, 2, NC, OCH)
  PRINT 79
  WRITE (6, 89) (EA(I), I = 1, NAP)
  PRINT 99
  CALL OUTPUT (V, NAP, 2, NC, OCH)
  PRINT 109
  WRITE (6, 89) (EB(I), I = 1, NAP)
  PRINT 119
  CALL OUTPUT (VB, NAP, 2, NC, OCH) CC
451 DO 100 I = 1, NAP
  SP(I) = PA(I, I) - PB(I, I) C  PP(I) = PT(I, I)
100 CONTINUE
  WRITE (6, 129)
  WRITE (6, 139) (I, SP(I), I = 1, NAP) C C...CALCULATE SPIN DENSITY RATIO C
SPOS = ZERO
SNEG = ZERO

```

```

DO 110 I= 1,NAP
  IF(SP(I) .LT. ZERO) GO TO 55
  SPOS = SPOS + SP(I)
  GO TO 110
55  SNEG = SNEG + SP(I)
110 CONTINUE
  SRAT = DABS(SNEG/SPOS)
  WRITE(6,149) SRAT C   WRITE(6,159) C   WRITE (6,139) (I,PP(I), I= 1,NAP) C
45 CONTINUE
65 CONTINUE
  RETURN C
  9 FORMAT (/ ,2X, 'ITERATION' ,I3,/)
  19 FORMAT (// ,2X, 'REPULSION MATRIX',//)
  29 FORMAT (// ,2X, 'H-MATRIX',//)
  39 FORMAT(// ,1X, ' AFTER ',I3, ' ITERATIONS, SCF DEVIATION ',D15.9,/)
  49 FORMAT (///5X, 'TOTAL DENSITY MATRIX',/)
  59 FORMAT (///5X, 'ALPHA-MATRIX',/)
  69 FORMAT (///5X, 'BETA-MATRIX',/)
  79 FORMAT (/ ,2X, 'ALPHA EIGENVALUES',/)
  89 FORMAT (5(2X,F8.4))
  99 FORMAT (/ ,2X, 'ALPHA ORBITALS',/)
  109 FORMAT (/ ,2X, 'BETA EIGENVALUES',/)
  119 FORMAT (/ ,2X, 'BETA ORBITALS',/)
  129 FORMAT (// ,2X, 'DIAGONAL SPIN DENSITY')
  139 FORMAT (5(I3,3X,F12.6,6X))
  149 FORMAT(/ ,10X, 'NEG. TO POS. S.D. RATIO = ',F12.8) C 159 FORMAT
(// ,2X, 'DIAGONAL CHARGE DENSITY')
  169 FORMAT (/ ,23X, 'SECOND ORDER ENERGY IS ',F12.6, ' EV ')
  179 FORMAT (/ ,3X, 'ALPHA 2ND ORDER MATRIX ELEMENTS',/)
  189 FORMAT (/ ,3X, 'BETA 2ND ORDER MATRIX ELEMENTS',/) C
  END C-----
  SUBROUTINE EDAMP(C,FA,NAP,NOC,A,CF,IA)
  IMPLICIT REAL*8 (A-H,P-Z) C....SUBROUTINE ADDS CONSTANT TO UNOCU-
PIED ORBITAL TO MIN. MIXING
  COMMON/SELF/DMP,CON
  DIMENSION C(60,60),FA(60,60),A(60,60)
  NOC1 = NOC + 1
  IF (IA .EQ. 2) GO TO 5
  CON = DMP*CF
  5 CONTINUE
  DO 10 I= 1,NAP
    DO 10 J= 1,NAP
      DELA = 0.D0
      DO 20 K = NOC1,NAP
        20  DELA = DELA + C(I,K)*C(J,K)
      10  A(I,J) = CON*DELA*CF
      DO 30 I= 1,NAP
        DO 30 J= 1,NAP
          30  FA(I,J) = FA(I,J) + A(I,J)
      IF (IA .EQ. 2) GO TO 15
      CF = 0.65D0*CF
  15 CONTINUE
  WRITE (6,9) CON
  9 FORMAT(3X, 'CON = ',F12.6)
  RETURN
  END C-----

```

```

SUBROUTINE SN2A(V,N,S)
  IMPLICIT REAL*8 (A-H,P-Z) C...SUBROUTINE CALCULATES SECOND ORDER
SELF-ENERGY MATRIX ELEMENTS FOR C...DIAGRAM 2A
  COMMON/EIG/C1(60,60),EA(60),C2(60,60),EB(60)
  COMMON/UHF/PA(60,60),PB(60,60)
  COMMON/PII/JCHG,NA,NB,NPIE,JSPIN,JUHF
  COMMON/SELF/DMP1,DMP2
  DIMENSION V(60,60),S(1)
  NAP=NA+1
  NBP=NB+1 C...FOR ODD ELECTRON SYSTEMS ONLY
  N2=(N+1)/2
  DO 5 I=1,N2
  TEMP4=S(I)
  DO 10 IR=1,N
    DO 10 IS=1,N
      PVA=PA(IR,IS)*V(IR,IS)
      PVB=PB(IR,IS)*V(IR,IS)
      DO 10 IT=1,N
        V1=V(I,IT)
        DO 20 L=1,NA
          TEMP1=C1(IR,L)
          TEMP2=C1(IT,L)
          TEMP3=EA(L)
          DO 20 M=NAP,N
            DELE=TEMP3-(EA(M)-DMP2)
            CS=TEMP1*C1(IS,M)
            C=CS*PVA*V1*TEMP2*C1(IT,M)/DELE
            TEMP4=TEMP4-C
20          CONTINUE
          DO 21 L=1,NB
            TEMP1=C2(IR,L)
            TEMP2=C2(IT,L)
            TEMP3=EB(L)
            DO 21 M=NBP,N
              DELE=TEMP3-(EB(M)-DMP2)
              CS=TEMP1*C2(IS,M)
              C=CS*PVB*V1*TEMP2*C2(IT,M)/DELE
              TEMP4=TEMP4-C
21          CONTINUE
10 CONTINUE
  S(I)=2.D0*TEMP4
  IP=N+1-I
  S(IP)=S(I)
5 CONTINUE
  RETURN
  END C-----
SUBROUTINE SN2B(V,PT,N,S)
  IMPLICIT REAL*8 (A-H,P-Z) C...SUBROUTINE CALCULATES SECOND ORDER
SELF-ENERGY MATRIX ELEMENTS FOR C...DIAGRAM 2B
  COMMON/EIG/C1(60,60),EA(60),C2(60,60),EB(60)
  COMMON/PII/JCHG,NA,NB,NPIE,JSPIN,JUHF
  COMMON/SELF/DMP1,DMP2
  DIMENSION V(60,60),PT(60,60)
  DIMENSION S(1)
  NAP=NA+1
  NBP=NB+1 C...FOR ODD ELECTRON SYSTEMS ONLY

```

```

N2=(N+1)/2
DO 5 I=1,N2
  TS=S(I)
DO 10 IR=1,N
  U1=V(I,IR)
  DO 10 IS=1,N
    PVA=PT(IS,IS)*U1
    DO 10 IT=1,N
      V1=V(IS,IT)
      DO 20 L=1,NA
        T1=C1(IR,L)
        T2=C1(IT,L)
        T3=EA(L)
        DO 20 M=NAP,N
          DELE=T3-(EA(M)-DMP2)
          CS=T1*C1(IR,M)*T2*C1(IT,M)
          C=CS*PVA*V1/DELE
          TS=TS+C
20      CONTINUE
      DO 21 L=1,NB
        T1=C2(IR,L)
        T2=EB(L)
        T3=C2(IT,L)
        DO 21 M=NBP,N
          DELE=T2-(EB(M)-DMP2)
          CS=T1*C2(IR,M)*T3*C2(IT,M)
          C=CS*PVA*V1/DELE
          TS=TS+C
21      CONTINUE
10 CONTINUE
  S(I)=2.D0*TS
  IP=N+1-I
  S(IP)=S(I)
5 CONTINUE
RETURN

```

END C-----
SUBROUTINE SN2C(N,NOCC,S,C1,EA,V,PA) C...SUBROUTINE CALCULATES
SECOND ORDER MATRIX ELEMENTS FOR DIAGRAM C 2C

```

IMPLICIT REAL*8 (A-H,P-Z)
COMMON/HH/H(60,60),R(60,60),PT(60,60),Z(60)
COMMON/PII/JCHG,NA,NB,NPIE,JSPIN,JUHF
COMMON/SELF/DMP1,DMP2
DIMENSION S(60,60),V(60,60),C1(60,60),EA(60),PA(60,60)
DATA TWO/2.D0/
DATA ZERO/0.D0/
NOCCP=NOCC+1
DO 5 I=1,N
  DO 5 J=1,I
    V1=V(I,J)
    TS=S(I,J)
    DO 10 IR=1,N
      DO 10 IT=1,N
        PAVV=PA(IR,IT)*V(IR,IT)*V1
        DO 20 L=1,NOCC
          X1=EA(L)
          X2=C1(IR,L)*PAVV

```

```

        X4=C1(J,L)
        X5=C1(I,L)
        DO 20 M=NOCCP,N
        DELE = X1-(EA(M)-DMP2)
        CR = X2*C1(IT,M)
        C = CR*(X5*C1(J,M) + X4*C1(I,M))/DELE
        TS = TS + C
20 CONTINUE
10 CONTINUE
   S(I,J) = TS
   S(J,I) = TS
5 CONTINUE
   RETURN
   END C-----
SUBROUTINE SN2D(N,NOCC,S,C,E,V) C...SUBROUTINE CALCULATES SECOND
ORDER MATRIX ELEMENTS FOR DIAGRAM C 2D
   IMPLICIT REAL*8 (A-H,P-Z)
   COMMON/HH/H(60,60),R(60,60),PT(60,60),Z(60)
   COMMON/SELF/DMP1,DMP2
   DIMENSION S(60,60),C(60,60),E(60),V(60,60)
   DATA TWO/2.D0/
   DATA ZERO/0.D0/
   NOCCP = NOCC + 1
   DO 10 I = 1,N
     DO 10 J = 1,I
       TS = S(I,J)
       V1 = V(I,J)
       DO 20 L = 1,NOCC
         T1 = C(I,L)
         T2 = C(J,L)
         T3 = E(L)
         DO 20 M = NOCCP,N
           C1 = T1*C(J,M) + C(I,M)*T2
           DELE = T3-(E(M)-DMP2)
           DO 30 IR = 1,N
             DO 30 IS = 1,N
               CT = C(IS,L)*C(IS,M)*C1
               TS = TS-CT*PT(IR,IR)*V1*V(IR,IS)/DELE
30 CONTINUE
20 CONTINUE
   S(I,J) = TS
   S(J,I) = TS
10 CONTINUE
   RETURN
   END C-----
SUBROUTINE SNDE (N,P,S,E) C C...ENERGY ROUTINE USED IF SELF-ENERGY
MATRIX IS DIAGONAL C
   IMPLICIT REAL*8 (A-H,P-Z) C...SUBROUTINE CALCULATES ENERGY CON-
TRIBUTION OF SECOND ORDER SELF- C...ENERGY FOR DIAGRAMS 2A & 2B
   DIMENSION P(60,60),S(1)
   DO 10 I = 1,N
     E = E + S(I)*P(I,I)
10 CONTINUE
   RETURN
   END C-----
SUBROUTINE SECE(N,P,S,EA)

```

```

IMPLICIT REAL*8(A-H,P-Z)
DIMENSION P(60,60),S(60,60)
DO 10 I= 1,N
  DO 10 J= 1,N
    EA = EA + S(I,J)*P(I,J)
10 CONTINUE
RETURN
END C-----
SUBROUTINE SYDI(NAP,FA,V,EA,MMS)
IMPLICIT REAL*8(A-H,P-Z)
COMMON/EIS/FV1(60),FV2(60),MATZ
COMMON/AAA/ED(60),FD(60,60),FVD(60,60),CD(60,60)
COMMON/SYM/S(60,60),ST(60,60),NSM(2),NOCC(2)
DIMENSION FA(60,60),V(60,60),EA(60),E1(60),E2(60) C..BLOCK FACTOR
CALL MMULT(FA,S,CD,NAP)
CALL MMULT(ST,CD,FVD,NAP)
NS1 = NSM(1)
CALL INIT (FA)
DO 10 I= 1,NS1
  DO 10 J= 1,NS1
    FA(I,J) = FVD(I,J)
10 CONTINUE
CALL RS(60,NS1,FA,E1,MATZ,FD,FV1,FV2,IERR)
NS2 = NSM(2)
CALL INIT (FA)
DO 20 I= 1,NS2
  I1 = I + NS1
  DO 20 J= 1,NS2
    J1 = J + NS1
    FA(I,J) = FVD(I1,J1)
20 CONTINUE
CALL RS(60,NS2,FA,E2,MATZ,CD,FV1,FV2,IERR)
CALL INIT (FVD)
NOC1 = NOCC(1)
IF(MMS.EQ.2) NOC1 = NOC1-1
NOC11 = NOC1 + 1
DO 30 I= 1,NS1
  DO 30 K = NOC11,NS1
    KP = NS2 + K
    EA(KP) = E1(K)
    FVD(I,KP) = FD(I,K)
30 CONTINUE
DO 40 K = 1,NOC1
  DO 40 I= 1,NS1
    EA(K) = E1(K)
    FVD(I,K) = FD(I,K)
40 CONTINUE
NOC2 = NOCC(2)
DO 50 K = 1,NS2
  KP = K + NOC1
  DO 60 I= 1,NS2
    IP = I + NS1
    EA(KP) = E2(K)
    FVD(IP,KP) = CD(I,K)
60 CONTINUE
50 CONTINUE C..BACK TRANSFORM

```

```

CALL MMULT(S,FVD,V,NAP)
RETURN
END C-----
SUBROUTINE PROJ(HCORE,EPI,OCH,NC,GAM)
IMPLICIT REAL*8 (A-H,P-Z)
CHARACTER OCH(60)
DIMENSION HCORE(60,60)
COMMON/UHF/RHOA(60,60),RHOB(60,60)
COMMON/CONTRO/NATOM,NBOND,NAP,NAO,NAT3
COMMON/MAT/BMAT(60,60),GMAT(60,60),HCORM(60,60)
COMMON/AAA/ED(60),FD(60,60),FVD(60,60),CD(60,60)
COMMON/PII/JCHG,NALPH,NBET,NPIE,JSPIN,JUHF
COMMON/SW/ISW,IPR,ISCR
COMMON/SYM/S(60,60),ST(60,60),NSM(2),NOCC(2)
COMMON/BLK5/N,M,NA,NB,NM,NPP,NAM,NBP,KIK
DIMENSION FA(61,61),CC(60,60),GAM(60,60)
DIMENSION CA(60,60),CB(60,60),EB(60),EA(60)
DIMENSION NC(60)
DIMENSION AX(60),BE(60),BX(60)
DIMENSION DELW(60),SPIN(61)
DIMENSION A2IJ(60),B(61),A(61),Q(60),SOMEGA(60)
DIMENSION T(60),U(60)
DIMENSION CSK(30,2),C0(2)
DATA ZERO/0.D0/ C C      CALCULATION OF BETA-ELECTRON CORRE-
SPONDING ORBITALS. C      REFERRED TO IN REF. (1) AS THE SET OF B(I). C
EIGENVALUES ARE D(I)**2 OF REF. (1). C
CALL MMULT(RHOA,RHOB,CD,NAP)
CALL MMULT(RHOB,CD,CC,NAP)
CALL SYMCOR(NAP,CC,CB,EB) C C      SET CONSTANTS C
NA = NALPH
NB = NBET
NBP = NB + 1
NAM = NA - 1
NBM = NB - 1
XNA = DFLOAT(NA)
XNB = DFLOAT(NB)
XM = 0.5D0*(XNA - XNB)
XN = 0.5D0*(XNA + XNB)
M = NA + NB
MP = M + 1
S2 = XM
MU = NA - NB + 1
MO = NA - NB
XAO1 = ZERO
XAT1 = ZERO
XATOT = ZERO
TOTSP = ZERO
N = NAP C C      INITIALIZE ARRAYS AND INVERT ORDER OF BETA
EIGENVALUES(EB'S) C
DO 10 I = 1,N C      SOMEGA(I) = EB(N-I + 1)
10 A(I) = ZERO
DO 20 I = 1,N
IF(EB(I) .LT. ZERO) EB(I) = ZERO
20 IF(EB(I) .GT. 1.D0) EB(I) = 1.D0 C C      THE EB(I) ARE THE D(I)**2 OF REF. (1).
C      THE EA(I) ARE EQUAL TO E(I)**2 OF REF. (1). C
DO 30 I = 1,NB

```

```

B(I) = ZERO
30 EA(I) = 1.D0-EB(I)
  I = 1
  B(I) = 1.D0
  A(I) = 1.D0
  B(NBP) = 1.D0
  A(NBP) = 1.D0
  IF (IPR .EQ. 0) GO TO 716
  WRITE(6,9)
  WRITE(6,19)(EB(I),I= 1,N)
716 CONTINUE C C      CALCULATE SUMS OF CONTINUING PRODUCTS C
  FA(1,1) = EB(1)
  FA(2,1) = ZERO
  IF(NB.LE.1)GO TO 135
  DO 50 J = 2,NB
  JM = J-1
  FA(1,J) = FA(1,JM) + EB(J)
  DO 40 K = 2,J
40 FA(K,J) = FA(K,JM) + EB(J)*FA(K-1,JM)
  FA(J+1,J) = ZERO
50 CONTINUE
135 DO 60 I = 1,NB
60 A(I+1) = FA(I,NB) C C      THESE ARE HARRIMAN'S ASUBK.  SEE EQN. (21)
OF REF. (2) C
  FA(1,1) = EA(1)
  FA(2,1) = ZERO
  IF(NB.LE.1)GO TO 145
  DO 80 J = 2,NB
  JM = J-1
  FA(1,J) = FA(1,JM) + EA(J)
  DO 70 K = 2,J
70 FA(K,J) = FA(K,JM) + EA(J)*FA(K-1,JM)
  FA(J+1,J) = ZERO
80 CONTINUE
145 DO 90 I = 1,NB
90 B(I+1) = FA(I,NB) C C      THESE ARE BSUBK OF REFS. (1), (2), AND (3).  C C
CALCULATION OF WEIGHTS FROM EQN. (26) OF REF. (1).  C
  DO 110 I = 1,NBP
  SI = XM + I-1.D0
  XZ = XN-SI
  MM = XZ + 1.01
  IS = 2.*SI + 0.01
  MS = SI + XM + 0.01
  NS = SI-XM + 0.01
  XS = DFLOAT(IS)
  SOMEGA(I) = ZERO
  DO 100 J = 1,MM
  JM = J-1
100 SOMEGA(I) = SOMEGA(I) + (-1.D0)**JM*(F(NS + JM,1)**2*B(NS + J))/(F(IS + J,1)
  1*F(JM,1))
  SOMEGA(I) = (XS + 1.D0)*F(MS,1)*SOMEGA(I)/F(NS,1)
  IM = I-1
  IF (IPR .NE. 1 .OR. I .GT. 5) GO TO 110
  WRITE(6,39)SI,SOMEGA(I)
110 CONTINUE C C      CALCULATE NATURAL ORBITALS OF CHARGE DENSITY
C

```

```

DO 7 IL= 1,N
DO 7 J= 1,N
CC(IL,J)= RHOA(IL,J)+ RHOB(IL,J)
7 FA(IL,J)= ZERO
CALL SYMNAT(NAP,CC,CA,EA)
DO 120 I= 1,N
IF (EA(I) .GT. 2.D0) EA(I)= 2.D0
120 IF (EA(I) .LT. ZERO) EA(I)= ZERO C C      CALCULATION OF A(K + 1)'S FROM
RECURSION RELATION C
DO 150 I= 1,N
150 FA(1,I)= 1.D0
FD(1,1)= FA(1,1)
DO 180 I= 2,NB
IM= I-1
DO 170 J= 1,NB C C      EQN. (31) OF REF. (2) C
FA(I,J)= A(I)-EB(J)*FA(IM,J)
170 FD(I,J)= FA(I,J)
180 CONTINUE C C      FA(K,L) IS ASUBK(L) OF REF. (2) C C C      CORRECT
PHASES OF NATURAL ORBITALS TO INSURE THAT TSUBI AND C      USUBI ARE
POSITIVE. SEE EQNS. (14), AND (15) OF REF. (1). C
NBMM= NBM
IF(NA.NE.NB)NBMM= NB
DO 210 I= 1,NB
JI= M-I+ 1
IF(JI.GT.N)GO TO 210
XV= 1.D-06
KK= 1
1875 IF(DABS(CA(KK,I)).GE.XV.AND.DABS(CA(KK,JI)).GE.XV.AND.
1 DABS(CB(KK,I)).GE.XV) GO TO 1900
KK= KK+ 1
GO TO 1875
1900 LL= KK+ 1
1905 IF(DABS(CA(LL,I)).GE.XV.AND.DABS(CA(LL,JI)).GE.XV.AND.
1 DABS(CB(LL,I)).GE.XV) GO TO 1910
1906 LL= LL+ 1
GO TO 1905
1910 XXV= CA(LL,JI)*CA(KK,I)-CA(LL,I)*CA(KK,JI)
IF(DABS(XXV).LT.1.D-06)GO TO 1906
XV= CA(LL,JI)/CA(KK,JI)
AX(I)= (CB(LL,I)-CB(KK,I)*XV)/(CA(LL,I)-CA(KK,I)*XV)
XV= CA(LL,I)/CA(KK,I)
BX(I)= (CB(LL,I)-CB(KK,I)*XV)/(CA(KK,JI)*XV-CA(LL,JI))
IF(AX(I).GT. ZERO) GO TO 15
DO 190 J= 1,N
FVD(J,I)= -FVD(J,I)
190 CA(J,I)= -1.D0*CA(J,I)
15 IF(BX(I).GE. ZERO)GO TO 210
DO 200 J= 1,N
FVD(J,JI)= -FVD(J,JI)
200 CA(J,JI)= -1.D0*CA(J,JI)
210 CONTINUE C C      NATURAL ORBITALS OF SPIN CALCULATION C
IF (IPR .EQ. 0) GO TO 717
WRITE(6,119)
WRITE(6,19)(EA(I),I= 1,N)
WRITE(6,49)
CALL OUTPUT(CA,NAP,2,NC,OCH)

```

```

717 CONTINUE
  DO 213 I = 1,M
    BX(I) = ZERO
213 AX(I) = ZERO
  AD = 1.D0/DSQRT(2.D0)
  DO 220 I = 1,NB
    N1 = M-I + 1
    DO 220 J = 1,N
      IF(N1.GT.N)GO TO 25
      CC(J,N1) = AD*(CA(J,I)-CA(J,N1))
      CC(J,I) = AD*(CA(J,I) + CA(J,N1))
      GO TO 220
25 CC(J,I) = CA(J,I)
220 CONTINUE
  IF(NA.EQ.NB)GO TO 35
  DO 230 I = NBP,NA
    DO 230 J = 1,N
230 CC(J,I) = CA(J,I)
35 CONTINUE
  DO 240 I = 1,N
    DELW(I) = DSQRT(1.D0-EB(I))
240 BE(I) = DSQRT(EB(I))
  MNM = M-N + 1 C C      ATOMIC SPIN DENSITIES CALCULATION C      SEE
TABLE II IN REF. (2) C
  KIK = 1.D0
  XKIK = KIK-1.D0
  S2 = XM + XKIK C NEW CALCULATION OF SANIBEL COEFFICIENTS
  YM = DFLOAT(NA-NB)/2.D0
  YMS = YM*YM
  S2S = S2*(S2 + 1.D0)
  DO 800 NLM = 1,2
    YNP = DFLOAT(NA + NB-2*NLM)/2.D0
    LL1 = YNP + YM + 0.01D0
    LL2 = YNP + S2 + 0.01D0
    LL3 = YNP-YM + 0.01D0
    LL4 = YNP-S2 + 0.01D0
    C0(NLM) = (2.D0*S2 + 1.D0)/(YNP + S2 + 1.D0)*F(LL3,LL4 + 1)/F(LL2,LL1 + 1)
    CSK(1,NLM) = C0(NLM)*(YNP + YMS-S2S)/(YMS-YNP*YNP)
    GG = 2.D0*(YNP-1.D0) + YNP + YMS-S2S
    CSK(2,NLM) = -(CSK(1,NLM)*GG + C0(NLM))/((YNP-1.D0)**2-YMS)
  JUP = NB-2
  IF(NLM.EQ.2) JUP = NB-3
  DO 802 J = 2,JUP
    YJ = J
    JM = J-1
    JP = J + 1
    GG = 2.D0*YJ*(YNP-YJ) + YNP + YMS-S2S
    GD = (YNP-YJ)**2-YMS
802 CSK(JP,NLM) = -(CSK(J,NLM)*GG + CSK(JM,NLM)*YJ**2)/GD
800 CONTINUE
  WRITE(6,59)S2
  IF(MU.EQ.1)GO TO 65
  P = -C0(1)*A(2)
  DO 250 K = 2,NB
    KM = K-1
250 P = P + (-1.D0)**K*CSK(KM,1)*A(K + 1)*K

```

```

Q(1) = ZERO
IF(NB.LE.1)GO TO 45
DO 260 I = 1,NB
Q(I) = -C0(2)*FA(2,I)
DO 260 K = 2,NBM
KP = K + 1
KM = K - 1
260 Q(I) = Q(I) + (-1.D0)**K*CSK(KM,2)*FA(KP,I)*K
45 CONTINUE
DO 270 I = 1,NB
BX(I) = C0(1)*FA(1,I)
DO 270 K = 2,NB
KM = K - 1
270 BX(I) = BX(I) + (-1.D0)**KM*CSK(KM,1)*FA(K,I)
DO 290 I = 1,NA
JI = M - I + 1
IF(JI.GT.N)GO TO 61
SS = XM/(S2*(S2 + 1.D0))
IF(I.GT.NB)GO TO 55
AA = SS + SS*(XN*SOMEQA(KIK) + P - XN*BX(I) - Q(I))/SOMEQA(KIK)
BB = SS*XM*BX(I)*DELW(I)/SOMEQA(KIK)
EA(I) = AA + BB
EA(JI) = AA - BB
GO TO 290
55 EA(I) = SS*(XM + 1.)
DO 280 J = 1,NB
280 EA(I) = EA(I) + SS*(1.D0 - BX(J))/SOMEQA(KIK))
GO TO 290
61 EA(I) = ZERO
290 CONTINUE
DO 301 I = 1,N
SPIN(I) = ZERO
DO 300 K = 1,M
IF(K.GT.N.OR.K.LT.MNM)GO TO 300
SPIN(I) = SPIN(I) + EA(K)*CC(I,K)**2
300 CONTINUE
301 TOTSP = TOTSP + SPIN(I)
IF (IPR .EQ. 0) GO TO 65
WRITE(6,69)S2
WRITE(6,19)(SPIN(I),I = 1,N)
WRITE(6,309) TOTSP
65 CONTINUE
SPOS = ZERO
SNEG = ZERO
DO 373 I = 1,N
IF(SPIN(I) .LT. ZERO) GO TO 374
SPOS = SPOS + SPIN(I)
GO TO 373
374 SNEG = SNEG + SPIN(I)
373 CONTINUE
SRAT = DABS(SNEG/SPOS)
WRITE(6,308) SRAT
308 FORMAT(/,10X,'NEG. TO POS. S.D. RATIO = ',F12.8)
309 FORMAT(/,10X,'TOTAL SPIN DENSITY = ',F12.8,/) C IF (IPR .EQ. 20) GO TO
375 C RETURN C C CALCULATION OF D PARAMETERS C FD(I,J) = D0(I,J);

```

```

CD(I,J) = D2(I,J); FVD(I,J) = D1(I,J); C      ED(I) = D1(I); AX(I) = D0(I) C      SEE REF.
(3), TABLE V AND EQN. (9) OF REF. (4) C
375 DO 360 I = 1,NB
    AX(I) = ZERO
    ED(I) = ZERO
    DO 310 J = 1,NB
        JM = J-1
        AX(I) = AX(I) + (-1.D0)**JM*CK(JM,0)*FA(J,I)
310 CONTINUE
    AX(I) = AX(I)/SOMEGA(KIK)
    IM = I-1
    DO 320 K = 1,NB
320 ED(I) = ED(I) + (-1.D0)**K*CK(K,0)*FA(K,I)
    ED(I) = ED(I)/SOMEGA(KIK)
    IF(I.EQ.1)GO TO 360
    DO 350 J = 1,IM
        A2IJ(1) = 1.D0
        IF(NB.LE.1)GO TO 165
        DO 324 K = 2,NB
324 A2IJ(K) = FA(K,I)-EB(J)*A2IJ(K-1) C C      A2IJ(K) IS ASUBK(I,J) OF REF. (2) C
165 FD(I,J) = ZERO
    IF(NB.LE.1)GO TO 175
    DO 330 K = 1,NBM
        KM = K-1
330 FD(I,J) = FD(I,J) + (-1.D0)**KM*CK(KM,0)*A2IJ(K)
175 FD(I,J) = FD(I,J)/SOMEGA(KIK)
340 FD(J,I) = FD(I,J)
    FVD(I,J) = (AX(I)-FD(I,J))/EB(J)
    CD(I,J) = (ED(I)-FVD(I,J))/EB(J)
67 FVD(J,I) = FVD(I,J)
350 CD(J,I) = CD(I,J)
360 CONTINUE C C      PROJECTED CHARGE DENSITY CALCULATION..PUT IN
BMAT C      SEE TABLE II OF REF. (2) C
    DO 380 I = 1,N
    DO 380 J = 1,I
    RHOIJ = ZERO
    DO 370 K = 1,M
        IF(K.LE.NB)GO TO 75
        IF(K.LE.NA)GO TO 85
        IF(K.GT.N)GO TO 370
        IF(K.GT.NA)GO TO 95
75 RHOIJ = RHOIJ + (1. + DSQRT(EB(K)))*(AX(K) + ED(K))*CA(I,K)*CA(J,K)
    GO TO 370
85 RHOIJ = RHOIJ + CA(I,K)*CA(J,K)
    GO TO 370
95 II = M-K + 1
    RHOIJ = RHOIJ + (1.D0-DSQRT(EB(II)))*(AX(II) + ED(II))*CA(I,K)*CA(J,K)
370 CONTINUE
    BMAT(I,J) = RHOIJ
380 BMAT(J,I) = RHOIJ
    CALL TRACAB(BMAT,HCORE,EPO,NAP)
    IF (IPR .EQ. 1) WRITE(6,89)EPO
    TRA = ZERO C C      CALCULATION OF SECOND ORDER DENSITY COMPO-
NENTS C      SEE TABLE I OF REF. (1). C
    EP2 = ZERO
    DO 460 KM = 1,N

```

```

DO 460 KN= 1,KM
QM=ZERO
DO 430 K= 1,NB
KP=M-K+1 C      CALCULATE IIII
GX=0.25D0*((1.D0+BE(K))**2)*(AX(K)+ED(K))
P=      (CA(KM,K)*CA(KN,K))**2
QM=QM+GX*P
IF(K.LT.MNM)GO TO 115 C      CALCULATE IIII'
GX=0.25D0*((1.D0-BE(K))**2)*(AX(K)+ED(K))
P=      (CA(KM,KP)*CA(KN,KP))**2
QM=QM+GX*P C      CALCULATE IIII'
GX=-0.25D0*(DELW(K)**2)*(AX(K)+ED(K))
P=      (CA(KM,K)*CA(KN,K)*CA(KM,KP)*CA(KN,KP))*2.D0
QM=QM+GX*P C      CALCULATE IIII'
GX=0.25D0*(DELW(K)**2)*(AX(K)-ED(K))
P=      ((CA(KM,K)*CA(KN,KP))**2+(CA(KM,KP)*CA(KN,K))**2)
QM=QM+GX*P C      CALCULATE IIII'
GX=-0.25D0*(DELW(K)**2)*(AX(K)-ED(K))
P=      CA(KM,K)*CA(KN,KP)*CA(KM,KP)*CA(KN,K)*2.D0
QM=QM+GX*P
115 IF(K.EQ.NB)GO TO 125
KAND=K+1
DO 410 LN=KAND,NB
LP=M-LN+1 C      CALCULATE IJII
GX=0.5D0*(1.D0+BE(K))*(1.D0+BE(LN))*(FD(K,LN)+(BE(K)+BE(LN))*FVD(K
I,LN)+BE(K)*BE(LN)*CD(K,LN))
P=      ((CA(KM,K)*CA(KN,LN))**2+(CA(KM,LN)*CA(KN,K))**2)
QM=QM+GX*P C      CALCULATE IJII
GX=-0.25D0*(1.D0+BE(K))*(1.D0+BE(LN))*(FD(K,LN)-FVD(K,LN)+2.D0*(BE
I(K)+BE(LN))*FVD(K,LN)-BE(K)*BE(LN)*(FVD(K,LN)-CD(K,LN)))
P=      CA(KM,K)*CA(KM,LN)*CA(KN,K)*CA(KN,LN)*2.D0
QM=QM+GX*P
IF(LN.LT.MNM)GO TO 116 C      CALCULATE IJII'
GX=0.5D0*(1.D0+BE(K))*(1.D0-BE(LN))*(FD(K,LN)+(BE(K)-BE(LN))*FVD(K
I,LN)-BE(K)*BE(LN)*CD(K,LN))
P=      ((CA(KM,K)*CA(KN,LP))**2+(CA(KM,LP)*CA(KN,K))**2)
QM=QM+GX*P C      CALCULATE IJII'
GX=-0.25D0*(1.D0+BE(K))*(1.D0-BE(LN))*(FD(K,LN)-FVD(K,LN)+2.D0*(BE
I(K)-BE(LN))*FVD(K,LN)+BE(K)*BE(LN)*(FVD(K,LN)-CD(K,LN)))
P=      CA(KM,K)*CA(KM,LP)*CA(KN,K)*CA(KN,LP)*2.D0
QM=QM+GX*P
116 IF(K.LT.MNM)GO TO 410 C      CALCULATE IJII'
GX=0.5D0*(1.D0+BE(LN))*(1.D0-BE(K))*(FD(LN,K)+(BE(LN)-BE(K))*FVD(L
IN,K)-BE(LN)*BE(K)*CD(LN,K))
P=      ((CA(KM,LN)*CA(KN,KP))**2+(CA(KM,KP)*CA(KN,LN))**2)
QM=QM+GX*P C      CALCULATE IJII'
GX=-0.25D0*(1.D0+BE(LN))*(1.D0-BE(K))*(FD(LN,K)-FVD(LN,K)+2.D0*(BE
I(LN)-BE(K))*FVD(LN,K)+BE(LN)*BE(K)*(FVD(LN,K)-CD(LN,K)))
P=      CA(KM,LN)*CA(KM,KP)*CA(KN,LN)*CA(KN,KP)*2.D0
QM=QM+GX*P C      CALCULATE IJII'
GX=0.5D0*(1.D0-BE(K))*(1.D0-BE(LN))*(FD(K,LN)-(BE(K)+BE(LN))*FVD(K
I,LN)+BE(K)*BE(LN)*CD(K,LN))
P=      ((CA(KM,KP)*CA(KN,LP))**2+(CA(KM,LP)*CA(KN,KP))**2)
QM=QM+GX*P C      CALCULATE IJII'
GX=-0.25D0*(1.D0-BE(K))*(1.D0-BE(LN))*(FD(K,LN)-FVD(K,LN)-2.D0*(BE
I(K)+BE(LN))*FVD(K,LN)-BE(K)*BE(LN)*(FVD(K,LN)-CD(K,LN)))

```

```

P= CA(KM, KP)*CA(KN, LP)*CA(KM, LP)*CA(KN, KP)*2.D0
QM=QM+GX*P C CALCULATE IJJ'I'

GX=-0.25D0*DELW(K)*DELW(LN)*(FD(K, LN)+FVD(K, LN)+BE(K)*BE(LN)*(FVD(
1K, LN)+CD(K, LN)))
P= (CA(KM, K)*CA(KN, LN)*CA(KM, LP)*CA(KN, KP)+CA(KM, LN)*CA(KN, K
1)*CA(KM, KP)*CA(KN, LP))*2.D0
QM=QM+GX*P C CALCULATE IJ'JI'
GX=-0.25D0*DELW(K)*DELW(LN)*(FD(K, LN)+FVD(K, LN)-BE(K)*BE(LN)*(FVD(
1K, LN)+CD(K, LN)))
P= (CA(KM, K)*CA(KN, LP)*CA(KM, LN)*CA(KN, KP)+CA(KM, LP)*CA(KN, K
1)*CA(KM, KP)*CA(KN, LN))*2.D0
QM=QM+GX*P
410 CONTINUE
125 IF(MO.LE.0)GO TO 430
DO 425 LQ=1,MO
LN=LQ+NB C CALCULATE ITIT
GX=0.5D0*(1.D0+BE(K))*(AX(K)+BE(K)*ED(K))
P= ((CA(KM, K)*CA(KN, LN))**2+(CA(KM, LN)*CA(KN, K))**2)
QM=QM+GX*P C CALCULATE ITTI
GX=-0.5D0*(1.D0+BE(K))*(0.5D0*(AX(K)-ED(K))+BE(K)*ED(K))
P= CA(KM, K)*CA(KN, LN)*CA(KM, LN)*CA(KN, K)*2.D0
QM=QM+GX*P
IF(K.LT.MNM) GO TO 425 C CALCULATE I'TI'T
GX=0.5D0*(1.D0-BE(K))*(AX(K)-BE(K)*ED(K))
P= ((CA(KM, KP)*CA(KN, LN))**2+(CA(KM, LN)*CA(KN, KP))**2)
QM=QM+GX*P C CALCULATE I'TTI'
GX=-0.5D0*(1.D0-BE(K))*(0.5D0*(AX(K)-ED(K))-BE(K)*ED(K))
P= CA(KM, KP)*CA(KN, LN)*CA(KM, LN)*CA(KN, KP)*2.D0
QM=QM+GX*P C CALCULATE ITTI'
GX=-0.25D0*(DELW(K)*(AX(K)+ED(K)))
420 P= (CA(KM, K)*CA(KN, LN)*CA(KM, LN)*CA(KN, KP)+CA(KM, LN)*CA(KN, K
1)*CA(KM, KP)*CA(KN, LN))*2.D0
QM=QM+GX*P
425 CONTINUE
430 CONTINUE
421 IF(MO.LE.1)GO TO 441
DO 440 KQ=1,MO
K=KQ+NB
IF(KQ.EQ.MO)GO TO 440
KQ1=KQ+1
DO 435 LQ=KQ1,MO
LN=LQ+NB C CALCULATE TUTU
QM=QM+0.50D0*((CA(KM, K)*CA(KN, LN))**2+(CA(KM, LN)*CA(KN, K))**2) C
CALCULATE TUUT
435 QM=QM-0.50D0*CA(KM, K)*CA(KN, LN)*CA(KM, LN)*CA(KN, K)*2.D0
440 CONTINUE
441 CONTINUE
IF(KM.EQ.KN)EP2=EP2+QM*GAM(KM, KN)
GMAT(KM, KN)=QM+0.5D0-0.5D0*(BMAT(KM, KM)+BMAT(KN, KN))
TRA=TRA+QM
IF(KM.NE.KN) TRA=TRA+QM
GMAT(KN, KM)=GMAT(KM, KN)
460 IF(KM.NE.KN)EP2=EP2+2.D0*QM*GAM(KM, KN)
IF (IPR .EQ. 1) WRITE(6,99) S2,EP2
EPI=EPO+EP2

```

```

IF (IPR .EQ. 1) WRITE(6,169) EPI
9 FORMAT(/,3X,'EB',/)
19 FORMAT(1X,5(1PD15.6,2X))
39 FORMAT(3X,'THE WEIGHTING FACTOR FOR THE S=' ,F6.4,' STATE =' ,1PD15
1.7)
49 FORMAT(/,3X,'NATURAL ORBITALS OF CHARGE',/)
59 FORMAT(/,25X,'RESULTS OF PROJECTION FOR S=' ,F6.4,/)
69 FORMAT(/,3X,'ATOMIC SPIN DENSITIES FOR S=' ,F6.4,/)
79 FORMAT(/,3X,'CORRESPONDING ORBITALS',/)
89 FORMAT(/,3X,'ONE-ELECTRON PART OF ENERGY =' ,1PD15.8,/)
99 FORMAT(/,3X,'FOR S=' ,F8.4,5X,'2 ELECTRON ENERGY =' ,1PD15.8,/)
119 FORMAT(/,3X,'NATURAL ORBITAL OCCUPATION NUMBERS',/)
139 FORMAT(/,3X,'THE WEIGHTED ENERGY FOR THIS PROJECTION =' ,1PD14.6,/)
169 FORMAT(/,3X,'PROJECTED ENERGY FOR S=0 STATE...' ,D15.6,/)
RETURN
END C-----
SUBROUTINE DENA(V,PA,NAP,NOC,IS)
IMPLICIT REAL*8 (A-H,P-Z)
COMMON/SYM/S(60,60),ST(60,60),NSM(2),NOCC(2)
COMMON/EXCI/IEX
DIMENSION V(60,60),PA(60,60)
DATA ZERO/0.D0/
IF (IEX .NE. 0) GO TO 5
1 CONTINUE C C...EVEN SYSTEM GROUND STATE CALCULATION C
DO 10 I= 1,NAP
DO 20 J= 1,I
SI= ZERO
DO 30 K= 1,NOC
SI= SI+ V(I,K)*V(J,K)
30 CONTINUE
PA(I,J)= SI
PA(J,I)= SI
20 CONTINUE
10 CONTINUE
RETURN
5 CONTINUE
IF (IEX .NE. 1) GO TO 35
2 CONTINUE C C...CALCULATION FOR ODD STATES C
NOCM= NOC-1
KOCC= NOC+ 1
KS= NOCC(1)
I1= (NAP+ 1)/2
I2= MOD(I1,2)
IF (I2 .EQ. 0) IS= 1
DO 40 I= 1,NAP
DO 50 J= 1,I
SI= ZERO
IF (IS .EQ. 2) GO TO 15
DO 60 K= 1,NOC
SI= SI+ V(I,K)*V(J,K)
60 CONTINUE
GO TO 25
15 CONTINUE
NOCP= NOC+ 1
DO 70 K= 1,NOCP
SI= SI+ V(I,K)*V(J,K)

```

```

70   CONTINUE
    SI = SI - V(I,KS)*V(J,KS)
25   CONTINUE
    PA(I,J) = SI
    PA(J,I) = SI
50   CONTINUE
40  CONTINUE
    RETURN
35  CONTINUE C C...CALCULATION FOR EXCITED SYSTEMS C
    KOCC = NOC + 1
    DO 80 I = 1, NAP
        DO 90 J = 1, I
            SI = ZERO
            DO 100 K = 1, NOC
                SI = SI + V(I,K)*V(J,K)
100   CONTINUE
        IF (IS .EQ. 2) GO TO 45
        SI = SI + V(I,KOCC)*V(J,KOCC) - V(I,NOC)*V(J,NOC)
45   CONTINUE
        PA(I,J) = SI
        PA(J,I) = SI
90   CONTINUE
80  CONTINUE
    RETURN
END C-----
SUBROUTINE MMULT(A,B,C,N)
IMPLICIT REAL*8 (A-H,P-Z)
DIMENSION A(60,60),B(60,60),C(60,60)
DATA ZERO/0.D0/
DO 10 I = 1, N
    DO 10 J = 1, N
        X = ZERO
        DO 20 K = 1, N
            X = X + A(I,K)*B(K,J)
20  CONTINUE
        C(I,J) = X
10  CONTINUE
    RETURN
END C-----
SUBROUTINE TRACAB(A,B,T,NAP)
IMPLICIT REAL*8 (A-H,P-Z)
DIMENSION A(60,60),B(60,60)
DATA ZERO/0.D0/
T = ZERO
DO 10 I = 1, NAP
    X = ZERO
    DO 20 K = 1, NAP
        X = X + A(I,K)*B(K,I)
20  CONTINUE
    T = T + X
10  CONTINUE
    RETURN
END C-----
SUBROUTINE UHFOCK(GAM,RA,RB,FA,NAP,S)
IMPLICIT REAL*8 (A-H,P-Z)
DIMENSION GAM(60,60),RA(60,60),RB(60,60),FA(60,60),S(60,60)

```

```

COMMON/MAT/BMAT(60,60),GMAT(60,60),HCORM(60,60)
DATA ZERO/0.D0/
DO 10 I= 1,NAP
  DO 20 J= 1,I
    EXC=ZERO C          IEX=I-J C          IF(IEX .EQ. 1 .OR. IEX .EQ. 0)
EXC=RA(J,I)*GAM(I,J)
    EXC=RA(J,I)*GAM(I,J)
    FA(I,J)=HCORM(I,J)-EXC+S(I,J)
    FA(J,I)=FA(I,J)
  20 CONTINUE
  X1=ZERO
  DO 30 K= 1,NAP
    X1=X1+(RA(K,K)+RB(K,K))*GAM(K,I)
  30 CONTINUE
  FA(I,I)=FA(I,I)+X1
10 CONTINUE
  RETURN
  END C-----
SUBROUTINE OUTPUT (B,N,IDI,NC,OCH)
IMPLICIT REAL*8 (A-H,P-Z)
CHARACTER OCH(60) C PRINTS THE SCF MATRICES
DIMENSION B(60,60) ,NC(1) C C
IF(IDI.GT.2) GO TO 5 C
J1= 1
J2= 10
DO 10 I= 1,N,10
  IF(J2.GT.N) J2= N
  PRINT 9,(OCH(J),NC(J),J= J1,J2)
  DO 20 K= 1,N
    PRINT 19,OCH(K),NC(K),(B(K,J),J= J1,J2)
  20 CONTINUE C
  J1=J2+ 1
  J2=J2+ 10
10 CONTINUE C
  RETURN
5 CONTINUE
J1= 1
J2= 10
DO 30 I= 1,N,10
  IF(J2.GT.N) J2= N
  PRINT 9,(OCH(J),NC(J),J= J1,J2)
  DO 40 K= 1,N
    PRINT 29,K,(B(K,J),J= J1,J2)
  40 CONTINUE C
  J1=J2+ 1
  J2=J2+ 10
30 CONTINUE C
  RETURN C
9 FORMAT(7X,10(5X,A1,I2,4X),/)
19 FORMAT(2X,A1,I2,10(2X,F10.4))
29 FORMAT(3X,I2,10(2X,F10.4))
  END C-----
SUBROUTINE ALPH(X,AL,NB) C C THIS SUBROUTINE CALCULATE ANGLE
BOND MAKES WITH X-AXIS
IMPLICIT REAL*8 (A-H,P-Z)
DIMENSION X(1),AL(1)

```

```

DATA ZERO/0.D0/
DO 10 I= 1,NB
  I3= 3*(I-1)+ 1
  J3= I3+ 3
  A= X(J3)-X(I3)
  B= X(J3+ 1)-X(I3+ 1)
  DB= DABS(B)
  IF (DB.LT.1.0D-04) GO TO 20
  AL(I)= DATAN(B/A)
  GO TO 10
20 CONTINUE
  AL(I)= ZERO
10 CONTINUE
RETURN
END C-----
SUBROUTINE CART(B,X,AL,NAT3,NATOM) C C CART CALCULATES NEW
COORD. AFTER BOND SHIFTS
IMPLICIT REAL*8 (A-H,P-Z)
DIMENSION X(1),B(1),AL(1)
DATA ZERO/0.D0/
E= ZERO
F= ZERO
DO 10 I= 1,NAT3
10 X(I)= ZERO
DO 20 I= 2,NATOM
  I1= I-1
  J= 3*I-2
  K= 3*I-1
  E= E+ B(I1)*DCOS(AL(I1))
  F= F+ B(I1)*DSIN(AL(I1))
  X(J)= E
  X(K)= F
20 CONTINUE
RETURN
END C-----
FUNCTION CK(I,NLM) C C SUMS FACTORIALS USING EQUATION (20) OF
REFERENCE (2) C CSUBK(S,M,NP) WHERE K=1, 2S= NA-NB+ 2*(KIK-1),
2M= NA-NB, C 2*NP= NA+ NB-NLM*2 C
IMPLICIT REAL*8 (A-H,P-Z)
COMMON/BLK5/N,M,NA,NB,NM,NPP,NAM,NBP,KIK
DATA ZERO/0.D0/
IB= NB-KIK+ 2-NLM
IS= KIK-1
JS= NA-NB+ KIK-1
NS= NB-NLM
IS2= NA-NB+ 2*KIK-2
X SX= DFLOAT(IS2)
WY= ZERO
IF(IB.LE.0)GO TO 45
IF((NS-I).LT.0)GO TO 45
DO 10 J= 1,IB
  JM= J-1
  IF((IB-JM-1).LT.0)GO TO 10
  I1= J
  I2= IS+ JM
  IF(IS.GT.0)GO TO 5

```

```

ZZ = 1.D0
GO TO 15
5 ZZ = F(I2,I1)
15 I1 = IS + J - I
   I2 = IS + JM
   IF((I1-1).LT.0)GO TO 10
   IF(I.EQ.0)GO TO 25
   YY = F(I2,I1)
   GO TO 35
25 YY = 1.D0
35 WY = (-1.D0)**JM*ZZ*YY*F(NS-I,2)/(F(IB-JM-1,2)*F(IS2 + J,2)) + WY
10 CONTINUE
   CK = (XSX + 1.D0)*F(JS,1)/F(IS,1)*WY
   RETURN
45 CK = ZERO
   RETURN
END C-----
FUNCTION F(INM,MNR) C C
FACTORIAL(INM)/FACTORIAL(MNR-1) C
IMPLICIT REAL*8 (A-H,P-Z)
XF = 1.D0
IF(INM.LE.1) GO TO 5
DO 10 J = MNR,INM
  XJ = J
10 XF = XF*XJ
5 F = XF
RETURN
END C-----
SUBROUTINE SYMNAT(NAP,FA,V,EA)
IMPLICIT REAL*8(A-H,P-Z)
COMMON/EIS/FV1(60),FV2(60),MATZ
COMMON/AAA/ED(60),FD(60,60),FVD(60,60),CD(60,60)
COMMON/SYM/S(60,60),ST(60,60),NSM(2),NOCC(2)
COMMON/EXCI/IEX
DIMENSION FA(60,60),V(60,60),EA(60),E1(60),E2(60) C..BLOCK FACTOR
CALL MMULT(FA,S,CD,NAP)
CALL MMULT(ST,CD,FVD,NAP)
NS1 = NSM(1)
CALL INIT (FA)
DO 10 I = 1,NS1
  DO 10 J = 1,NS1
    FA(I,J) = FVD(I,J)
10 CONTINUE
CALL RS(60,NS1,FA,E1,MATZ,FD,FV1,FV2,IEERR)
CALL INIT (FA)
NS2 = NSM(2)
DO 20 I = 1,NS2
  I1 = I + NS1
  DO 20 J = 1,NS2
    J1 = J + NS1
    FA(I,J) = FVD(I1,J1)
20 CONTINUE
CALL RS(60,NS2,FA,E2,MATZ,CD,FV1,FV2,IEERR)
CALL INIT (FVD)
K = 0
KS = 0 C...CHECK FOR SYM. OCC. NUMBERS > = 2

```

CALCULATES

```

DO 40 LL= 1,NS1
  L=NS1+1-LL
  DE= 2.D0-E1(L)
  IF(DE.GT.1.0D-08) GO TO 5
  K= K + 1
  KS= KS + 1
  EA(K)= E1(L)
  DO 50 I= 1,NS1
    FVD(I,K)= FD(I,L)
50  CONTINUE
40  CONTINUE
5  KSP= KS + 1
  KA= 0 C...CHECK FOR ANTISYM. OCC. NUMBERS > = 2
DO 60 LL= 1,NS2
  L= NS2+ 1-LL
  DE= 2.D0-E2(L)
  IF(DE.GT.1.0D-08) GO TO 15
  K= K + 1
  KA= KA + 1
  EA(K)= E2(L)
  DO 70 I= 1,NS2
    IP= I+ NS1
    FVD(IP,K)= CD(I,L)
70  CONTINUE
60  CONTINUE
15 KAP= KA + 1 C...CHECK FOR SYM OCC NUMBERS > 1 , < 2
DO 80 LL= KSP,NS1
  L= NS1+ 1-LL
  DE= 1.01D0-E1(L)
  IF(DE.GT.1.0D-06) GO TO 25
  K= K + 1
  KS= KS + 1
  EA(K)= E1(L)
  DO 90 I= 1,NS1
    FVD(I,K)= FD(I,L)
90  CONTINUE
80  CONTINUE
25 KSP= KS + 1 C...CHECK FOR ANTISYM OCC NUMBERS > 1 , < 2
DO 100 LL= KAP,NS2
  L= NS2+ 1-LL
  DE= 1.0D0-E2(L)
  IF (DE .GT. 1.0D-08) GO TO 35
  K= K + 1
  KA= KA + 1
  EA(K)= E2(L)
  DO 110 I= 1,NS2
    IP= I+ NS1
    FVD(IP,K)= CD(I,L)
110 CONTINUE
100 CONTINUE
35 KAP= KA + 1 C...CHECK FOR SYM OCC NUMBERS = 1
DO 120 LL= KSP,NS1
  L= NS1+ 1-LL
  DE= 0.99999999D0-E1(L)
  IF(DE.GT.1.0D-08) GO TO 55
  K= K + 1

```

```

    KS = KS + 1
    EA(K) = E1(L)
    DO 130 I = 1, NS1
        FVD(I, K) = FD(I, L)
130    CONTINUE
120    CONTINUE
    55 KSP = KS + 1
    45 CONTINUE
    DO 140 LL = KAP, NS2
        L = NS2 + 1 - LL
        IF(E2(L).LT.1.0D-08) GO TO 65
        K = K + 1
        KA = KA + 1
        EA(K) = E2(L)
        DO 150 I = 1, NS2
            IP = I + NS1
            FVD(IP, K) = CD(I, L)
150    CONTINUE
140    CONTINUE
    65 KAP = KA + 1
    DO 160 LL = KSP, NS1
        L = NS1 + 1 - LL
        K = K + 1
        EA(K) = E1(L)
        DO 170 I = 1, NS1
            FVD(I, K) = FD(I, L)
170    CONTINUE
160    CONTINUE
    IF(KAP.GT.NS2) GO TO 75
    DO 180 LL = KAP, NS2
        L = NS2 + 1 - LL
        K = K + 1
        EA(K) = E2(L)
        DO 190 I = 1, NS2
            IP = I + NS1
            FVD(IP, K) = CD(I, L)
190    CONTINUE
180    CONTINUE C..BACK TRANSFORM
    75 CALL MMULT(S, FVD, V, NAP)
    RETURN
    END C-----
SUBROUTINE SYMCOR(NAP, FA, V, EA)
IMPLICIT REAL*8(A-H, P-Z)
COMMON/EIS/FV1(60), FV2(60), MATZ
COMMON/AAA/ED(60), FD(60,60), FVD(60,60), CD(60,60)
COMMON/SYM/S(60,60), ST(60,60), NSM(2), NOCC(2)
DIMENSION FA(60,60), V(60,60), EA(60), E1(60), E2(60) C..BLOCK FACTOR
CALL MMULT(FA, S, CD, NAP)
CALL MMULT(ST, CD, FVD, NAP)
NS1 = NSM(1)
CALL INIT(FA)
DO 10 I = 1, NS1
    DO 10 J = 1, NS1
        FA(I, J) = FVD(I, J)
10    CONTINUE
    CALL RS(60, NS1, FA, E1, MATZ, FD, FV1, FV2, IERR)

```

```

NS2 = NSM(2)
CALL INIT (FA)
DO 20 I = 1, NS2
  I1 = I + NS1
  DO 20 J = 1, NS2
    J1 = J + NS1
    FA(I, J) = FVD(I1, J1)
20 CONTINUE
CALL RS(60, NS2, FA, E2, MATZ, CD, FV1, FV2, IERR)
CALL INIT (FVD)
K = 0
KS = 0
DO 40 LL = 1, NS1
  L = NS1 + 1 - LL
  DE = 1.D0 - E1(L)
  IF(DE.GT.1.0D-08) GO TO 5
  K = K + 1
  KS = KS + 1
  EA(K) = E1(L)
  DO 50 I = 1, NS1
    FVD(I, K) = FD(I, L)
50 CONTINUE
40 CONTINUE
5 KSP = K + 1
KA = 0
DO 60 LL = 1, NS2
  L = NS2 + 1 - LL
  DE = 1.D0 - E2(L)
  IF(DE.GT.1.0D-08) GO TO 15
  K = K + 1
  KA = KA + 1
  EA(K) = E2(L)
  DO 70 I = 1, NS2
    IP = I + NS1
    FVD(IP, K) = CD(I, L)
70 CONTINUE
60 CONTINUE
15 KAP = KA + 1
DO 80 LL = KSP, NS1
  L = NS1 + 1 - LL
  IF(E1(L).LT.1.0D-08) GO TO 25
  K = K + 1
  KS = KS + 1
  EA(K) = E1(L)
  DO 90 I = 1, NS1
    FVD(I, K) = FD(I, L)
90 CONTINUE
80 CONTINUE
25 KSP = KS + 1
DO 100 LL = KAP, NS2
  L = NS2 + 1 - LL
  K = K + 1
  EA(K) = E2(L)
  DO 110 I = 1, NS2
    IP = I + NS1
    FVD(IP, K) = CD(I, L)

```

```

110 CONTINUE
100 CONTINUE
  IF(KSP.GT.NS1) GO TO 35
  KAP = KA + 1
  DO 120 LL = KSP, NS1
    L = NS1 + 1 - LL
    K = K + 1
    EA(K) = E1(L)
    DO 130 I = 1, NS1
      FVD(I, K) = FD(I, L)
130 CONTINUE
120 CONTINUE C..BACK TRANSFORM
35 CALL MMULT(S, FVD, V, NAP)
  RETURN
  END C-----
SUBROUTINE VEFF(N, NBOND, IE)
IMPLICIT REAL*8 (A-H, P-Z)
INTEGER*4 LDA, IPVT(60), JOB
COMMON/PII/JCHG, NALPH, NBET, NPIE, JSPIN, JUHF
COMMON/EIG/C1(60,60), E1(60), C2(60,60), E2(60)
COMMON/POL/RI(60,60), P(60,60)
COMMON/FINAL/BN(60), X(180), AL(60), NC(60)
COMMON/HH/H(60,60), V(60,60), PT(60,60), ZZ(60)
COMMON/DER/DB(60), DR(60), DV(60), VOP(60,60), D(60)
COMMON/SCR/A(60,60), B(60,60), C(60,60), E(60)
DIMENSION DET(2), WORK(60), Z(60), V0(60,60)
DATA ZERO/0.D0/ C...SET CONSTANTS
KOC = MOD(N, 2)
NALP = NALPH + 1
NBETP = NBET + 1 C...INITIALIZE PI-MATRIX
CALL INIT (P) C...IF SCF ORBITALS ARE USED, IE=1 C...ALPHA CONTRIB-
UTION
  DO 20 I = 1, N
    DO 20 J = 1, I
      DO 30 IO = 1, NALPH
        DO 30 IU = NALP, N
          DEL = E1(IU) - E1(IO)
          CO = -2.D0 * C1(I, IU) * C1(I, IO) * C1(J, IU) * C1(J, IO)
          P(I, J) = P(I, J) + CO / DEL
30 CONTINUE
        DO 40 IO = 1, NBET
          DO 40 IU = NBETP, N
            DEL = E2(IU) - E2(IO)
            CO = -2.D0 * C2(I, IU) * C2(I, IO) * C2(J, IU) * C2(J, IO)
            P(I, J) = P(I, J) + CO / DEL
40 CONTINUE
        P(J, I) = P(I, J)
20 CONTINUE
  CALL VZERO(N, V0, 0)
  CALL MMULT(P, V0, B, N) C...CALCULATE R MATRIX (CALLED 'A' HERE)
  DO 50 I = 1, N
    DO 50 J = 1, N
      DEL = ZERO
      IF(I .EQ. J) DEL = 1.D0
      A(I, J) = DEL - B(I, J)
50 CONTINUE C...FIND R INVERSE

```

```

CALL DGECO(A,60,N,IPVT,RCOND,Z)
JOB = 1
CALL DGEDI(A,60,N,IPVT,DET,WORK,JOB)
DO 60 I = 1,N
  DO 60 J = 1,N
    RI(I,J) = A(I,J)
60 CONTINUE C...CALCULATE V-EFFECTIVE AS V0*R-INV
CALL MMULT (V0,RI,V,N)
RETURN
END C-----
SUBROUTINE VZERO(N,V0,ISC) C...CALCULATES BARE POTENTIAL USING
OHNO FORM
IMPLICIT REAL*8 (A-H,P-Z)
COMMON/DER/D1(60),D2(60),D3(60),D(60,60),DT(60)
COMMON/FINAL/B(60),X(180),AL(60),NC(60)
DIMENSION V0(60,60),DX(3)
DATA ZERO/0.D0/ C...SET CONSTANTS
ESQ = 14.397D0
GAMO = 11.13D0
CON = 23.062D0
AO = ESQ/GAMO
PF = .5D0
DO 10 I = 1,N
  DO 10 J = 1,I
    IF (J .NE. I) GO TO 20
    V0(I,I) = GAMO
    GO TO 10
20 CONTINUE
  I3 = 3*(I-1)
  J3 = 3*(J-1)
  BI = ZERO
  DO 30 K = 1,3
    DX(K) = X(J3 + K) - X(I3 + K)
    BI = BI + DX(K)*DX(K)
30 CONTINUE
  BI = DSQRT(BI)
  BR = BI/AO
  C1 = 1.D0 + BR**2
  C2 = DSQRT(C1)
  GIJ = GAMO/C2
  V0(I,J) = GIJ
  V0(J,I) = V0(I,J)
  DFR = (-GIJ*BR)/(AO + C1)
  D(I,J) = DFR
  D(J,I) = D(I,J)
10 CONTINUE
RETURN
END C-----
SUBROUTINE VPRIME(N,NBOND) C...SUBROUTINE CALCULATES
DVEFF/DBOND
IMPLICIT REAL*8(A-H,P-Z)
COMMON/SW/ISW,IPR,ISCR
COMMON/MAT/BMAT(60,60),GMAT(60,60),HCORM(60,60)
COMMON/HH/H(60,60),V(60,60),PT(60,60),Z(60)
COMMON/DER/D1(60),D(60),D3(60),V0P(60,60),DT(60)
COMMON/POL/RI(60,60),P(60,60)

```

```

COMMON/FINAL/BN(60),X(180),AL(60),NC(60)
DIMENSION VP(60,60),DV(60,60),A(60,60),B(60,60)
DIMENSION DB(60),DX(3)
DATA CON/23.062D0/
DATA ZERO/0.D0/ C...CALCULATE (I+V*PI)
CALL MMULT(V,P,A,N)
  DO 10 I= 1,N
    DO 10 J= 1,N
      DEL= 1.D0
      IF ( I .NE. J ) DEL= ZERO
      B(I,J)= DEL + A(I,J)
10  CONTINUE
  DO 20 K= 1,NBOND
    CALL INIT (DV)
    DO 40 I= 1,K
      KP= K + 1
      DO 40 J= KP,N
        I3= (I-1)*3
        J3= (J-1)*3
        DO 50 L= 1,3
          DX(L)= X(J3+L)-X(I3+L)
50  CONTINUE
      BI= LENGTH(DX)
      CALL DFBON(DX,DB,BI,AL,I,J)
      KMI= K-I+ 1
      IF (KMI .LE. 0) GO TO 40
      DV(I,J)= V0P(I,J)*DB(KMI)
      DV(J,I)= DV(I,J)
40  CONTINUE
    CALL MMULT(B,DV,A,N)
    CALL MMULT(A,RI,VP,N)
    DO 60 I= 1,N
      DO 60 J= 1,N
        IF (I .EQ. J) GO TO 60
        Y= VP(I,J)*GMAT(I,J)*CON
        D(K)= D(K)+ Y
60  CONTINUE
20 CONTINUE
  RETURN
  END C-----
SUBROUTINE INIT (A) C... THIS SUBROUTINE ZEROES 2-D ARRAYS
IMPLICIT REAL*8 (A-H,P-Z)
DIMENSION A(60,60)
DATA ZERO/0.D0/
DO 10 I= 1,60
  DO 10 J= 1,I
    A(I,J)= ZERO
    A(J,I)= ZERO
10 CONTINUE
  RETURN
  END

```

References

1. R. P. Feynman, Phys. Rev., **76** 749 (1949); **76** 769 (1949).
2. F. J. Dyson, Phys. Rev., **75** 486 (1949); **75** 1736 (1949).
3. Seminal works in the application of polarization insertion screening are: L. Hedin, Phys. Rev., **139** A796 (1965) and A. D. Mclachlan and M. A. Ball, Mol. Phys., **7** 501 (1964). Work on calculations of excitation energies using second-order self-energies: O. Tanimoto and K. Shimada, Mol. Phys., **23** 745 (1972); Mol. Phys., **23** 765 (1972).
4. D. Bohm and D. Pines, Phys. Rev., **92** 609 (1953).
5. D. Pines, Phys. Rev., **92** 626 (1953).
6. H. Gutfreund and W. A. Little, Phys. Rev. **183** 68 (1969).
7. H. Gutfreund and W. A. Little, J. Chem. Phys. **50** 4468 (1969).
8. R. Pariser and R. G. Parr, J. Chem. Phys., **21** 466 (1953); **21** 767 (1953).

9. J. A. Pople, *Trans. Faraday Soc.*, **49** 1375 (1953).
10. J. A. Pople and R. K. Nesbet, *J. Chem. Phys.*, **22** 571 (1954).
11. A. Brickstock and J. A. Pople, *Trans. Faraday Soc.*, **50** 901 (1954).
12. A. L. Fetter and J. D. Walecka "Quantum Theory of Many Particle Systems" (McGraw-Hill, New York, 1971).
13. K. A. Brueckner, *Phys. Rev.*, **100** 36 (1955).
14. J. Goldstone, *Proc. Royal Soc. London*, **A239** 267 (1957).
15. W. P. Su, J. R. Schrieffer and A. J. Heeger, *Phys. Rev. Lett.* **42** 1698 (1979).
16. W. P. Su, J. R. Schrieffer and A. J. Heeger, *Phys. Rev. B* **22** 2099 (1980).
17. S. Kivelson and D. E. Heim, *Phys. Rev. B* **26** 4278 (1982).
18. K. R. Subbaswamy and M. Grabowski, *Phys. Rev. B*. **24** 2168 (1981).
19. J. E. Hirsch and M. Grabowski, *Phys. Rev. Lett.* **52** 1713 (1984).
20. D. S. Boudreaux, R. R. Chance, J. L. Bredas and R. Silbey, *Phys. Rev. B* **28** 6927 (1983).
21. H. Fukutome and M. Sasai, *Prog. Theor. Phys.* **67** 41 (1982) **69** 1 (1983); **69** 373 (1983).
22. S. Etemad, A. J. Heeger and A. G. MacDiarmid, *Ann. Rev. Phys. Chem.* **33** 443 (1982).
23. M. J. Rice, *Phys. Lett.* **71A** 152 (1979).
24. J. A. Krumhansl and J. R. Schrieffer, *Phys. Rev. B* **11**, 3535 (1975).

25. D. K. Campbell and A. Bishop, *Phys. Rev. B* **24** 4859 (1981).
26. E. J. Mele and M. J. Rice, *Phys. Rev. Lett.* **45** 926 (1980).
27. S. Ikehata, J. Karfen, T. Woerner, A. Pron, M. A. Druy, A. Sivak, A. J. Heeger and A. G. MacDiarmid, *Phys. Rev. Lett.* **45** 1123 (1980).
28. N. Suzuki, M. Osaki, S. Etemad, A. J. Heeger and A. G. MacDiarmid, *Phys. Rev. Lett.* **45** 1209 (1980).
29. Salem, "The Molecular Orbital Theory of Conjugated Systems" (W. A. Benjamin, New York, 1966).
30. J. A. Pople and S. H. Walmsley, *Mol. Phys.* **5** 15 (1962).
31. B. Kirtman, W. B. Nilson and W. E. Palke, *Solid State Commun.* **46** 791 (1983).
32. C. R. Fincher, E. E. Chin, A. J. Heeger, A. G. MacDiarmid, and J. B. Hastings, *Phys. Rev. Lett.* **48** 100 (1982).
33. C. S. Yannoni and T C. Clarke, *Phys. Rev. Lett.* **51** 1191 (1983).
34. M. J. Duijvestijn, A. Manenshijn, J. Schmidt and R. A. Wind, *J. Mag. Res.* **64** 461 (1985).
35. R. E. Peierls, "Quantum Theory of Solids", (Oxford Univ. Press, London, 1955).
36. H. W. Gibson, *J. Amer. Chem. Soc.* (to be published).
37. S. Kuroda and H. Shirakawa, *Solid State Commun.* **43** 591 (1982).

38. H. Thomann, L. R. Dalton, Y. Tomkiewicz, N. S. Shiren and T. C. Clarke, *Phys. Rev. Lett.* **50** 533 (1983).
39. M. Nechtschein, F. Devreux, F. Genoud, M. Guglielmi and K. Holczer, *Phys. Rev. B* **27** 61 (1983).
40. H. Thomann, J. F. Cline, B. M. Hoffman, H. Kim, A. Morrobel-Sosa, B. H. Robinson and L. R. Dalton, *J. Phys. Chem.* **89** 1994 (1985).
41. M. Mehring, H. Seidel, W. Muller and G. Wegner, *Solid State Commun.* **45** 1075 (1983).
42. A. J. Heeger and J. R. Schrieffer, *Solid State Commun.* **48** 207 (1983).
43. R. K. Bullough and P. J. Caudrey "The Soliton and its History" in R. K. Bullough and P. J. Caudrey (eds.) "Topics in Current Physics: Solitons", (Springer-Verlag, Berlin, 1980).
44. J. Goldstone and R. Jackiw, *Phys. Rev. D*, **11** 1486 (1975).
45. M. J. S. Dewar and W. Thiel, *J. Amer. Chem. Soc.*, **99** 4899 (1977).
46. W. A. Little, *J. Chem. Phys.* **49** 420 (1968).
47. J. N. Murrell and A. J. Harget, "Semi-Empirical SCF-MO Theory of Molecules" (Wiley and Sons, London, 1972).
48. N. Mataga and K. Nishimoto, *Z. Phys. Chem.* **113** 140 (1957).
49. K. Ohno, *Theor. Chim. Acta* **2** 219 (1964).
50. S. Mazumdar and D. K. Campbell, *Phys. Rev. Lett.*, **55** 2067 (1985).

51. A potential is downwardly convex if, for all j , $V_{j+1} + V_{j-1} \geq 2V_j$,
where V_j is the Coulomb interaction with a site j sites away.
52. C. A. Coulson and H. C. Longuet-Higgins, Proc. Roy. Soc. A 191 39 (1947).
53. T. Terasaka, T. Iijima, Y. Fujimura, and T. Nakajima, Bull. Chem. Soc. Japan 46 1301 (1973).
54. I. L. Cooper and J. Linderberg, Mol. Phys. 25 265. (1973).
55. A. Warshel and M. Karplus, J. Amer. Chem. Soc. 94 5612 (1972).
56. K. Schulten, I. Ohmine and M. Karplus, J. Chem. Phys. 64 4422 (1976); 65 2298 (1978).
57. P. O. Lowdin, "Quantum Theory of Atoms, Molecules and the Solid State" (Academic, New York, 1966).
58. J. E. Harriman, J. Chem. Phys. 40 2827 (1962); D. H. Phillips and J. C. Schug, J. Chem. Phys. 61 1031 (1974).
59. S. Suhai, Chem. Phys Lett. 96 619 (1983); Phys. Rev. B 27 3506 (1983).
60. H. Thomann, L. R. Dalton, M. Grabowski, Y. Tomkiewicz and T. C. Clarke, Phys. Rev. B 31 3141 (1985).
61. D. K. Campbell "A Field Theorist's View of Conducting Polymers: Solitons in Polyacetylene and Related Systems" in S. Takeno (ed.) "Dynamical Problems in Soliton Systems", (Springer-Verlag, Berlin, (1984).

**The vita has been removed from
the scanned document**